U.PORTO
INSTITUTO DE CIÊNCIAS BIOMÉDICAS ABEL SALAZAR
UNIVERSIDADE DO PORTO

NOTCH SIGNALING PATHWAY AS A MEDIATOR FOR EARLY DETECTION AND MODULATION OF AGGRESSIVENESS OF PROSTATE CANCER

FILIPE LA FUENTE CARVALHO
TESE DE DOUTORAMENTO APRESENTADA
AO INSTITUTO DE CIÊNCIAS BIOMÉDICAS ABEL SALAZAR
DA UNIVERSIDADE DO PORTO EM CIÊNCIAS MÉDICAS

2013

FILIPE LA FUENTE DE CARVALHO

NOTCH SIGNALING PATHWAY AS A MEDIATOR FOR EARLY DETECTION AND MODULATION OF AGGRESSIVENESS OF PROSTATE CANCER

Tese de Candidatura ao grau de Doutor em Ciências Médicas submetida ao Instituto de Ciências Biomédicas Abel Salazar da Universidade do Porto

Orientador — Doutor David M. Berman
Categoria — Professor Associado
Afiliação — Department of Pathology and Molecular Medicine, Queen's University

Coorientador — Doutor Rui Henrique
Categoria — Professor Auxiliar
Afiliação — Instituto de Ciências Biomédicas Abel Salazar da Universidade do Porto

Coorientador — Doutor Carlos Lopes
Categoria — Professor Catedrático
Afiliação — Instituto de Ciências Biomédicas Abel Salazar da Universidade do Porto

FILIPE CRISTA LA FUENTE ISAAC DE CARVALHO

NOTCH SIGNALING PATHWAY AS A MEDIATOR FOR EARLY DETECTION AND MODULATION OF AGGRESSIVENESS OF PROSTATE CANCER

Porto, 2013

Dissertação de candidatura ao grau de Doutor apresentada ao Instituto de Ciências Biomédicas Abel Salazar Universidade do Porto

VIA DE SINALIZAÇÃO NOTCH COMO MEDIADOR DA DETECÇÃO PRECOCE E MODULAÇÃO DA AGRESSIVIDADE DO CANCRO DA PRÓSTATA

Orientador — Prof. Doutor David M. Berman
Coorientadores — Prof. Doutor Rui Henrique e
Prof. Doutor Carlos Lopes

PREFACE

O homem é do tamanho do seu sonho.
(A Man is the size of his dream)
Fernando Pessoa

A scientific breakthrough requires hard-work, a significant amount of hours dedicated to a specific problem and reproducible methods to validate the discovery. However, one needs a fair amount of creativity to address new questions and the ability to dream about unthinkable scenarios that might lead to unexpected findings. When I started my first year of medical school, I was far from imaging that I would pursue a Ph.D. and perform all my research at Johns Hopkins University. After completing the second year of my medical degree at Faculdade de Medicina da Universidade do Porto, Prof. Adelino Leite Moreira involved me in research projects studying pulmonary hypertension in animal models. At that time, Prof. Tiago Henriques-Coelho was very interested in understanding the roles of a peptide, thymulin, in the pathophysiology of pulmonary hypertension. With kindness and patience, Profs. Leite Moreira and Henriques-Coelho introduced me to the fundamental steps of scientific method and the laboratory routine, and at the same time encouraged me to come to the United States as a summer student to enrich my knowledge and mature scientific ideas. Therefore, I spent two summers doing research while in medical school, one at Maine Medical Center with Prof. Calvin Vary working in endoglin and TGFb signaling, and another at Harvard Medical School supervised by Prof. Tiago Outeiro developing an assay for studying protein oligomerization in Parkinson's disease. Tiago and I were already good friends at the time, and few years later when he returned to Portugal to start his own laboratory, Tiago assigned me a project focused on renal tubular dysenesis, a kidney disease caused by misfolding of an important enzyme. I had just graduated from medical school and was about to start my internship, so I started experiencing the physician-scientist life: clinical commitments in the morning and early afternoon; basic research at late hours and throughout the weekend. I am very grateful to Tiago and the members of his laboratory, namely Rita Oliveira, Leonor Fleming, and Sandra Tenreiro, who taught me the fundamental techniques of cellular and molecular biology.

In the middle of crowded emergency rooms and unexpected scientific results, Pipa, an oncology resident at the time, got my attention and my mind was no longer only divided between science and medicine, but also between Portugal and the United States. A few months after we met, Pipa was offered a position for a residency program in Washington, DC and I was about to start urology residency at Hospital de Santo António, Porto. As any first year urology resident, one of the

clinical tasks assigned to me was to perform prostate biopsies. I became intrigued with the fact that besides all the advances in medical imaging and cancer diagnostics, urologists still struggle to detect prostate cancers and there is an unmet need for new predictors of outcome. In Europe and in the USA there are prostate cancer screening programs using prostate-specific antigen (PSA) serum levels. In general, men with elevated PSA levels are recommended to undergo a prostate biopsy to detect cancer at an early stage. However, this improvement in diagnosis resulted in overtreatment of harmless low-grade tumors. Only men with aggressive cancers are likely to derive any survival benefit from treatment and prostate biopsies often do not accurately distinguish indolent from aggressive cancers. Therefore, I decided to interrupt my residency training and move to the United States (meanwhile Pipa and I were engaged and planning to get married) and devote my Ph.D. research to the understanding of molecular mechanisms involved in prostate cancer progression and metastasis. All the bench work of this Ph.D. project was performed at the Departments of Pathology and Oncology of Johns Hopkins School of Medicine, Baltimore supervised by Prof. David Berman. I am profoundly grateful to Prof. Berman for accepting me in his laboratory as his mentee, for all his challenging scientific questions that became cornerstones to begin a solid scientific career. I also wish to thank my colleagues at the Berman laboratory and other collaborative laboratories, particularly William Brandt, Brian Simons, Luigi Marchionni, Tamara Lotan, Edward Schaeffer, Ashley Ross, Zhenhua Huang, Zeshaan Rasheed, Emmanuel Antonarakis and William Matsui, for their help, advice and scientific input to all the projects. My gratitude also to my co-mentors Prof. Rui Henrique and Prof. Carlos Lopes, who always made short the distance between USA and Portugal. I should also acknowledge financial support from Fundação para a Ciência e Tecnologia through a Ph.D. scholarship.

A special final word of gratefulness to Pipa for all her love, patience and incentive throughout these years; and to my parents, sister and the rest of the family that although far away continuously supported me.

The structure of this Thesis is well accepted by Instituto de Ciências Biomêdicas Abel Salazar, Universidade do Porto and other academic institutions. The Thesis is written in English because all the results have already been published or submitted for publication in peer-reviewed international scientific journals contributing to a broad spectrum of potential readers. I should mention that the contents of the Thesis surpass the initial project that motivated the official title — Notch signaling pathway as a mediator for early detection and modulation of aggressiveness of prostate cancer — proposed in the beginning of experimental work. The main focus of this Thesis is the molecular mechanisms involved in prostate cancer progression and metastasis. The Thesis is organized in five sections: an Introduction paper providing an overview of Notch pathway in cancer, particularly in prostate cancer, highlighting questions that remain open in the field; the “Rationale and Aims” present the main goals of my research projects; a summary of all the “Materials and Methods” used in all the experiments to generate the results; a section of “Results and Discussion” contains 3 original papers focused on different aspects of prostate cancer progression; and to conclude a list of references and a summary of the Thesis in English and Portuguese. Overall, the results presented in this Thesis provide new insights into the roles of Notch pathway members in prostate cancer progression, the benefit of molecular markers in distinguishing indolent from aggressive tumors, and the biological activity of prostate circulating tumor cells.

Washington, D.C., October 15, 2013

INDEX

Abbreviations

AS	Active surveillance
CTCs	Circulating tumor cells
FISH	Fluorescent in situ hybridization
HES1	Hairy and enhancer of split–1
HES6	Hairy and enhancer of split–6
HEY1	Hairy/enhancer-of-split related with YRPW motif 1
PSA	Prostate-specific antigen
PTEN	Phosphatase and tensin homolog
RBPJ	Recombination signal binding protein for immunoglobulin kappa J region
TRAMP	Transgenic adenocarcinoma of the mouse prostate

PART I — INTRODUCTION

CHAPTER 1 —
NOTCH SIGNALING IN PROSTATE CANCER: A MOVING TARGET

NOTCH SIGNALING IN PROSTATE CANCER: A MOVING TARGET

Filipe LF Carvalho[1], Brian W. Simons[1,2], Charles G. Eberhart[1], David M Berman[1,3,4]
[1]*Department of Pathology,* [2]*Department of Molecular and Comparative Pathobiology,* [3]*Urology and Oncology, Johns Hopkins University School of Medicine, Baltimore, Maryland, USA,* [4]*Department of Pathology and Molecular Medicine and Cancer Biology and Genetics Program, Cancer Research Institute, Queen's University, Kingston, Ontario, Canada*

Abstract

By regulating cell fate, Notch pathway signaling provides critical input into differentiation, organization and function of multiple tissues. Notch signaling is becoming an increasingly recognized feature of a number of cancers, where it may play oncogenic or tumor suppressive roles. In benign prostate, Notch controls the proportion of cells with stem cell properties, as well as the differentiation state and architecture of the gland. In prostate cancer, similar features correlate with lethal potential and may be influenced by Notch. Increased Notch1 can confer a survival advantage on prostate cancer cells, and levels of Notch family members, such as Jagged2, Notch3 and Hes6 increase with higher cancer grade. However, Notch signaling can also antagonize growth and survival of both benign and malignant prostate cells. Since Notch antagonists are being tested in clinical trials for cancer, it will be critically important to know whether Notch normally supports or suppresses prostate cancer progression prior to applying this body of research to patient care. Here we review the operation of Notch signaling in prostate development and disease and point out further opportunities for therapeutic, diagnostic, and biologic inquiry.

Keywords: Notch pathway; tumor progression; prostate cancer; active surveillance, targeted therapy

How Notch regulates cell fate and tissue organization

General roles for Notch in biology

Named for the notched wing phenotype of mutant *Drosophila* and encoding a family of evolutionarily conserved cell surface receptors, Notch is one of the most widely studied pathways in biology (1). Notch signaling has especially dramatic effects on cell fate, determining the shape and composition of organs and tissues throughout the animal(2). For example, Notch signaling in intestinal stem cells favors enterocyte rather than endocrine differentiation (3), whereas in lymphopoietic precursors, Notch activation favors the development of T cell over B cell progeny (4). These cell fate decisions typically occur in a specialized stem cell niche where stem cells and progeny monitor each other's differentiation states. Notch signaling requires direct contact between the sending and receiving cells (see below), and is therefore well suited for this purpose.

General mechanisms of Notch signaling

To initiate Notch signaling, a membrane-bound ligand on the sending cell binds to a receptor on the receiving cell (Fig. 1A). Ligand binding catalyzes a unique series of proteolytic cleavages that convert the full-length membrane-bound receptor into a smaller transcriptional transactivator, the notch intracellular domain (NICD), which is released from the cell surface and translates into the nucleus (Fig. 1B). NICDs bind to RBPJ/CBP transcription factors to activate Notch target genes, including those encoding members of the Hairy and enhancer of split (HES) and the Hairy/enhancer-of-split related with YRPW motif (HEY) protein families (Fig. 1B). Notably, these well-established pathway components have less well known family members with emerging roles in the prostate. Two examples of particular interest in the prostate are DLK1 and HES6. DLK1 (Delta like 1 homolog) is highly related to delta ligands, but lacks the Delta-Serrate-LAG–2 (DSL) activating domain and is therefore likely a naturally occurring antagonist of Notch signaling (5). HES6 is structurally related with other HES family members, such as HES1, but is not a direct target of cannonical Notch signaling. In fact, HES6 determines an opposite cell fate in neural stem cells than HES1, a well established Notch target (6).

Research into Notch function in the prostate and other organs has been skewed towards Jagged1, Delta-like 1 and Notch1. A more complete understanding of Notch function will require additional attention to other Notch receptors and ligands.

A

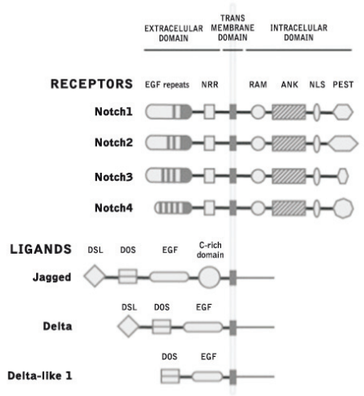

B

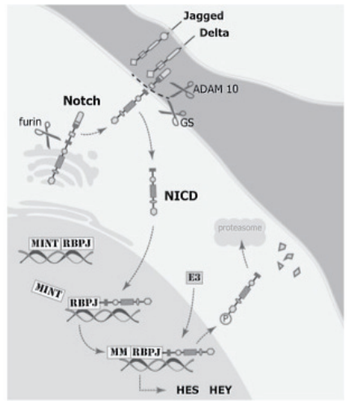

Figure 1 — **A** In mammals, the pathway is composed of four receptors (Notch1 through Notch4) and five ligands (Jagged1 and 2 and Delta-like 1, 3, and 4). Both ligands and receptors are single-pass transmembrane proteins composed by different structural domains. Ligands have an extracellular domain with three related structural motifs: the Delta/Serrate/LAG–2 (DSL) motif; the Delta and OSM–11-like proteins (DOS) motif; and the third motif is compose of EGF-like repeats, both calcium binding and non calcium-binding, that can affect signaling efficiency. Jagged ligands also have a citosine-rich (C-rich) domain. The extracellular domain of Delta-like 1 homolog (DLK1) only has a DOS motif and EGF repeats. The structure of the transmembrane and intracellular portion of the ligands remains largely unknown. Notch receptors have an extracellular domain that contains EGF-like repeats and a negative regulatory region; a transmembrane domain; and an intracellular domain composed RBPJ association module (RAM) that binds the transcription complex, the nuclear localization sequence (NLS), seven ankyrin repeats (ANK), and a proline (P)/glutamic acid (E)/serine (S)/threonine (T) motif (PEST) that targets protein for degradation.
B The receptor is activated in a juxtacrine manner through its interaction with a ligand presented by an adjacent cell. An appropriate ligand binding produces a conformational change in the Notch receptor, exposing the extracellular domain for ADAM10 enzyme cleavage. After cleavage, there is a second cleavage within the transmembrane domain, performed by the gamma-secretase (GS) complex. GS cleavage releases the active form of the receptor — Notch intracellular domain (NICD) — into the cytoplasm from which it translocates into the nucleus. Here NICD complexes with the DNA-binding transcription activator factor RBPJ (other allies CBF1, CSL) to displace the transcriptional repressor Mint. This displacement facilitates the recruitment of activators such as Mastermind (MM) and thereby the transcription of pathway target genes. The main targets of the Notch pathway are two families of transcriptional repressors: the Hairy and enhancer of split (HES) and the Hairy/enhancer-of-split related with YRPW motif (HEY) proteins. Although it remains unknown if HES6 is a target of Notch pathway, recent studies reveal that HES6 may play an important role in prostate cancer progression. In order to quench Notch pathway activation, the NICD is phosphorylated on the PEST domain by E3 ubiquitin ligases, thereby targeting it for proteosomal degradation.

Notch pathway in cancer

The T-ALL link

Physiologic roles for the Notch pathway were established in the 1920s, but it took another 70 years to link genetic alterations that directly activate Notch signaling to cancer. In the 1990s, Ellisen and collaborators (7) found a translocation that generated a ligand-independent, autonomously activated form of the Notch receptor (NICD) in T-cell acute lymphoblastic leukemia (T-ALL) cells. Bringing together chromosomes 7 and 9, the translocation placed NICD under the transcriptional control of T-cell receptor β. By engineering the t(7,9) translocation into transgenic mice, Pear and colleagues demonstrated that NICD1 overexpression could cause leukemia (8). Data from human patients show that NOTCH1 overexpression correlates with poor survival, although it derives only rarely from t(7,9) translocation. Instead, Notch1 activation usually occurs through mutations in the receptor that render it constitutively active and/or resistant to degradation (9, 10). These and other experiments laid the groundwork for Notch signaling became a popular topic in cancer research with the ascendance of the idea that embryonic pathways may be reactivated in the development of cancer (11–13), and with the identification of Notch pathway expression in common solid tumors (Figure 2).

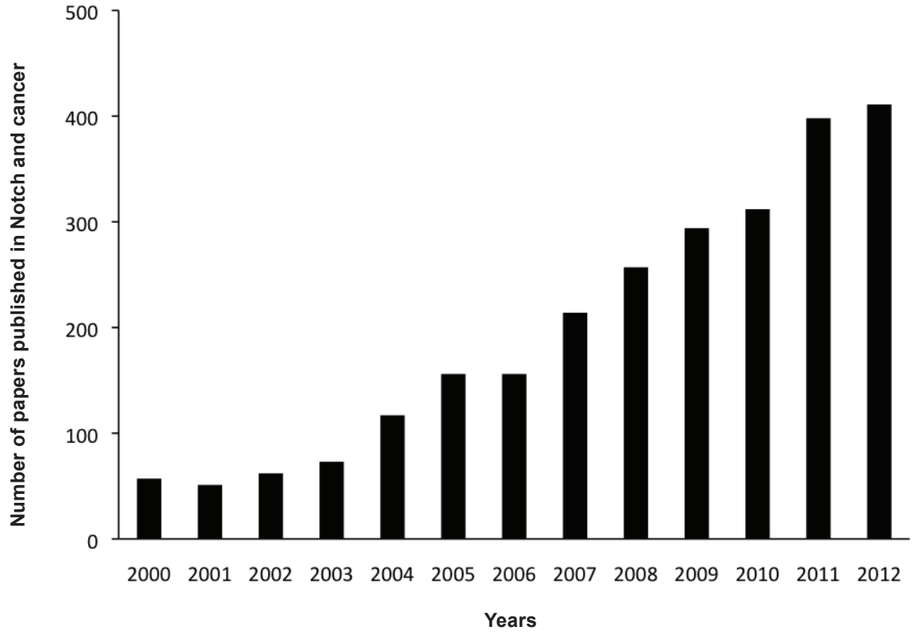

Figure 2 — The number of indexed publications about Notch pathway and cancer continuous increase over the last 10 years.

Notch in solid tumors

Mechanisms of Notch activation in Solid Tumors

Notch signaling can be aberrantly activated in tumor cells through different mechanisms, such as genetic and epigenetic alterations or cross-talk with other oncogenic pathways. Over the last decade, several studies showed that DNA alterations can activate Notch signaling in a variety of solid tumors. For example, ovary and breast cancers have somatic mutations, copy number alterations (14), amplifications (15), gene rearrangements (16) implicate Notch pathway members in tumor pathophysiology. In addition, histone methylation that regulate the dynamics of gene transcription can also induce Notch signaling during tumorigenesis (17). Lastly, Notch can also be activated by intracellular cross-talk with other pathways. For example, Notch activation in a human B cell leukemia/lymphoma model resulted from induction of JAGGED2 ligand by the MYC oncogene (18). Alternatively, Notch activity can be mimicked by other transcription factors. For example, hypoxia-inducible transcriptional factor 1 alpha (HIF1A) can bypass Notch receptors cleavage by gamma-secretase to directly activate Notch-responsive promoters and increase the expression of Notch downstream targets (19). Since both Myc and HIF1A have established roles in prostate cancer these alternative routes to Notch activation may play a role in the disease.

Effects of Notch activation in solid tumors

Once activated, Notch signalling can promote cell growth in a variety of solid tumors (Table 1). Of these, breast (mammary gland) cancer has drawn the much attention and can serve as one paradigm for understanding the effects of Notch signalling. Activation of Notch1 in transgenic mice disrupts mammary gland homeostasis — interfering with normal expansion, differentiation, and regression programs associated with pregnancy and lacation (20). Enforced activation can also induce breast cancer, as shown by the oncogenic activity of Notch1 in the mouse mammary gland (20–22). In human breast cancers, high levels of JAGGED1 and NOTCH1 proteins have been linked to particularly aggressive cancers (23). The poor prognosis seen in these tumors may derive from a role for Notch in the development of drug-resistance. In particular, Notch signaling levels increase in breast cancer cells that become resistant to the estrogen receptor antagonist tamoxifen, the HER2 receptor antagonist trastuzumab (Herceptin), and the epidermal growth factor receptor (EGFR) antagonists gefitinib and lapatinib (24–27). Within the heterogeneity of breast tumors, there are subpopulations of cells, called breast cancer stem cells, that are responsible for tumor repopulation after chemotherapy and the generation of metastasis (28). Although,

breast cancer stem cells are resistant to chemotherapy, recent evidence shows that these cells are sensitive to HER2 targeting agents (29,30). Moreover, Notch signaling is essential for breast cancer stem cells survival and self-renewal (31–32). Altogether, resistance HER2 targeted therapy can be delayed or overcome by combining these agents with Notch antagonists (gamma secretase inhibitors), and that effective dosing can be attained in vivo. Therefore, Notch antagonism may be useful in treating solid tumors that become resistant to targeted therapies, including therapies that target endocrine pathways. Given the central role of endocrine therapy in treating prostate cancer, this indication deserves further attention.

Notch signaling in the prostate

Notch signaling in prostate development and homeostasis

During male fetal development, rising androgen levels initiate prostate morphogenesis and induce prostate buds to form in the urogenital sinus (UGS) at 10 weeks gestation in humans and at embryonic day 17.5 in mice (33–35). Progression from the relatively simple UGS to the complex branching structure of the mature prostate involves carefully orchestrated patterns of proliferation, invasion, and differentiation. During this process, multiple cell-fate decisions are made in both the mesenchyme and the epithelium that generate basal, luminal, and neuroendocrine cells, and results in zone-or lobe-specific epithelial identity. During early embryonic development, the primitive prostatic epithelium is somewhat uniform and cells express markers of both basal and luminal cells (36). As the prostate matures, multipotent basal progenitor cells differentiate along a basal or luminal phenotype. Both layers contain stem cells capable of generating the complete spectrum of basal and luminal cells (37, 38). After maturation, the two layers are maintained independently by luminal and basal stem cells and transdifferentiation from basal to luminal phenotype is uncommon (39, 40). Notably, both populations can be the cell of origin for prostate cancer in mice (38, 39).

In the prostate, Notch signaling is induced during times of rapid growth corresponding to the formation of the organ in the embryo and its regeneration after castration. Whether Notch inhibits or promotes growth in the prostate, is controversial. One of the earliest studies on this topic (41), showed that Notch1 mRNA was upregulated in embryonic and postnatal prostate epithelia and dramatically downregulated upon maturation of the gland in adulthood. Using a Notch1-GFP transgenic mouse in which the activity of a Notch1 gene regulatory region was visualized through expression of green fluorescent protein (GFP) the same group attempted to further delineate Notch1 expression in the mouse prostate (41). The investigators concluded that Notch1 was concentrated in basal cells, however, no clear basal

Tumor type	Notch pathway member	Role in tumor biology	References
Oncogenic			
Mammary	JAGGED1 and JAGGED2	Critical for breast cancer tumor progression and bone metastasis	(84, 85)
	NOTCH1 and NOTCH4	In Mouse mammary tumor virus models contributed to breast tumor cell initiation	(21, 86–88)
	NOTCH1 and NOTCH2	Gene rearrangements with MAST kinase family members confers tumor growth advantage	(16)
Ovary cancer	JAGGED1, JAGGED2 and NOTCH3	Somatic mutations and copy number alterations important for proliferation of ovarian cancer cells	(14, 89)
Lung Cancer	NOTCH1 and NOTCH3	NOTCH3 translocation in human lung cancers NOTCH1 promotes tumor cell growth and survival through regulation of IGF pathway	(90) (91)
Kidney	JAGGED1 and NOTCH1	Pathway is constitutively active and promotes growth of renal cell carcinoma	(92)
Tumor suppressive			
Head and Neck	NOTCH1	Exome sequencing revealed NOTCH1 inactivation suggesting it may function as a tumor suppressor gene	(93)
Skin	NOTCH1	Deletion in keratinocytes causes skin cancer through microenviroment	(94)

Table 1 — A partial list of oncogenic and tumor suppressive effects of several Notch pathway members in solid tumors.

expression pattern was demonstrated for Notch1–GFP, and by in situ hybridization, Notch1 appeared more luminal than basal. Nevertheless, this study clearly demonstrated a dynamic expression pattern for Notch1 in prostate epithelium that coincided with key phases of organogenesis and epithelial differentiation.

In mouse adult prostate, the expression levels of the receptors and functional role are slightly different from those described during neonatal stage. Both basal and luminal cells express Notch ligands and receptors (Table 2), but their expression is higher in luminal cells and Notch activation induces luminal cells proliferation (42). On the contrary, Notch activation in basal cells inhibits proliferation and induces differentiation. Valdez and collaborators identified a positive feedback loop between TGFβ signals coming from the stroma that activate Notch in basal cells, contributing to inhibit proliferation of prostate basal cells and counterbalance androgen growth stimuli.

	MOUSE		HUMAN	
Notch member	**Basal Layer**	**Luminal layer**	**Basal Layer**	**Luminal layer**
Notch1	+	+	+	+
Notch2	+	+	-	-
Notch3	-	+	-	-
Notch4	-	-	-	-
Jagged1	+	-	-	+
Jagged2	+	-	-	-
Delta-like 1	-	-	-	-

Table 2 — Expression of Notch ligands and receptor in normal prostate. The expression of other Delta-like ligands has not yet been described. The expression of Notch receptors and ligands in each layer is represented by (+) and (-) represents the absence of expression.

Notch signaling was also implicated in the proliferative response of basal cells in response to androgen stimulation. Following castration, Notch1 expression rose, suggesting a role for the receptor in involution or regeneration (43). Notch inhibition through pharmacologic or genetic (Notch1 deletion) means slowed prostate epithelial differentiation while stimulating proliferation, particularly in cells with an “intermediate” phenotype (i.e., those that expressed both basal and luminal cell markers) (44). Another mouse model with Rbpj deletion in both basal and luminal cells (42) (to impair Notch canonical signaling) found overproliferation of basal cells during prostate regeneration in response to androgens. Thus, several studies in mice have supported a growth-inhibitory role for Notch in the prostate.

Subsequent work (45), in contrast, found that Notch signaling promoted prostate growth. Unlike previous studies, this work was performed in adult human prostate tissue. In these samples, DLK1, a noncanonical Notch ligand that inhibits Notch signaling, was expressed in basal cells, whereas the NOTCH1 receptor and JAGGED1 ligand were co-expressed in luminal secretory cells — suggesting that in these human tissues, the cell types sending and receiving Notch signals were switched in relation to the mouse. Using an antibody specific for activated NICD1, Notch signaling activity was detected in endothelial cells lining blood vessels, but not in epithelial cells of the quiescent adult prostate. These data indicated that Notch was inactive in adult quiescent prostate. However, through expression of NOTCH1, mature prostate epithelial cells had the capacity to activate the Notch signaling pathway, whereas immature/stem cells used DLK1 to repress Notch activation.

The investigators confirmed this scenario by studying prostate growth in a human organ culture model. In growing prostate epithelium, Notch was dramatically activated, with downregulation of the Notch inhibitor DLK1, as well as increased NOTCH1 and nuclear accumulation of its activated product, NICD1 (45). Importantly, as demonstrated by culture with Notch antagonist (gamma secretase inhibitor, or GSI), Notch inhibition halted prostate epithelial cell growth (45).

Why do the roles of Notch in prostate growth appear to switch polarity from one study to the next? Additional work will need to be carried out to answer this question, but it seems more likely to be a question of experimental technique. An explanation may lie in the use of tissues at different stages of maturation by the different groups. One group inhibited Notch in postnatal prostate, at a time when many epithelial cells in the prostate had not yet matured. Others used mature prostates in these assays. The observed data to date might fit a model in which Notch signaling drives proliferation and maturation in mature cells, but prevents these processes in immature cells.

Notch suppresses two central pathways in prostate development and disease: Androgen receptor and PI3K/AKT

Notch interacts with two signaling mechanisms that are central to prostate development, growth, homeostasis and carcinogenesis: the androgen receptor (AR) pathway and the Phosphoinositide 3–kinase (PI3k) / Akt pathway (46, 47). AR signaling is

sufficient to promote prostate growth and differentiation in the embryo and to support glandular homeostasis throughout adulthood. Androgen binding to AR in the cytoplasm induces the receptor homodimerization and translocation to the nucleus. The homodimers bind to the DNA at specific regulatory elements and recruit coactivators (such as Steroid Receptor Coactivator 1 (SRC1) and p300/CBP) to transcribe AR target genes (47). Humans with genetic mutations that disrupt AR signaling do not develop a prostate and never get prostate cancer (48). In the prostate, AR activation leads to prostate cancer formation (49) and in advanced cases, AR signaling is not only maintained, but it can become promiscuous — triggered by a variety of steroid hormones — or even ligand-independent. Thus, signaling by this pathway is a cardinal feature of prostate cancers, and interfering with AR signaling is one of the first examples of targeted therapy in oncology.

A recent study suggested a role for Notch in the acquisition of castration resistance. Belandia and collaborators (50) observed that the Notch target HEY1 directly bound the N-terminal activation domain of AR, suppressing androgen signaling. NICD also suppressed AR activity, was active in cells with different origins — myoblasts, prostate and breast cancer — and suppressed AR activity more effectively than HEY1 alone. The latter effect occurred most likely as a consequence of the induction of related transcriptional repressors, such as HES1 (50). In contrast to these in vitro interactions between Notch and AR, the real process in the prostate may be more complex. Using immunohistochemistry, strong nuclear HEY1 staining was observed in benign prostate hyperplasia, but in prostate cancer this transcription factor localized only to the cytoplasm, indicating reduced nuclear activity of HEY1 in cancer and supporting the idea that cancers downregulate Notch signaling (50). In the same study, however, AR always localized to the nucleus in both benign and malignant tissues (50). Thus although HEY1 has the ability to inhibit AR signaling when expressed at high levels in cell lines, in actual human cancers, HEY1 appeared to be excluded from the nucleus, leaving AR free to transcribe its target genes.

PI3K/AKT activates growth and migration in the prostate (51,52). This pathway is triggered when G protein-coupled or tyrosine kinase receptors activate PI3–Kinase. Then, PI3K phosphorylates cell membrane proteins necessary for AKT binding so it can also be phosphorylated by its activating kinases. PI3K/AKT signaling is suppressed by the phosphatase activity of the Phosphatase and tensin homolog (PTEN), an important tumor suppressor gene. Deletions in PTEN gene and consequent deregulation of PI3k/mTOR signaling contribute to malignant transformation of prostate cells in vitro and in mice models and are common features of advanced human prostate cancers (53–55). Whelan and colleagues (56) found decreased expression of Notch1 in prostate cancer compared with benign prostate and further observed that NICD1 directly induced PTEN expression, resulting in diminished PI3K/AKT activity.

These data suggest the possibility of a tumor suppressive effect of Notch signaling, particularly when triggered by Notch1.

Interestingly, a reciprocal feedback mechanism has been recently described that links the PI3/AKT and AR pathways. Carver and collaborators (57) recently found that suppression of either pathway induces activity in the other. Thus, inactivation of PI3K/AKT lead to increased AR activity, whereas suppressing AR lead to increased PI3K/AKT. It is well established that PI3K/AKT signaling increases in advanced prostate cancer (58). Thus one might expect that decreased Notch signaling permits this increase in PI3/AKT in prostate cancer.

Notch signaling in prostate cancer

Notch pathway expression and function in prostate cancer cell lines

In prostate cancer, there is good agreement between various studies on the expression of Notch components in prostate cancer cell lines. However, the functional significance of Notch signaling in prostate cancer is controversial. Studies from different laboratories consistently detect high level constitutive expression of NOTCH1 and NICD1 in all of the frequently studied human prostate cancer cell lines (PC3, DU145, 22Rv1, and LNCaP) (41, 59). In these cells, knockdown of NOTCH1 levels by small interfering RNA can suppress malignant properties, including cell invasion (59), survival, and proliferation (60). The latter result was surprising, given that earlier work had shown that Notch pathway activation, as achieved through engineered overexpression of NICD, had a similar growth inhibitory effect (41). One possible reason for both inhibition and activation of the pathway to inhibit growth is that Notch pathway activation could have different effects at different levels, a so called “Goldilocks effect.” Moderate Notch signaling could support growth whereas extreme levels of pathway activity (high or low) may inhibit growth. Another potential contributor to different laboratories having different results stems from the vagaries of research using cultured cells. In particular, calcium levels vary significantly in different commonly used culture media components and can have dramatic effects on epithelial cell growth and differentiation (61). High levels of calcium can promote cell autonomous Notch receptor cleavage, producing the active NICD form with little or no contribution of ligand presentation by adjacent cells (62). These results indicate the need for additional studies that carefully titrate levels of Notch signaling while controlling for calcium levels and culture conditions. Until then, the roles of the pathway in prostate cancer are likely to remain controversial. In the meantime, examining research done on prostate cancer tissues might provide some insight.

Expression of pathway components in prostate cancer tissue

Most studies demonstrate an upregulation of Notch pathway members in prostate cancer compared to benign tissue. In the TRansgenic Adenocarcinoma of the Mouse Prostate (TRAMP) model, *Notch1* mRNA levels rose upon metastasis to regional lymph nodes (41), suggesting a role for the pathway in metastasis. In humans, an analysis of mRNA expression databases showed decreased mRNA levels of *NOTCH1* and *HEY1* in prostate cancer compared to benign glands (44). Studies focusing on protein levels, in contrast have found increasing levels of Notch pathway members in human cancers along the progression spectrum. Using immunohistochemistry, Bin Hafeez and collaborators found that levels of NOTCH1 protein increased with increasing Gleason grade (59). Their finding that NOTCH1 levels were particularly high in cancer cells surrounding capillaries provided further support to the idea that Notch signaling might enhance the ability of such cells to escape into the bloodstream and metastasize. Indeed, when compared to localized tumor or benign tissue, metastases showed distinctly elevated levels of JAGGED1 protein (63). Intriguingly, tumors with highest levels of JAGGED1 were least likely to be cured by radical prostatectomy, suggesting that JAGGED1 contributes to the ability of these cancers to metastasize prior to surgery. Thus, bearing in mind contradictory evidence in mice (41), the preponderance of evidence supports upregulation rather than downregulation of Notch components with human prostate cancer progression. While far from proof, this increased level of pathway expression is consistent with a functional role for Notch in prostate cancer progression. Approaches to further explore Notch function in this disease could include conditional knockout of Notch pathway members in mouse models of prostate cancer and trials of Notch antagonists in prostate cancer-bearing mice and humans (see below).

Notch pathway members distinguish high grade from low grade prostate cancers and serve as biomarkers to improve biopsy accuracy

When considering the potential function of any signalling pathway in prostate cancer, it is useful to do so in the context of Gleason Grade. In particular, it is only Gleason grades of 7 and above that have the potential to metastasize and kill (64, 65). Thus, when properly evaluated (i.e., through comprehensive examination of a surgically removed prostate gland), the Gleason grade accurately distinguishes between indolent aggressive prostate cancers. Unfortunately, biopsies often do not accurately distinguish indolent cancers from their more aggressive counterparts (66, 67), leading to frequent “overtreatment” of cancers that do not warrant treatment. At the other end of the spectrum, high grade tumors can rapidly recur after treatment and kill patients regardless of primary treatment. New evidence suggests that members of the Notch pathway are distinctive features of aggressive prostate cancers with high Gleason grade. For example, comparing gene expression profiles from purely high-grade (Gleason 4+4=8) vs. purely low grade (Gleason 3+3=6) microdissected cancer cells, Notch signaling was the foremost distinguishing feature. This observation was confirmed in a meta-analysis using gene profling data form other labororaties. In particular, cancer cells with metastatic potential (Gleason 4+4=8) upregulated the Notch ligand *JAGGED2*, the *NOTCH3* receptor, and the potential Notch target gene, Hairy enhancer of split family member, *HES6* (68, Filipe LF Carvalho and David Berman, submitted) (Figure 3). Thus, a particular Notch ligand, receptor, and response gene, appeared to distinguish aggressive prostate cancers. The arrangement of these components into a potential signaling cascade suggests that the pathway is functional in aggressive prostate cancers.

These findings raise new questions regarding potential uses of Notch pathway members as diagnostic and therapeutic targets in prostate cancer. One such question is whether Notch signalling might be a useful drug target in aggressive prostate cancers.

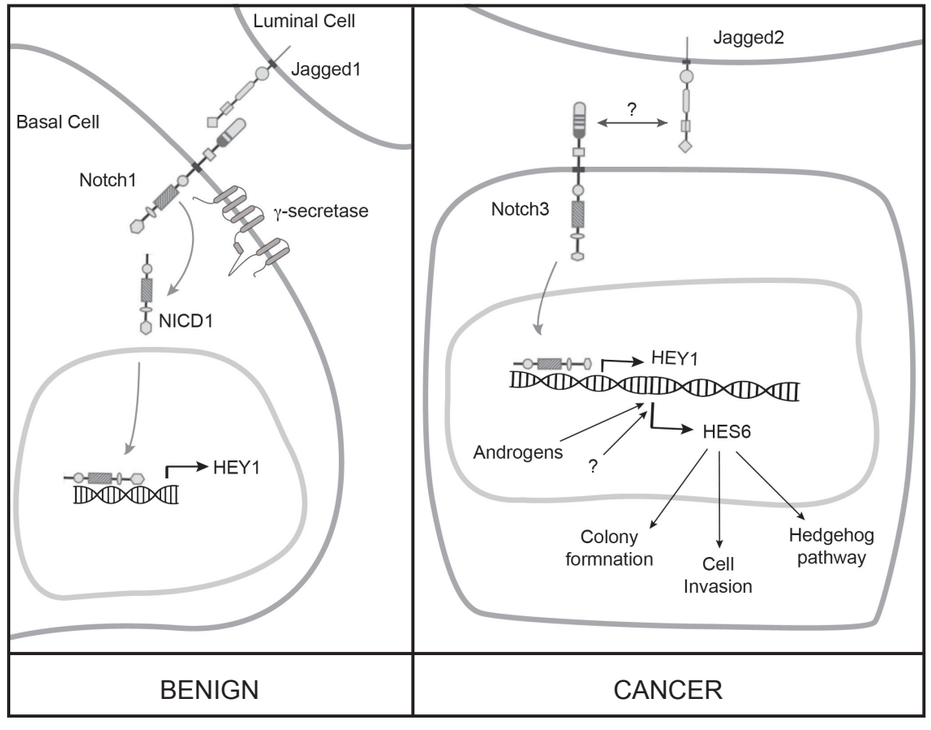

Figure 3 — Schematic representation of possible Notch signaling dynamics in prostate benign glands and cancer cells.

Notch pathway inhibitors

Gamma-Secretase inhibitors

The most widely used compounds to inhibit Notch pathway are gamma-secretase inhibitors (GSI). These drugs were initially developed in an effort to reduce amyloid–β protein aggregates in Alzheimer's disease. GSIs were subsequently found to be an attractive candidate treatment method for cancers involving active Notch signaling. Initially tested in T-ALL lines and later in prostate, breast, and lung cell lines and xenografts, GSI treatment was found to result in growth suppression (10, 24, 60, 69, 70). In early mouse studies it quickly became evident that these drugs caused toxicity in other Notch-dependent tissues, particularly the gastrointestinal tract and the thymus (71, 72). However, alternative dosing strategies have been found to limit this toxicity. For example, intermittent dosing, as well as co-administration of dexamathosone have been shown to reduce gastrointestinal toxicity in animals exposed to GSIs without compromising anti-tumor effects (73, 74).

Selective Notch inhibitors

More precisely targeted approaches have emerged to effectively shut down the Notch pathway. By focusing on individual ligands or receptors, these agents have the potential to avoid side-effects associated with pan-Notch inhibition (75). Antibodies binding the receptors Notch1 and Notch2, and the ligand Delta-like 4, have been used experimentally and shown to inhibit cancer cell proliferation with minimal intestinal toxicity (76, 77). These approaches rely on cancer cells having relatively more stringent requirements for the targeted ligand or receptor compared to intestinal enterocytes. A second approach utilized synthetic peptides that inhibit Notch1 from engaging the transcriptional machinery. Stabilized alpha-helical peptides have been produced that can specifically block NICD1 binding to RBPJ. Used in vivo in a Notch1 driven mouse leukemia model, these peptides repressed Notch1 target gene expression and leukemegenesis while avoiding gastrointestinal toxicity (78). This agent could have lower toxicity than GSIs because it does not affect signaling by other Notch receptors (Notch2, 3, or 4), or because it spares other GSI targets outside of the Notch pathway. Ultimately, it will be critical to explore whether cancer cells and enterocytes have differential requirements for signaling by each of the 4 Notch receptors. These differential requirements may form the basis for enhancing the therapeutic index of strategies to more safely and effectively target Notch signaling.

Clinical trials with Notch inhibitors

There are currently twenty-eight clinical trials registered at the NIH recruiting patients to study the effects of Notch inhibitors, mainly GSI, in cancer. Among these trials, there is one specific for prostate cancer patients: it combines the anti-androgen bicalutamide with a GSI in patients whose cancers recur after surgery (prostatectomy) or prostate radiation. There are another seven trials recruiting patients with unspecified metastatic solid tumors that can enroll patients with prostate cancer. Results from two Phase I clinical trials with escalate doses of GSI recently published reported that these drugs were well tolerated and there was potential clinical benefit in brain tumor (glioma), colorectal adenocarcinoma and melanoma patients (79, 80). No benefits, however, have been reported for prostate cancer patients. As mentioned above, the lack of consistent experimental data about the role of Notch on prostate cancer makes it difficult to predict the therapeutic effects of GSIs or to pinpoint the types of patients that will benefit most from these drugs. A better understanding of differential activities of individual Notch ligands and receptors — within the pathway and in interactions with other pathways — will reveal whether these drugs should be added to the therapeutic armamentarium of prostate cancer and how best to do so.

Conclusion

Evidence increasingly supports the notion that the Notch pathway interacts with many different signaling cascades to regulate critical cellular processes. In the prostate, there is evidence that Notch is important for the normal development of the gland and that its deregulation may be involved in tumorigenesis. It remains unclear whether the pathway stimulates or inhibits prostate cancer progression. Thus, despite the emergence of effective and non-toxic inhibitors of Notch signaling, it is not currently clear what to expect when these agents are used in prostate cancer patients. Future studies should clarify this important issue. In the meantime, the pathway appears to be upregulated in more aggressive prostate cancers compared to indolent cases. This differential expression pattern could be exploited in selecting patients who need treatment as opposed to those that can be maintained in active surveillance programs.

References

1 Artavanis-Tsakonas S, Muskavitch MA. Notch: the past, the present, and the future. Curr Top Dev Biol. 2010;92:1–29.

2 Artavanis-Tsakonas S, Rand MD, Lake RJ. Notch signaling: cell fate control and signal integration in development. Science. 1999;284:770–6.

3 Ohlstein B, Spradling A. Multipotent Drosophila intestinal stem cells specify daughter cell fates by differential notch signaling. Science. 2007;315:988–92.

4 Radtke F, Wilson A, Stark G, Bauer M, van Meerwijk J, MacDonald HR, et al. Deficient T cell fate specification in mice with an induced inactivation of Notch1. Immunity. 1999;10:547–58.

5 Falix FA, Aronson DC, Lamers WH, Gaemers IC. Possible roles of DLK1 in the Notch pathway during development and disease. Biochim Biophys Acta. 2012;1822:988–95.

6 Jhas S, Ciura S, Belanger-Jasmin S, Dong Z, Llamosas E, Theriault FM, et al. Hes6 inhibits astrocyte differentiation and promotes neurogenesis through different mechanisms. J Neurosci. 2006;26:11061–71.

7 Ellisen LW, Bird J, West DC, Soreng AL, Reynolds TC, Smith SD, et al. TAN–1, the human homolog of the Drosophila notch gene, is broken by chromosomal translocations in T lymphoblastic neoplasms. Cell. 1991;66:649–61.

8 Pear WS, Aster JC, Scott ML, Hasserjian RP, Soffer B, Sklar J, et al. Exclusive development of T cell neoplasms in mice transplanted with bone marrow expressing activated Notch alleles. J Exp Med. 1996;183:2283–91.

9 Zhu YM, Zhao WL, Fu JF, Shi JY, Pan Q, Hu J, et al. NOTCH1 mutations in T-cell acute lymphoblastic leukemia: prognostic significance and implication in multifactorial leukemogenesis. Clin Cancer Res. 2006;12:3043–9.

10 Weng AP, Ferrando AA, Lee W, Morris JPt, Silverman LB, Sanchez-Irizarry C, et al. Activating mutations of NOTCH1 in human T cell acute lymphoblastic leukemia. Science. 2004;306:269–71.

11 Beachy PA, Karhadkar SS, Berman DM. Tissue repair and stem cell renewal in carcinogenesis. Nature. 2004;432:324–31.

12 Taipale J, Beachy PA. The Hedgehog and Wnt signalling pathways in cancer. Nature. 2001;411:349–54.

13 Reya T, Morrison SJ, Clarke MF, Weissman IL. Stem cells, cancer, and cancer stem cells. Nature. 2001;414:105–11.

14 Integrated genomic analyses of ovarian carcinoma. Nature. 2011;474:609–15.

15 Park JT, Li M, Nakayama K, Mao TL, Davidson B, Zhang Z, et al. Notch3 gene amplification in ovarian cancer. Cancer Res. 2006;66:6312–8.

16 Robinson DR, Kalyana-Sundaram S, Wu YM, Shankar S, Cao X, Ateeq B, et al. Functionally recurrent rearrangements of the MAST kinase and Notch gene families in breast cancer. Nat Med. 2011;17:1646–51.

17 Liefke R, Oswald F, Alvarado C, Ferres-Marco D, Mittler G, Rodriguez P, et al. Histone demethylase KDM5A is an integral part of the core Notch-RBP-J repressor complex. Genes Dev. 2010;24:590–601.

18 Yustein JT, Liu YC, Gao P, Jie C, Le A, Vuica-Ross M, et al. Induction of ectopic Myc target gene JAG2 augments hypoxic growth and tumorigenesis in a human B-cell model. Proc Natl Acad Sci U S A. 2010;107:3534–9.

19 Gustafsson MV, Zheng X, Pereira T, Gradin K, Jin S, Lundkvist J, et al. Hypoxia requires notch signaling to maintain the undifferentiated cell state. Dev Cell. 2005;9:617–28.

20 Hu C, Dievart A, Lupien M, Calvo E, Tremblay G, Jolicoeur P. Overexpression of activated murine Notch1 and Notch3 in transgenic mice blocks mammary gland development and induces mammary tumors. Am J Pathol. 2006;168:973–90.

21 Dievart A, Beaulieu N, Jolicoeur P. Involvement of Notch1 in the development of mouse mammary tumors. Oncogene. 1999;18:5973–81.

22 Politi K, Feirt N, Kitajewski J. Notch in mammary gland development and breast cancer. Semin Cancer Biol. 2004;14:341–7.

23 Reedijk M, Odorcic S, Chang L, Zhang H, Miller N, McCready DR, et al. High-level coexpression of JAG1 and NOTCH1 is observed in human breast cancer and is associated with poor overall survival. Cancer Res. 2005;65:8530–7.

24 Rizzo P, Miao H, D'Souza G, Osipo C, Song LL, Yun J, et al. Cross-talk between notch and the estrogen receptor in breast cancer suggests novel therapeutic approaches. Cancer Res. 2008;68:5226–35.

25 Pandya K, Meeke K, Clementz AG, Rogowski A, Roberts J, Miele L, et al. Targeting both Notch and ErbB–2 signalling pathways is required for prevention of ErbB–2–positive breast tumour recurrence. Br J Cancer. 2011;105:796–806.

26 Piechocki MP, Yoo GH, Dibbley SK, Lonardo F. Breast cancer expressing the activated HER2/neu is sensitive to gefitinib in vitro and in vivo and acquires resistance through a novel point mutation in the HER2/neu. Cancer Res. 2007;67:6825–43.

27 Osipo C, Patel P, Rizzo P, Clementz AG, Hao L, Golde TE, et al. ErbB–2 inhibition activates Notch–1 and sensitizes breast cancer cells to a gamma-secretase inhibitor. Oncogene. 2008;27:5019–32.

28 Liu S, Wicha MS. Targeting breast cancer stem cells. J Clin Oncol. 2010;28:4006–12.

29 Korkaya H, Paulson A, Iovino F, Wicha MS. HER2 regulates the mammary stem/progenitor cell population driving tumorigenesis and invasion. Oncogene. 2008;27:6120–30.
30 Korkaya H, Wicha MS. HER2 and breast cancer stem cells: more than meets the eye. Cancer Res. 2013;73:3489–93.
31 Harrison H, Farnie G, Brennan KR, Clarke RB. Breast cancer stem cells: something out of notching? Cancer Res. 2010;70:8973–6.
32 Pannuti A, Foreman K, Rizzo P, Osipo C, Golde T, Osborne B, et al. Targeting Notch to target cancer stem cells. Clin Cancer Res. 2010;16:3141–52.
33 Kellokumpu-Lehtinen P, Santti R, Pelliniemi LJ. Correlation of early cytodifferentiation of the human fetal prostate and Leydig cells. Anat Rec. 1980;196:263–73.
34 Timms BG, Mohs TJ, Didio LJ. Ductal budding and branching patterns in the developing prostate. J Urol. 1994;151:1427–32.
35 Cunha GR. The role of androgens in the epithelio-mesenchymal interactions involved in prostatic morphogenesis in embryonic mice. Anat Rec. 1973;175:87–96.
36 Wang Y, Hayward S, Cao M, Thayer K, Cunha G. Cell differentiation lineage in the prostate. Differentiation. 2001;68:270–9.
37 Leong KG, Wang BE, Johnson L, Gao WQ. Generation of a prostate from a single adult stem cell. Nature. 2008;456:804–8.
38 Wang X, Kruithof-de Julio M, Economides KD, Walker D, Yu H, Halili MV, et al. A luminal epithelial stem cell that is a cell of origin for prostate cancer. Nature. 2009;461:495–500.
39 Choi N, Zhang B, Zhang L, Ittmann M, Xin L. Adult murine prostate basal and luminal cells are self-sustained lineages that can both serve as targets for prostate cancer initiation. Cancer Cell. 2012;21:253–65.
40 Ousset M, Van Keymeulen A, Bouvencourt G, Sharma N, Achouri Y, Simons BD, et al. Multipotent and unipotent progenitors contribute to prostate postnatal development. Nat Cell Biol. 2012;14:1131–8.
41 Shou J, Ross S, Koeppen H, de Sauvage FJ, Gao WQ. Dynamics of notch expression during murine prostate development and tumorigenesis. Cancer Res. 2001;61:7291–7.
42 Valdez JM, Zhang L, Su Q, Dakhova O, Zhang Y, Shahi P, et al. Notch and TGFbeta form a reciprocal positive regulatory loop that suppresses murine prostate basal stem/progenitor cell activity. Cell Stem Cell. 2012;11:676–88.
43 Wang XD, Shou J, Wong P, French DM, Gao WQ. Notch1-expressing cells are indispensable for prostatic branching morphogenesis during development and re-growth following castration and androgen replacement. J Biol Chem. 2004;279:24733–44.
44 Wang XD, Leow CC, Zha J, Tang Z, Modrusan Z, Radtke F, et al. Notch signaling is required for normal prostatic epithelial cell proliferation and differentiation. Dev Biol. 2006;290:66–80.
45 Ceder JA, Jansson L, Helczynski L, Abrahamsson PA. Delta-like 1 (Dlk-1), a novel marker of prostate basal and candidate epithelial stem cells, is downregulated by notch signalling in intermediate/transit amplifying cells of the human prostate. Eur Urol. 2008;54:1344–53.
46 Shen MM, Abate-Shen C. Molecular genetics of prostate cancer: new prospects for old challenges. Genes Dev. 2010;24:1967–2000.
47 Sarker D, Reid AH, Yap TA, de Bono JS. Targeting the PI3K/AKT pathway for the treatment of prostate cancer. Clin Cancer Res. 2009;15:4799–805.
48 Batch JA, Williams DM, Davies HR, Brown BD, Evans BA, Hughes IA, et al. Androgen receptor gene mutations identified by SSCP in fourteen subjects with androgen insensitivity syndrome. Hum Mol Genet. 1992;1:497–503.
49 Han G, Foster BA, Mistry S, Buchanan G, Harris JM, Tilley WD, et al. Hormone status selects for spontaneous somatic androgen receptor variants that demonstrate specific ligand and cofactor dependent activities in autochthonous prostate cancer. J Biol Chem. 2001;276:11204–13.
50 Belandia B, Powell SM, Garcia-Pedrero JM, Walker MM, Bevan CL, Parker MG. Hey1, a mediator of notch signaling, is an androgen receptor corepressor. Mol Cell Biol. 2005;25:1425–36.
51 Ghosh S, Lau H, Simons BW, Powell JD, Meyers DJ, De Marzo AM, et al. PI3K/mTOR signaling regulates prostatic branching morphogenesis. Dev Biol. 2011;360:329–42.
52 Stiles B, Groszer M, Wang S, Jiao J, Wu H. PTENless means more. Dev Biol. 2004;273:175–84.
53 Davies MA, Koul D, Dhesi H, Berman R, McDonnell TJ, McConkey D, et al. Regulation of Akt/PKB activity, cellular growth, and apoptosis in prostate carcinoma cells by MMAC/PTEN. Cancer Res. 1999;59:2551–6.
54 Wang S, Gao J, Lei Q, Rozengurt N, Pritchard C, Jiao J, et al. Prostate-specific deletion of the murine Pten tumor suppressor gene leads to metastatic prostate cancer. Cancer Cell. 2003;4:209–21.
55 McMenamin ME, Soung P, Perera S, Kaplan I, Loda M, Sellers WR. Loss of PTEN expression in paraffin-embedded primary prostate cancer correlates with high Gleason score and advanced stage. Cancer Res. 1999;59:4291–6.

56 Whelan JT, Kellogg A, Shewchuk BM, Hewan-Lowe K, Bertrand FE. Notch–1 signaling is lost in prostate adenocarcinoma and promotes PTEN gene expression. J Cell Biochem. 2009;107:992–1001.
57 Carver BS, Chapinski C, Wongvipat J, Hieronymus H, Chen Y, Chandarlapaty S, et al. Reciprocal feedback regulation of PI3K and androgen receptor signaling in PTEN-deficient prostate cancer. Cancer Cell. 2011;19:575–86.
58 Lotan TL, Gurel B, Sutcliffe S, Esopi D, Liu W, Xu J, et al. PTEN protein loss by immunostaining: analytic validation and prognostic indicator for a high risk surgical cohort of prostate cancer patients. Clin Cancer Res. 2011;17:6563–73.
59 Bin Hafeez B, Adhami VM, Asim M, Siddiqui IA, Bhat KM, Zhong W, et al. Targeted knockdown of Notch1 inhibits invasion of human prostate cancer cells concomitant with inhibition of matrix metalloproteinase–9 and urokinase plasminogen activator. Clin Cancer Res. 2009;15:452–9.
60 Zhang Y, Wang Z, Ahmed F, Banerjee S, Li Y, Sarkar FH. Down-regulation of Jagged–1 induces cell growth inhibition and S phase arrest in prostate cancer cells. Int J Cancer. 2006;119:2071–7.
61 Hager B, Bickenbach JR, Fleckman P. Long-term culture of murine epidermal keratinocytes. J Invest Dermatol. 1999;112:971–6.
62 Dalrymple S, Antony L, Xu Y, Uzgare AR, Arnold JT, Savaugeot J, et al. Role of notch–1 and E-cadherin in the differential response to calcium in culturing normal versus malignant prostate cells. Cancer Res. 2005;65:9269–79.
63 Santagata S, Demichelis F, Riva A, Varambally S, Hofer MD, Kutok JL, et al. JAGGED1 expression is associated with prostate cancer metastasis and recurrence. Cancer Res. 2004;64:6854–7.
64 Han M, Partin AW, Pound CR, Epstein JI, Walsh PC. Long-term biochemical disease-free and cancer-specific survival following anatomic radical retropubic prostatectomy. The 15–year Johns Hopkins experience. Urol Clin North Am. 2001;28:555–65.
65 Stephenson AJ, Kattan MW, Eastham JA, Bianco FJ, Jr., Yossepowitch O, Vickers AJ, et al. Prostate cancer-specific mortality after radical prostatectomy for patients treated in the prostate-specific antigen era. J Clin Oncol. 2009;27:4300–5.
66 Davies JD, Aghazadeh MA, Phillips S, Salem S, Chang SS, Clark PE, et al. Prostate size as a predictor of Gleason score upgrading in patients with low risk prostate cancer. J Urol. 2011;186:2221–7.
67 Kvale R, Moller B, Wahlqvist R, Fossa SD, Berner A, Busch C, et al. Concordance between Gleason scores of needle biopsies and radical prostatectomy specimens: a population-based study. BJU Int. 2009;103:1647–54.

68 Ross AE, Marchionni L, Vuica-Ross M, Cheadle C, Fan J, Berman DM, et al. Gene expression pathways of high grade localized prostate cancer. Prostate. 2011.
69 Rasul S, Balasubramanian R, Filipovic A, Slade MJ, Yague E, Coombes RC. Inhibition of gamma-secretase induces G2/M arrest and triggers apoptosis in breast cancer cells. Br J Cancer. 2009;100:1879–88.
70 Konishi J, Kawaguchi KS, Vo H, Haruki N, Gonzalez A, Carbone DP, et al. Gamma-secretase inhibitor prevents Notch3 activation and reduces proliferation in human lung cancers. Cancer Res. 2007;67:8051–7.
71 van Es JH, van Gijn ME, Riccio O, van den Born M, Vooijs M, Begthel H, et al. Notch/gamma-secretase inhibition turns proliferative cells in intestinal crypts and adenomas into goblet cells. Nature. 2005;435:959–63.
72 Wong GT, Manfra D, Poulet FM, Zhang Q, Josien H, Bara T, et al. Chronic treatment with the gamma-secretase inhibitor LY–411,575 inhibits beta-amyloid peptide production and alters lymphopoiesis and intestinal cell differentiation. J Biol Chem. 2004;279:12876–82.
73 Real PJ, Tosello V, Palomero T, Castillo M, Hernando E, de Stanchina E, et al. Gamma-secretase inhibitors reverse glucocorticoid resistance in T cell acute lymphoblastic leukemia. Nat Med. 2009;15:50–8.
74 Wei P, Walls M, Qiu M, Ding R, Denlinger RH, Wong A, et al. Evaluation of selective gamma-secretase inhibitor PF–03084014 for its antitumor efficacy and gastrointestinal safety to guide optimal clinical trial design. Mol Cancer Ther. 2010;9:1618–28.
75 Wu Y, Cain-Hom C, Choy L, Hagenbeek TJ, de Leon GP, Chen Y, et al. Therapeutic antibody targeting of individual Notch receptors. Nature. 2010;464:1052–7.
76 Noguera-Troise I, Daly C, Papadopoulos NJ, Coetzee S, Boland P, Gale NW, et al. Blockade of Dll4 inhibits tumour growth by promoting non-productive angiogenesis. Nature. 2006;444:1032–7.
77 Ridgway J, Zhang G, Wu Y, Stawicki S, Liang WC, Chanthery Y, et al. Inhibition of Dll4 signalling inhibits tumour growth by deregulating angiogenesis. Nature. 2006;444:1083–7.
78 Moellering RE, Cornejo M, Davis TN, Del Bianco C, Aster JC, Blacklow SC, et al. Direct inhibition of the NOTCH transcription factor complex. Nature. 2009;462:182–8.
79 Tolcher AW, Messersmith WA, Mikulski SM, Papadopoulos KP, Kwak EL, Gibbon DG, et al. Phase I study of RO4929097, a gamma secretase inhibitor of Notch signaling, in patients with refractory metastatic or locally advanced solid tumors. J Clin Oncol. 2012;30:2348–53.

80 Krop I, Demuth T, Guthrie T, Wen PY, Mason WP, Chinnaiyan P, et al. Phase I pharmacologic and pharmacodynamic study of the gamma secretase (Notch) inhibitor MK–0752 in adult patients with advanced solid tumors. J Clin Oncol. 2012;30:2307–13.
81 Hartmann D, de Strooper B, Serneels L, Craessaerts K, Herreman A, Annaert W, et al. The disintegrin/metalloprotease ADAM 10 is essential for Notch signalling but not for alpha-secretase activity in fibroblasts. Hum Mol Genet. 2002;11:2615–24.
82 De Strooper B, Annaert W, Cupers P, Saftig P, Craessaerts K, Mumm JS, et al. A presenilin–1–dependent gamma-secretase-like protease mediates release of Notch intracellular domain. Nature. 1999;398:518–22.
83 Fryer CJ, White JB, Jones KA. Mastermind recruits CycC:CDK8 to phosphorylate the Notch ICD and coordinate activation with turnover. Mol Cell. 2004;16:509–20.
84 Sethi N, Dai X, Winter CG, Kang Y. Tumor-derived JAGGED1 promotes osteolytic bone metastasis of breast cancer by engaging notch signaling in bone cells. Cancer Cell. 2011;19:192–205.
85 Xing F, Okuda H, Watabe M, Kobayashi A, Pai SK, Liu W, et al. Hypoxia-induced Jagged2 promotes breast cancer metastasis and self-renewal of cancer stem-like cells. Oncogene. 2011;30:4075–86.
86 Gallahan D, Callahan R. Mammary tumorigenesis in feral mice: identification of a new int locus in mouse mammary tumor virus (Czech II)-induced mammary tumors. J Virol. 1987;61:66–74.
87 Jhappan C, Stahle C, Wolff M, Merlino G, Pastan I. An epidermal growth factor receptor promoter construct selectively expresses in the thymus and spleen of transgenic mice. Cell Immunol. 1993;149:99–106.
88 Raafat A, Bargo S, Anver MR, Callahan R. Mammary development and tumorigenesis in mice expressing a truncated human Notch4/Int3 intracellular domain (h-Int3sh). Oncogene. 2004;23:9401–7.
89 Choi JH, Park JT, Davidson B, Morin PJ, Shih Ie M, Wang TL. Jagged–1 and Notch3 juxtacrine loop regulates ovarian tumor growth and adhesion. Cancer Res. 2008;68:5716–23.
90 Dang TP, Gazdar AF, Virmani AK, Sepetavec T, Hande KR, Minna JD, et al. Chromosome 19 translocation, overexpression of Notch3, and human lung cancer. J Natl Cancer Inst. 2000;92:1355–7.
91 Eliasz S, Liang S, Chen Y, De Marco MA, Machek O, Skucha S, et al. Notch–1 stimulates survival of lung adenocarcinoma cells during hypoxia by activating the IGF–1R pathway. Oncogene. 2010;29:2488–98.
92 Sjolund J, Johansson M, Manna S, Norin C, Pietras A, Beckman S, et al. Suppression of renal cell carcinoma growth by inhibition of Notch signaling in vitro and in vivo. J Clin Invest. 2008;118:217–28.
93 Agrawal N, Frederick MJ, Pickering CR, Bettegowda C, Chang K, Li RJ, et al. Exome sequencing of head and neck squamous cell carcinoma reveals inactivating mutations in NOTCH1. Science. 2011;333:1154–7.
94 Demehri S, Turkoz A, Kopan R. Epidermal Notch1 loss promotes skin tumorigenesis by impacting the stromal microenvironment. Cancer Cell. 2009;16:55–66.

CHAPTER 2 —
RATIONAL AND AIMS

RATIONAL AND AIMS

A major drawback of prostate-specific antigen (PSA) screening is the diagnosis and overtreatment of indolent prostate cancer. Therefore it is necessary to find new biomarkers and pathways that better distinguish indolent from lethal prostate cancer. Microarray gene expression studies showed that in high grade localized prostate cancer one of the most overexpressed signaling cascades is the Notch pathway. Among all the members of Notch pathway, Hairy enhancer of Split 6 (HES6) was the most upregulated in tumors with lethal potential (high-grade tumors). Thus, one of the aims of this research project was to understand the molecular mechanisms and interactions of HES6 in prostate cancer that may contribute to its aggressiveness and progression.

Due to my medical background and a career goal to establish as an independent physician-scientist in urology, I was excited by the idea of working on new predictive and prognostic markers. As mentioned before, PSA screening of prostate cancer results in overdiagnosis of indolent tumors and consequently overtreatment with important adverse effects, such as incontinence or erectile dysfunction. So an option to manage tumors with low grade features, called Active Surveillance, is to perform intermittent digital rectal exams and prostate biopsies with the intent to avoid treatment until the cancer progresses. While I evaluate the contribution of Notch signaling for tumor progression, we also evaluated the potential of established assays as biomarkers guiding active surveillance. One particularly promising assay is the expression of the tumor suppressor Phosphatase and tensin homolog (PTEN) protein in prostate biopsies. The question we addressed was whether the loss of PTEN can distinguish the tumors that will upgrade and need treatment from those who can be managed on active surveillance.

When prostate cancer cells metastasize to bone, 3⁄4 of the patients die within a period of 5 years. Due to the lack of good tissue resources during the progression of prostate cancer, the molecular events that contribute to metastasis development and treatment failure are largely unknown. To address this problem and as a platform on which to study Notch and other potential mediators of the lethal phenotype, we developed experimental systems that without relying in cell surface markers, isolated viable circulating tumor cells (CTCs). To test CTCs tumor-forming ability, we xenografted CTCs, from the Transgenic Adenocarcinoma of the Mouse Prostate (TRAMP) mice and from patients with late-stage prostate cancer, into immunodeficient mice. This approach allowed us to determine that viable CTCs contain tumor-initiating cells.

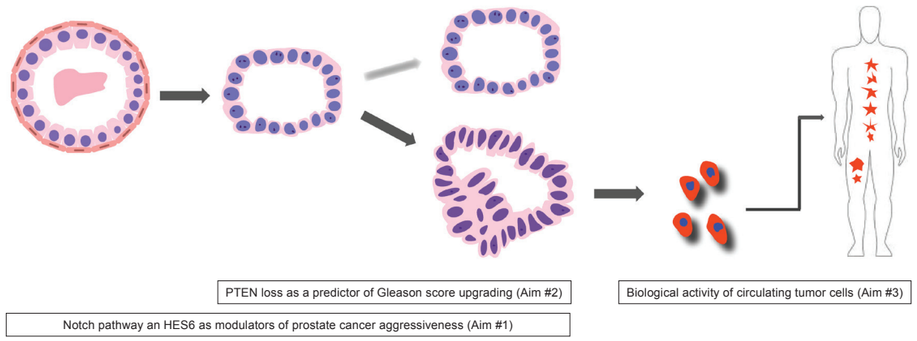

Figure 1 — Schematic representation of prostate cancer progression. The aims of this thesis address different stages of prostate cancer. The length of the black boxes indicates the period focused by each aim during cancer progression.

Therefore, the major goal of this doctoral project was to understand the molecular and cellular characteristics of prostate cancer cells with lethal potential and provide reliable markers to ameliorate clinical decisions.
Specifically, the aims of this project were:

1 Notch signaling pathway as modulation of prostate cancer aggressiveness

- Characterize the expression of all canonical Notch pathway components in benign and cancer prostate cells.
- Determine the responsiveness of Notch receptor and main targets to androgen stimulation.
- Evaluate the response of prostate cell lines to Notch pathway blockade with a gamma-secretase inhibitor.
- Identify the molecular pathways controlled by HES6 in prostate cells.
- Using in vitro cellular assays, analyze HES6 contributions for cancer progression.

2 PTEN as a molecular marker to predict upgrading of prostate cancer from biopsy to radical prostatectomy

- Determine whether loss of PTEN protein expression can improve the selection criteria of prostate cancer patients to active surveillance.

3 Proving and harnessing the biological activity of circulating prostate cancer cells

- Without relying on cell size or the expression of differentiation markers, isolate viable prostate CTCs from mice and humans.
- Generate xenografts using circulating tumor cells in immunodeficient mice to assay their ability to initiate new tumors.

CHAPTER 3 —
METHODS

METHODS

This section describes the methods that successfully generated data presented in the following chapters. I divided the methods according to the chapters where they were used to smoother the reader's pilgrimage throughout this section.

Chapter 4
Materials and Methods

Plasmids, virus and construct generation HES6 (clone LIFESEQ7399489, Open Biosystems) was subcloned into the lentiviral vector pNL-EGFP/CMV-WPREdU3 to establish overexpressing stable cell lines. shRNAs targeting HES6 mRNAs were obtained from the Expression Arrest-TRC shRNA Libraries (TRCN0000017828). Notch3 intracellular domain construct (gift from Dr Nicolas Gaiano) was subcloned into pcDNA 3.1(-) (Invitrogen). The vectors used in dual-luciferase reporter assay experiments were CBFRE-luc (Addgene #26897) and pGL2 (Promega).

Cell lines and cell culture Human cancer cell lines were obtained from the American Type Culture Collection and maintained in RPMI 1640 (Gibco) supplemented with 10% fetal bovine serum (FBS) and Penicillin-Streptomycin (Invitrogen), except VCaP and LnCaP96. VCaP were provided by Dr William B. Isaacs (Brady Urological Institute, The Johns Hopkins University School of Medicine) and maintained in DMEM/10% FBS (Gibco) and LnCaP96 cells were a gift from Dr Alan K. Meeker (Brady Urological Institute, The Johns Hopkins University School of Medicine) generated by long-term culture of LnCaP in charcoal-stripped FBS. Prostate epithelial cells RWPE–1 and PrEC were cultured according to vendor's instructions. All cell line identities were confirmed by forensic identity analyses within 6 months of use. For the androgen withdrawn experiments, LnCaP cells were washed with charcoal-stripped FBS three times for 1h and incubated in 10% charcoal-stripped FBS containing medium for 48h before stimulation with 10nM of dihydrotestosterone (DHT).

Real-time PCR analysis Total RNA was isolated with RNeasy Mini kit (Qiagen) and cDNA was synthesized with 1 mg of total RNA using High-Capacity cDNA Reverse Transcription kit (Applied Biosystems). cDNA was amplified on a StepOne Plus (Applied Biosystems) using TaqMan gene-specific oligonucleotide primers or custom designed primers (Supplementary Table S1). To determine the genes differentially

expressed in cancer and benign cell lines, we designed Taqman gene plates comprising all Notch pathway members described in mammals and five housekeeping genes. Results are presented as a heatmap using Euclidean distance and ward linkage for clustering using median centered delta CT values for each gene.

Immunoblotting Protein lysates in NuPAGE buffer (Invitrogen) were separated by gradient 4–12% BisTris Gel and transferred to polyvinylidene difluoride membrane. Primary antibodies used were rabbit monoclonal anti-Notch1 (D1E11; 1:1000; Cell Signaling), rabbit polyclonal anti-cleaved Notch1 (Val1744; 1:1000; Cell Signaling), rabbit monoclonal anti-Notch2 (8A1; 1:1000; Cell Signaling), rabbit polyclonal anti-Notch3 (Pro2311; 1:1000; Cell Signaling), rabbit polyclonal anti-HES1 (ab71559; 1:1000; Abcam), rabbit polyclonal anti-HEY1 (ab22614; 1:500; Abcam), rabbit polyclonal anti-HES6 (ab66461; 1:1000; Abcam), mouse monoclonal anti-glyceraldehyde–3–phosphate dehydrogenase (GAPDH) (clone 6C5; 1:1000; Santa Cruz Biotechnology). The membrane was incubated sequentially with primary antibodies (overnight at 4oC), horseradish peroxidase (HRP)-conjugated anti-rabbit or anti-mouse and chemiluminescent substrate (Thermo Fisher) before exposure to film.

Luciferase reporter assay Cells were plated in 24–well plates and 24 hours later transfected using Lipofectamine2000 (Invitrogen) with pGL2 (control) or with CBFRE-luc to determine endogenous Notch pathway activity in prostate cells. After 48 hours, luciferase activity was determined using Dual-Luciferase Reporter Assay system (Promega) and normalized to PrEC basal luminescence. All experiments were performed in triplicate.

siRNA transient knockdown Notch3 siRNA (Supplementary Table 2) transient transfections (final concentration of 10 nmol/L) were carried out by using Lipofectamine 2000 (Invitrogen), following the manufacturer's instructions. Nontargeting siRNA was used as a control. Cells were lysated for western blot 24 hours after siRNA transfection.

DAPT treatment and IC50 assay 24 hours after seeding the cells, gamma secretase inhibitor N-[N–(3,5–Difluorophenacetyl)-L-alanyl]-S-phenylglycine t-butyl ester (DAPT) was added to 200 ml of growth media per well in final concentrations ranging from 1 nmol/L to 400 mmol/L. Viability was assayed (see below) after 96 hours. The half maximum inhibitory concentration (IC50) of DAPT was calculated using GraphPad Prism software.

Cell viability and proliferation assays 22Rv1 and LnCaP with stable shRNA HES6 knockdown or PC3 stably overexpressing HES6 were seeded (500 cells per well) in 96–well black flat-bottom tissue culture plates. Cell viability and growth was determined using Alamar Blue vital dye (Invitrogen) according to the manufacturer's instructions. Values were reported as mean standard error of optical density of triplicate wells fro each concentration and time point.

Immunohistochemistry and Immunofluorescence IHC and IF staining were performed as described previously (1, 2) using anti-Hes6 antibody (ab66461; 1:1000; Abcam). Mann-Whitney test used for statistical analysis of HES6 staining intensity was measured automatic quantitative analysis.

Androgen-deprived tissue in tissue microarray (TMA) We used a previously described TMA comprising formalin-fixed paraffin-embedded prostate cancer tissue from (n=55) patients treated with androgen-deprivation therapy prior to prostatectomy and from (n=12) untreated controls (3).

Invasion assays 22Rv1 or LnCaP cells infected with control or shHES6 lentiviruses (see plasmids and viruses above) were seeded at 7.5 x 10^4 cells/well or 5 x 10^4 PC3 cells infected with control or HES6 overexpression lentiviruses. The assay was performed in triplicate and in two independent experiments as previously described (4). Student t test was used to evaluate significant differences and a statistical significance was considered at $p < 0.05$.

Colony-forming efficiency assay Colony-forming efficiency assays were conducted as described earlier (5). All visible were counted and results presented as total number colonies stander error in two individual experiments.

Gene expression arrays and data analysis Differential gene expression analysis was performed as previously described (6–8), using statistical packages from the R/Bioconductor project (9, 10). Briefly, gene expression was measured on the Illumina HT–12 v4 whole genome gene expression microarray. For each individual microarray feature a generalized linear model was fit to estimate expression differences between groups. Moderated t-statistics were obtained by empirical Bayesian shrinkage of log2 fold-change standard errors (11), and adjustment for multiple testing was obtained using the Benjamini and Hochberg method (12). Gene annotation for the microarray used in this study was obtained from the corresponding R-Bioconductor metadata packages.

Patients and tissue samples

After obtaining institutional review board approval, the Johns Hopkins Hospital (JHH) Pathology database was queried for all needle biopsies performed at JHH or Johns Hopkins Bayview Medical Center (BMC) that contained only Gleason Score 3+3=6 (GS 6) tumor followed by a radical prostatectomy (RP) specimen that contained GS > 6 tumor occurring between 2000–2011. Controls with GS 6 tumor on biopsy followed by only GS 6 tumor on RP were selected from sequential biopsies occurring between 2000–2004 at JHH and 2000–2011 at BMC. Patients who underwent any neoadjuvant therapies (hormonal therapy, radiation therapy) were excluded. As is routine at JHH and BMC, all RP specimens were entirely submitted and processed for histologic analysis. All biopsies and RP slides were re-reviewed and re-graded by trained uropathologists using the 2005 modified International Society of Urologic Pathology (ISUP) grading system. Each case was assigned a primary, secondary and tertiary (for RP specimens) Gleason pattern. Cases where the slides were not available for re-review and cases with biopsy GS > 6 on re-review were excluded from the analysis. A single block (generally consisting of two needle biopsy cores) containing the largest percentage involvement by tumor was selected for PTEN immunostaining (described below). In order to assure that there was enough tumor available for reliable evaluation, cases with less than 5% tumor involvement on any single needle core were excluded.

Clinico-pathologic parameters

Clinical parameters were extracted from the Johns Hopkins Brady Urological Institute database and included age, race where available (white vs. non-white), pre-operative serum prostate-specific antigen (PSA) measured closest to time of biopsy, and clinical stage. PSA density was calculated by dividing the pre-operative PSA by the prostate gland weight at radical prostatectomy. PSA recurrence was defined as a serum PSA level >0.2 ng/mL following RP. Pathologic parameters were extracted for each case from the Johns Hopkins Department of Pathology database and included the total number of needle cores sampled, the absolute number of cores involved by tumor, the percent tumor present on the maximally involved core, the presence of tumor on bilateral cores (right and left) and the presence of perineural invasion. The fraction of cores involved by tumor was calculated by dividing the number of involved cores by the total number of cores sampled in each case.

PTEN Immunohistochemistry

4 µm biopsy sections were deparaffinized and re-hydrated under standard conditions. Antigen unmasking was performed by steaming in EDTA buffer (pH 8.0) for 45 minutes. Endogenous peroxidase activity was quenched by incubation with peroxidase block for 5 minutes at RT. Slides were incubated for 45 minutes at room temperature with a rabbit anti-human PTEN antibody (Clone D4.3 XP; Cell Signaling, Danvers, MA; 1:50 dilution). A horseradish peroxidase-labeled polymer (PowerVision, Leica Microsystems, Bannockburn IL) was applied for 30 minutes at RT and signal detection was performed using 3,3'–diaminobenzidine tetrahydrochloride (DAB) as the chromagen. Slides were counterstained with hematoxylin, dehydrated, and mounted.

IHC interpretation

PTEN IHC on each case was independently scored by two uropathologists using a previously validated dichotomous scoring system. Cases were considered to have PTEN protein loss if the intensity of cytoplasmic staining was markedly decreased or entirely negative across >10% of tumor cells compared to surrounding benign glands and/or stroma. In cases where the two scoring uropathologists disagreed about the PTEN IHC scoring (17/174 or 10% of total), a third uropathologist blindly scored the case to break the tie.

PTEN FISH

A four-color FISH method was designed based on methods used previously. As described, FISH analysis was performed on needle cores using adjacent sections stained with DAPI (40,6–diamidino – 2–phenylindole, dihydrochloride) in selected areas of tumor with PTEN loss by immunohistochemistry. H&E needle cores sections were scanned digitally and available for side-by-side comparison with the FISH images to confirm delineated marked regions of interest. PTEN copy number was evaluated by counting spots for each probe in 50 non-overlapping, intact, interphase nuclei per case. In cases where the PTEN status was inconclusive, 100 cells were evaluated. Variation of nuclear size in tumor cells required the use of non-PTEN-deleted prostate cancer cores as controls to define the threshold for classifying the PTEN copy number. Overall, the mean + 3 standard deviations was used as the cutoff value for assigning hemizygous deletion status in each case. This approach was particularly useful for cores exhibiting more cellular heterogeneity where cells differed in shape, size or density. Homozygous deletion status for PTEN was defined by more conservative criteria, a simultaneous lack of both

PTEN locus signals in 30% of scored nuclei. Background information on the assay, cell selection criteria and on determining cut-off thresholds is also available on the website (www.ptendeletion.net).

Statistical analysis

Means and proportions of characteristics of cases and controls were compared using the two-sample t-test and the chi-square test, respectively. Multivariable logistic regression was used to estimate the odds ratios (ORs) and 95% confidence intervals (CI) of a biopsy upgrade among men with markedly decreased PTEN. First, ORs were estimated adjusted for age at diagnosis. Next, results were adjusted for preoperative PSA (continuous, log-transformed) and clinical stage (binary, T2 or higher). Results were further adjusted for race (binary, nonwhite). Statistical analyses were performed using SAS 9.3 (Cary, NC).

Chapter 6

Patient selection for CTCs collection

Patients treated at the Johns Hopkins Sidney Kimmel Comprehensive Cancer Center (Baltimore, MD) with castration-resistant PCa and radiologic evidence of distant osseous or soft tissue metastatic disease were recruited according to an institutional review board (IRB)-approved protocol. All patients signed a written informed consent. A total of 14 patients (Table 1, CHAPTER 6) donated 7 mL of blood on one or more occasions for CTCs immunocytochemistry or xenograft. Blood from healthy individuals without evidence of PCa was spiked with DU145 cells.

Cell Culture

Human DU145 and LnCaP prostate cancer cells were obtained from the American Type Culture Collection, maintained in RPMI 1640 media (Gibco) supplemented with 10% fetal bovine serum (Gibco) and Penicillin-Streptomycin (Invitrogen).

Cell isolation

Blood drawn into a heparinized tube followed two different approaches (Fig. 1 and 4, CHAPTER 6) to remove red blood cells and collect nucleated cells: red cell lysis or density gradient centrifugation. After red cell removal, nucleated cells present in blood were collected, incubated with anti-leukocyte antibody CD45 magnetic microbeads (Miltenyi Biotec), placed into magnetic depletion columns (Miltenyi Biotec) to deplete white blood cells and all tumor cells that flow through the columns were collected for further studies. As a “proof-of-principle” for isolation of viable circulating cells, human DU145 prostate cancer (1×10^6) cells were spiked in blood from healthy individuals and placed back in culture for 48 hours to monitor if the cells were viable and able to expand in culture. CTCs from PCa patients were either spread across microscopic slides for immunofluorescent analysis or xenografted in mice.

Generation of CTC xenografts and determination of engraftment with PSA

CTCs from both TRAMP mice and human prostate cancer patients were inserted into anesthetized male highly immunodeficient *NOD.Cg-Prkdcscid Il2rgtm-1Wjl/SzJ* mice (Figure 1 and 4, CHAPTER 6), also known as NOD SCID gamma (NSG) mice (13). NSG mice lack functional T cells, B cells, and NK cells and have markedly reduced dendritic cell and macrophage activity. This high degree of immunodeficiency results in superior engraftment of human cells (14).

Approximately 700 mL of blood from TRAMP mice (n=9) went through the red cell lysis step and nucleated cells were afterwards injected into the tail vein of NSG mice. To confirm the existence of CTCs in TRAMPs blood, we spread TRAMP nucleated cells in a microscope slide and performed Wright's stain.

CTCs isolated from PCa patient blood were injected into the tail vein of NSG mice (n=4) or wrapped in mouse newborn seminal vesicle mesenchyme (SVM) and inserted under the renal capsule (n=7) as described previously (15). Briefly, this technique consists in the isolation of SVM from newborn (day 0) C57BL/6 mice (15), 1×10^5 SVM cells were combined with CTCs isolated from patients in a matrigel (BD Biosciences) disk. The disk, containing CTCs and the SVM were combined and cultured 12 hours in RPMI supplemented with 1 mM of dihydrotestosterone, and then introduced under the renal capsule. To confirm the capacity of SVM to support prostate epithelial growth, benign primary mouse prostate epithelial cells (1×10^6) were combined with SVM and also grafted under the kidney capsule. PSA-producing cancer cells LnCaP (1×10^6) cells were also used as controls, to confirm that the grafting conditions supported human prostate cancer growth and to confirm the performance of ultrasensitive PSA tests (see below) on mouse serum. Since mice do not make PSA, human CTC engraftment was monitored monthly by ultrasensitive nano-PSA assays (Nanosphere Inc, Chicago, IL) performed on serum prepared from 50 mL of mouse blood (16). NSG mice injected with TRAMP CTCs were euthanized 3 months after grafting, and the NSGs grafted with human circulating cells were euthanized 8 months after grafting. An expert veterinary pathologist performed comprehensive necropsies as well as histologic examination of the liver, lungs, spleen and the grafts from all animals.

Immunohistochemistry and immunofluorescence

Formalin-fixed, paraffin-embedded tissue samples from the liver, lungs, spleen and CTC xenografts were sectioned (4 mm) and immunohistochemistry was performed as described using anti-SV40 T-Ag (clone Pab101 Santa Cruz, 1:1000) or anti-androgen receptor (clone N–20 Santa Cruz, 1:500) antibodies for immunodetection.

Immunofluorescent staining for cytokeratin 8 (1:500; clone M20 Abcam) and EpCAM (1:500; clone VU–1D9 Abcam) was performed to confirm the collection of CTCs from castration-resistant PCa patients. Cells obtained after CD45 depletion were spread onto a microscope slide, stained as previously described and analyzed under a 100x oil immersion objective using a Nikon E400 fluorescence microscope (Nikon).

PART II — RESULTS

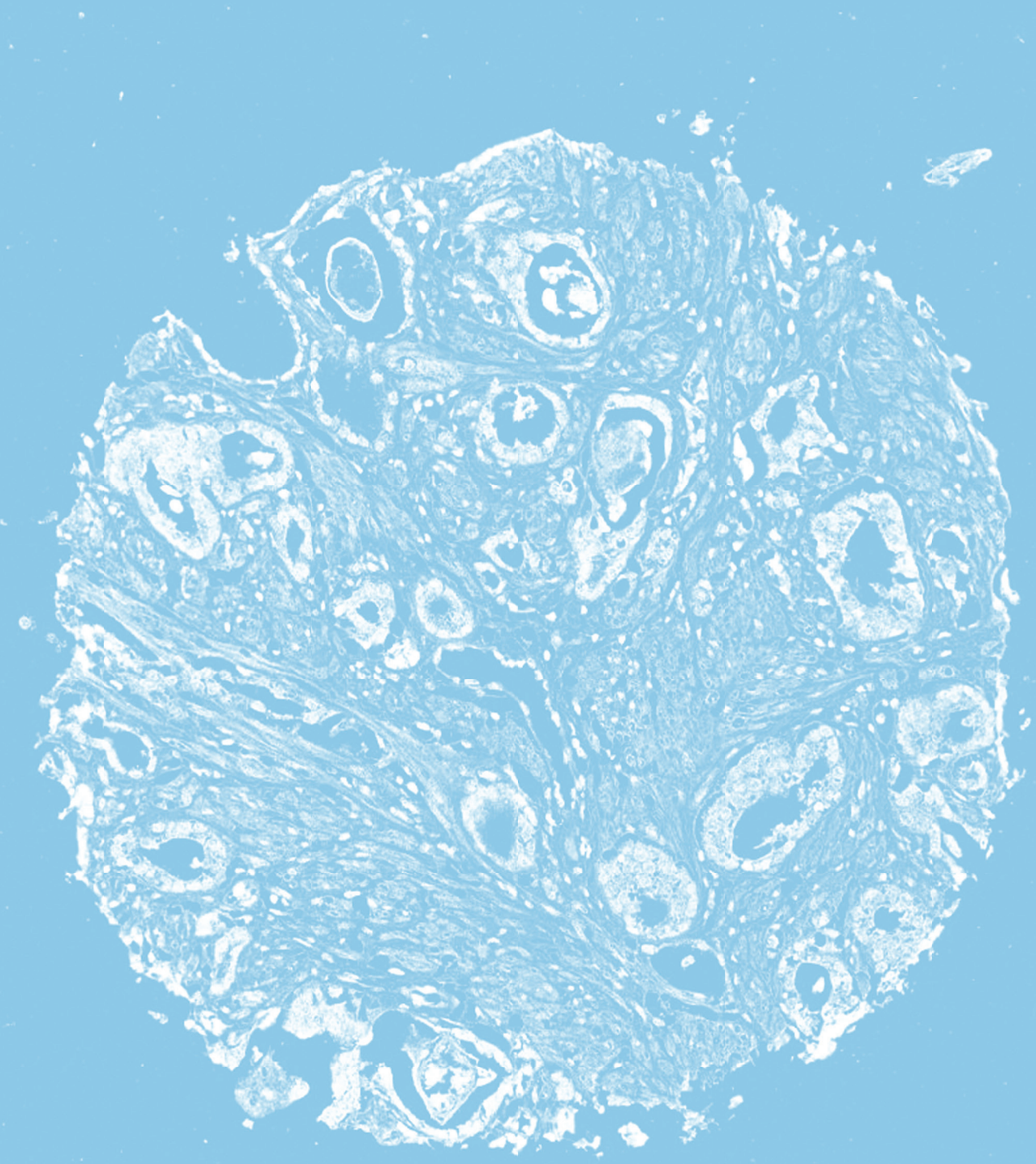

CHAPTER 4 —
EXPRESSION OF NOTCH PATHWAY MEMBERS IN PROSTATE CELLS AND HES6 CONTRIBUTION FOR TUMOR AGGRESSIVENESS

EXPRESSION OF NOTCH PATHWAY MEMBERS IN PROSTATE CELLS AND HES6 CONTRIBUTION FOR TUMOR AGGRESSIVENESS

Title HES6 promotes prostate cancer aggressiveness independently of Notch signaling

Filipe LF. Carvalho[1,2], Luigi Marchionni[2], Anuj Gupta[2], Basheer Ahamad[1], Edward M. Schaeffer[1,2,3], Ashley E. Ross[1,3], David M. Berman[1–4]
[1]*Department of Pathology,* [2]*Department of Oncology,* [3]*Brady Institute of Urology, Johns Hopkins University School of Medicine, Baltimore, MD, USA,* [4]*Departments of Pathology and Molecular Medicine and Cancer Biology and Genetics, Cancer Research Institute, Queen's University, Kingston, Ontario, Canada*

Running title HES6 promotes prostate cancer aggressiveness

Keywords: Gleason score; HES6; NOTCH3; Notch pathway; prostate cancer
Financial Support: PhD grant from Fundação para Ciência e Tecnologia (SFRH/ BD/ 69819/ 2010 to FLFC)

Corresponding author
David M. Berman,
Department of Pathology and Molecular Medicine,
Division of Cancer Biology and Genetics
Cancer Research Institute
Queen's University
18 Stuart St., 329 Botterell Hall
Kingston, ON K7L 3N6
Mobile: +12026649226
Email: bermand@queensu.ca

Conflicts of Interest DMB has consulted and/or performed sponsored research for Myriad Genetics and Metamark Genetics

Word count 5000
Total number of figures 7

Abstract

Notch signaling is implicated in the pathogenesis of a variety of cancers, but its role in prostate cancer is poorly understood. However, selected Notch pathway members are overrepresented in high-grade prostate cancers. We comprehensively profiled Notch pathway components in prostate cells and found prostate cancer-specific upregulation of *NOTCH3* and *HES6*. Their expression was particularly high in androgen-responsive lines. Notch stimulation in these cells induced canonical Notch targets, HES1 and HEY1. We found that androgen stimulation also induced HES and HEY protein family members HES1 and HEY1, which are well known canonical targets of Notch signaling. Androgen simultaneously suppressed Notch receptor expression, suggesting that androgens can activate Notch target genes in a receptor-independent manner. Using a Notch-sensitive RBPJ reporter assay, we found that basal levels of Notch signaling were significantly lower in prostate cancer cells compared to benign cells. Accordingly pharmacological Notch pathway blockade did not inhibit cancer cell growth or viability. In contrast to canonical Notch targets, HES6, a HES family member known to antagonize Notch signaling, was not regulated by Notch signaling, but relied instead on androgen levels, as we were able to demonstrate both in culture and in human patients. When engineered into prostate cancer cells, reduced levels of HES6 resulted in reduced cancer cells invasion and clonogenic growth. By molecular profiling, we identified potential roles for HES6 in regulating hedgehog signaling, apoptosis, and cell migration. These results contraindicate an oncogenic role for Notch signaling in the prostate, but implicate HES6 as a protagonist in prostate cancer progression.

Introduction

Prostate-specific antigen (PSA) screening has vastly improved detection of prostate cancer at an early, curable stage (1, 2). However, early detection with PSA has resulted in overtreatment of harmless low-grade cancers (3). Only men with aggressive cancers are likely to derive any survival benefit from treatment (4). Safely addressing overtreatment in prostate cancer will require a more sophisticated understanding of pathways that distinguish indolent prostate cancers that do not merit treatment from those that are potentially harmful. Recent mRNA profiling studies have revealed molecular features that may aid in this distinction, including the Hairy and Enhancer of Split transcriptional repressor, HES6 and other members of the Notch pathway (5, 6). Here, we intensively investigate Notch pathway expression in prostate cancer and further investigate HES6 regulation and function.

The Notch signaling pathway is composed of four receptors Notch1 through Notch4, and five ligands Jagged 1 and 2 (JAG1 and JAG2) and Delta-like 1, 3, and 4 (DLL1, DLL3, DLL4). Ligand bound to the surface of a neighboring cell binds to the Notch receptor, inducing a conformational change that facilitates cleavage by the γ-secretase complex. γ-secretase cleavage releases the active form of the receptor — Notch intracellular domain (NICD) — into the cytoplasm. Cytoplasmic NICD translocates into the nucleus to complex with the DNA-binding transcriptional co-activator RBPJ. The resulting NICD/RBPJ complex activates Notch target genes, which include two families of transcription repressors: Hairy and enhancer of split (HES) and Hairy/enhancer-of-split related with YRPW motif (HEY). Expression of these repressors, particularly HES1 and HEY1, are used to monitor Notch pathway activation. In addition, there is increasing evidence for regulatory feedback loops between HES family members. One member, HES6, is of particular interest, because it is preferentially expressed in aggressive prostate cancers (6), and its status as a member of the Notch signaling pathway is not well understood. In malignant gliomas, HES6 plays important roles in cell proliferation and migration (8). HES6 can antagonize Notch signaling by interacting with HES1 (9). Despite the fact that HES6 bears strong homology to known Notch pathway targets, whether Notch signaling regulates HES6 is unknown.

Notch signaling is critical for cell-fate decisions in many organs (7), including the prostate. Adult prostate glands are composed of basal and luminal layers that have distinct androgen-responsiveness. Luminal cells express high androgen receptor (AR) levels and undergo apoptosis after androgen deprivation (10, 11). In contrast, basal cells do not rely on androgen to survive and are able to regenerate prostate glands after castration, once androgens are replenished (11). Studies of benign mouse prostate epithelium have revealed that Notch ligands and receptors are expressed in both basal and luminal cells and can mediate physiologic proliferative responses that include response to androgen (12, 13). Prostate cancer cells almost universally emerge as androgen-dependent cells with a luminal cell phenotype. Upon androgen-deprivation, growth pauses until cells adapt to androgen-independent growth. Prostate cancer cell lines have been isolated from patients at different stages in this process, and can be classified as androgen-responsive or androgen-unresponsive.

In comparison to indolent cancers, aggressive prostate cancer cells upregulate not only HES6 but also the Notch ligand Jagged2, and the Notch3 receptor (5,6). Induction of a Notch ligand, a receptor, and a potential response gene, could represent an active signaling cascade in aggressive prostate cancers. If this is the case, then measuring and targeting Notch signaling could be helpful in the diagnosis and treatment of aggressive prostate cancers. If HES6 is not a Notch target, then other pathways that regulate this gene might be useful for the same purposes. Here, we investigate expression and function of Notch signaling and HES6 in benign prostate and prostate cancer cells.

Materials and Methods

Plasmids, virus and construct generation HES6 (clone LIFESEQ7399489, Open Biosystems) was subcloned into the lentiviral vector pNL-EGFP/CMV-WPREdU3 to establish overexpressing stable cell lines. shRNAs targeting HES6 mRNAs were obtained from the Expression Arrest-TRC shRNA Libraries (TRCN0000017828). Notch3 intracellular domain construct (gift from Dr Nicolas Gaiano) was subcloned into pcDNA 3.1(-) (Invitrogen). The vectors used in dual-luciferase reporter assay experiments were CBFRE-luc (Addgene #26897) and pGL2 (Promega).

Cell lines and cell culture Human cancer cell lines were obtained from the American Type Culture Collection and maintained in RPMI 1640 (Gibco) supplemented with 10% fetal bovine serum (FBS) and Penicillin-Streptomycin (Invitrogen), except VCaP and LnCaP96. VCaP were provided by Dr William B. Isaacs (Brady Urological Institute, The Johns Hopkins University School of Medicine) and maintained in DMEM/10% FBS (Gibco) and LnCaP96 cells were a gift from Dr Alan K. Meeker (Brady Urological Institute, The Johns Hopkins University School of Medicine) generated by long-term culture of LnCaP in charcoal-stripped FBS. Prostate epithelial cells RWPE–1 and PrEC were cultured according to vendor's instructions. All cell line identities were confirmed by forensic identity analyses within 6 months of use. For the androgen withdrawn experiments, LnCaP cells were washed with charcoal-stripped FBS three times for 1h and incubated in 10% charcoal-stripped FBS containing medium for 48h before stimulation with 10nM of dihydrotestosterone (DHT).

Real-time PCR analysis Total RNA was isolated with RNeasy Mini kit (Qiagen) and cDNA was synthesized with 1 mg of total RNA using High-Capacity cDNA Reverse Transcription kit (Applied Biosystems). cDNA was amplified on a StepOne Plus (Applied Biosystems) using TaqMan gene-specific oligonucleotide primers or custom designed primers (Supplementary Table S1). To determine the genes differentially expressed in cancer and benign cell lines, we designed Taqman gene plates comprising all Notch pathway members described in mammals and five housekeeping genes. Results are presented as a heatmap using Euclidean distance and ward linkage for clustering using median centered delta CT values for each gene.

Immunoblotting Protein lysates in NuPAGE buffer (Invitrogen) were separated by gradient 4–12% BisTris Gel and transferred to polyvinylidene difluoride membrane. Primary antibodies used were rabbit monoclonal anti-Notch1 (D1E11; 1:1000; Cell Signaling), rabbit polyclonal anti-cleaved Notch1 (Val1744; 1:1000; Cell Signaling), rabbit monoclonal anti-Notch2 (8A1; 1:1000; Cell Signaling), rabbit polyclonal anti-Notch3 (Pro2311; 1:1000; Cell Signaling), rabbit polyclonal anti-HES1 (ab71559; 1:1000; Abcam), rabbit polyclonal anti-HEY1 (ab22614; 1:500; Abcam), rabbit polyclonal anti-HES6 (ab66461; 1:1000; Abcam), mouse monoclonal anti-glyceraldehyde–3–phosphate dehydrogenase (GAPDH) (clone 6C5; 1:1000; Santa Cruz Biotechnology). The membrane was incubated sequentially with primary antibodies (overnight at 4oC), horseradish peroxidase (HRP)-conjugated anti-rabbit or anti-mouse and chemiluminescent substrate (Thermo Fisher) before exposure to film.

Luciferase reporter assay Cells were plated in 24–well plates and 24 hours later transfected using Lipofectamine2000 (Invitrogen) with pGL2 (control) or with CBFRE-luc to determine endogenous Notch pathway activity in prostate cells. After 48 hours, luciferase activity was determined using Dual-Luciferase Reporter Assay system (Promega) and normalized to PrEC basal luminescence. All experiments were performed in triplicate.

siRNA transient knockdown Notch3 siRNA (Supplementary Table 2) transient transfections (final concentration of 10 nmol/L) were carried out by using Lipofectamine 2000 (Invitrogen), following the manufacturer's instructions. Nontargeting siRNA was used as a control. Cells were lysated for western blot 24 hours after siRNA transfection.

DAPT treatment and IC50 assay 24 hours after seeding the cells, gamma secretase inhibitor N-[N-(3,5–Difluorophenacetyl)-L-alanyl]-S-phenylglycine t-butyl ester (DAPT) was added to 200 ml of growth media per well in final concentrations ranging from 1 nmol/L to 400 mmol/L. Viability was assayed (see below) after 96 hours. The half maximum inhibitory concentration (IC50) of DAPT was calculated using GraphPad Prism software.

Cell viability and proliferation assays 22Rv1 and LnCaP with stable shRNA HES6 knockdown or PC3 stably overexpressing HES6 were seeded (500 cells per well) in 96–well black flat-bottom tissue culture plates. Cell viability and growth was determined using Alamar Blue vital dye (Invitrogen) according to the manufacturer's instructions. Values were reported as mean standard error of optical density of triplicate wells fro each concentration and time point.

Immunohistochemistry and Immunofluorescence IHC and IF staining were performed as described previously (14, 15) using anti-Hes6 antibody (ab66461; 1:1000; Abcam). Mann-Whitney test used for statistical analysis of HES6 staining intensity was measured automatic quantitative analysis.

Androgen-deprived tissue in tissue microarray (TMA) We used a previously described TMA comprising formalin-fixed paraffin-embedded prostate cancer tissue from (n=55) patients treated with androgen-deprivation therapy prior to prostatectomy and from (n=12) untreated controls (14).

Invasion assays 22Rv1 or LnCaP cells infected with control or shHES6 lentiviruses (see plasmids and viruses above) were seeded at 7.5 x 10^4 cells/well or 5 x 10^4 PC3 cells infected with control or HES6 overexpression lentiviruses. The assay was performed in triplicate and in two independent experiments as previously described (16). Student t test was used to evaluate significant differences and a statistical significance was considered at $p < 0.05$.

Colony-forming efficiency assay Colony-forming efficiency assays were conducted as described earlier (17). All visible were counted and results presented as total number colonies stander error in two individual experiments.

Gene expression arrays and data analysis Differential gene expression analysis was performed as previously described (6, 18, 19), using statistical packages from the R/Bioconductor project (20, 21). Briefly, gene expression was measured on the Illumina HT–12 v4 whole genome gene expression microarray. For each individual microarray feature a generalized linear model was fit to estimate expression differences between groups. Moderated t-statistics were obtained by empirical Bayesian shrinkage of log2 fold-change standard errors (22), and adjustment for multiple testing was obtained using the Benjamini and Hochberg method (23). Gene annotation for the microarray used in this study was obtained from the corresponding R-Bioconductor metadata packages.

Results

Notch pathway components in prostate carcinogenesis

We investigated the expression of the 36 known and presumed Notch pathway components in a panel of commonly used prostate cell lines. Of the two benign prostate lines studied, RWPE–1 and PrEC have been reported to show relatively luminal

and basal epithelial phenotypes (24, 25). The 5 cancer cell lines studied included two androgen unresponsive lines (DU145 and PC3), and three that are androgen responsive (22Rv1, LnCaP, and VCaP) (26, 27). Quantitative TaqMan PCR (qPCR) assays on cDNA prepared from prostate cell lines revealed Notch gene expression patterns that organized the cell lines clearly into distinct benign and cancer clusters (Fig. 1A). HES6 was most differentially expressed gene between benign cells and cancer cells with 4–fold higher transcript levels in cancer (Fig. 1B). Although not as dramatically, other targets, such as HEY1, HEY2 and HES4 also exhibited increased expression levels in cancer cells (Fig. 1B). In contrast, many canonical Notch signaling components were downregulated in cancer cells, including DLL1 and JAG1 ligands, NOTCH1, 2, and 4 receptors, and the target gene, HES2 (Fig. 1B).

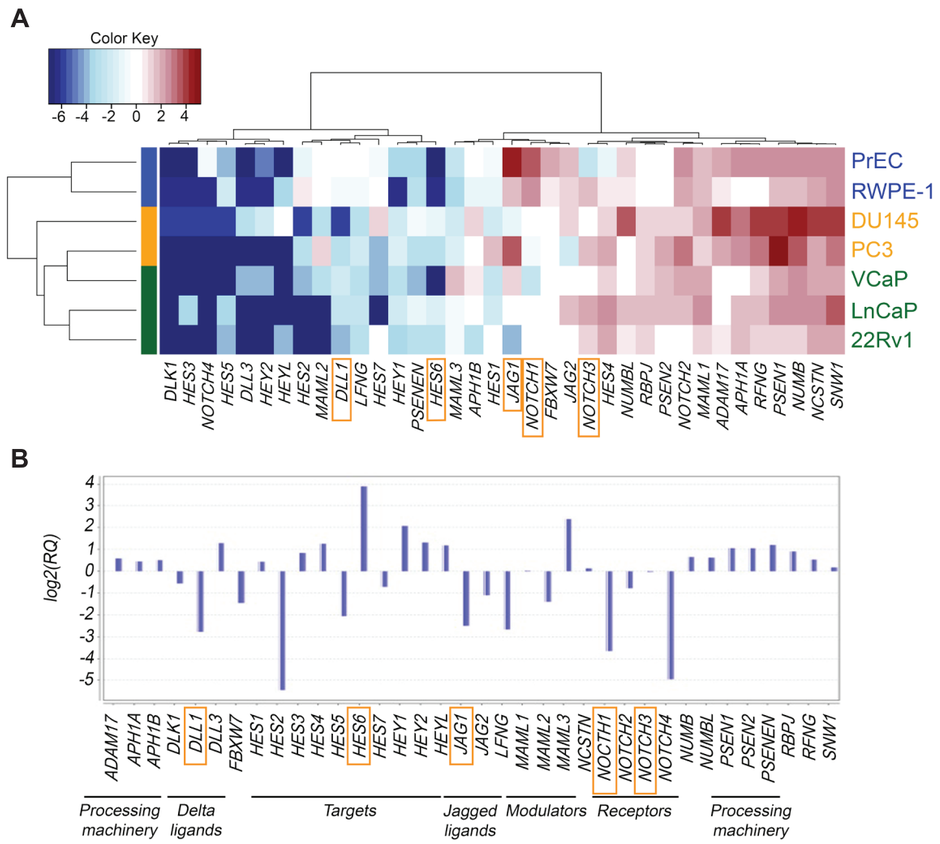

Figure 1 — Notch pathway members' expression in prostate cells

A Heatmap with gene expression results of Notch pathway members across commonly used prostate cells. Color bars at the top of the heatmap represent groups of cells with similar phenotypes: blue — benign cells; yellow — androgen-independent cancer cell lines; green — androgen-responsive cancer cell lines. Hierarchical clustering of gene expression patterns clearly distinguishes benign from cancer cells. Genes circled in yellow are, along with HES6 and NOTCH3 that are relevant for our analysis, the most studied members of Notch pathway.

B qRT-PCR analysis of relative expression of Notch pathway members in cancer relative to benign cell lines. A log2 fold increase in the y axis represents an enrichment of the genes in cancer cells and negative values correspond to genes downregulated in cancer cells. HES6 was most differentially expressed gene in cancer cells. In contrast, canonical Notch signaling components, including DLL1 and JAG1 ligands, NOTCH1 and NOTCH2 receptors, were downregulated in cancer cells.

Notch signaling components in prostate cancer cell lines

Since Notch3 levels were previously shown to be lowest in indolent prostate cancers and highest in aggressive, high Gleason grade tumors, we performed a subanalysis to further investigate receptor expression in cancer. Interestingly, the benign RWPE–1 cell line showed the highest levels of Notch3 expression, whereas benign PrEC cells showed the lowest Notch3 levels (Fig. 2A and Supplementary Fig. S1), contributing to an overall lower expression of Notch3 in cancer. The exclusion of RWPE would make Notch3 the second most overexpressed gene in cancer, after HES6 (Supplementary Fig. S2). Of further interest, those cell lines with high Notch3 expression also showed increased HES6, and both of these genes were particularly elevated in three of four androgen-responsive prostate cell lines (RWPE–1, 22Rv1 and LnCaP but not VCaP) compared to androgen-independent lines (DU–145, PC3) (Fig. 2A). These results prompted us to explore whether or not Notch3 and androgens regulate HES6.

Notch signaling dynamics in prostate cancer

Few previous studies have presented Notch signaling dynamics in prostate cells. We genetically and pharmacologically manipulated benign prostate cells and prostate cancer cells, and used a variety of assays to measure effects on Notch pathway activity and cell viability. At baseline, benign prostate cells showed significantly higher levels of Notch1 and Notch2 receptor protein than did prostate cancer cells (Fig. 2B). To explore Notch activity levels, we introduced a Notch dependent luciferase reporter (28) into the 7 benign and malignant prostate lines profiled in this study. The benign cell lines RWPE–1 and PrEC showed the highest levels of RBPJ promoter basal activity, consistent with their overall higher expression of Notch receptors (Fig. 2C). These results demonstrate lower levels of Notch signaling in prostate cancer cells compared to their benign counterparts and suggest a neutral or anti-oncogenic role for Notch in prostate epithelia.

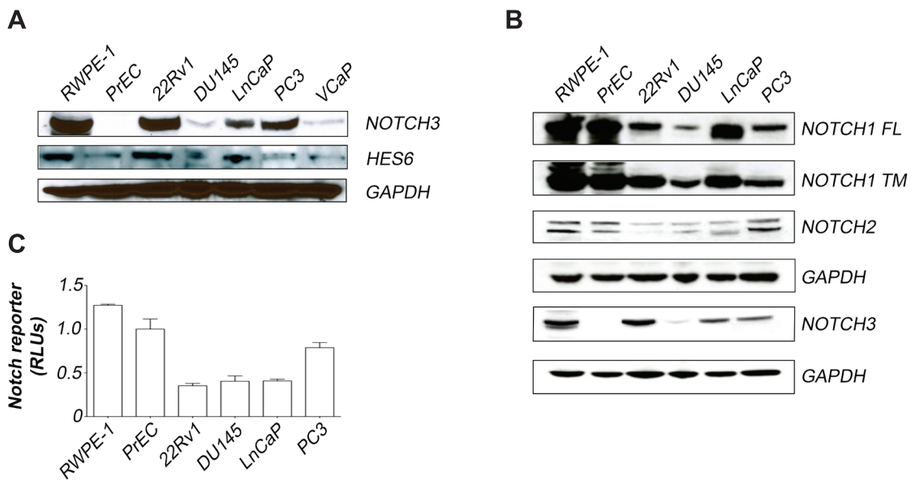

Figure 2 — Dynamics of Notch signaling in prostate cells

A Cell lines with high NOTCH3 expression also presented increased HES6. Immunoblot showing basal NOTCH3 and HES6 expression are globally higher in cancer cells confirming the expression pattern presented in the heatmap (Fig. 1A).

B Benign cells have significantly higher levels of Notch receptor protein than cancer cells. Immunoblot showing basal Notch1, Notch2, and Notch3. FL, full length NOTCH1; TM, transmembrane NOTCH1.

C Notch dependent luciferase reporter showed higher activity levels of RBPJ in benign cell lines. In benign cells a higher RBPJ promoter activity is consistent with overall high expression of Notch receptors. RLUs, Relative Luminescence Units.

Contributions of Notch3 receptor to Notch signaling and HES6 expression

Different Notch receptor species can have different effects (29). Having established through its expression pattern that Notch3 was the receptor most correlated with HES6 expression in prostate cancer (Fig. 2A), we introduced constitutively active Notch3 intracellular domain (NICD3) into benign (RWPE–1 and PrEC) and cancer (22Rv1 and LnCaP) cells (Supplementary Fig. S3). Interestingly, qPCR analysis demonstrated that NICD3 overexpression in benign cell lines did not induce HES or HEY family members (Fig. 3A and data not shown), indicating that Notch signaling was unresponsive to NICD3 in these cells. Whereas most cancer cell lines also showed only modest responses to NICD3, 22RV1 cells responded with a 50% induction of HES1 and five-times induction of HEY1 and HES5. Most notably, HES6 was not induced by NICD3 in any of the cell lines we tested. These results indicate that some prostate cancer cell lines respond to Notch signaling, but that HES6 induction is not part of that response.

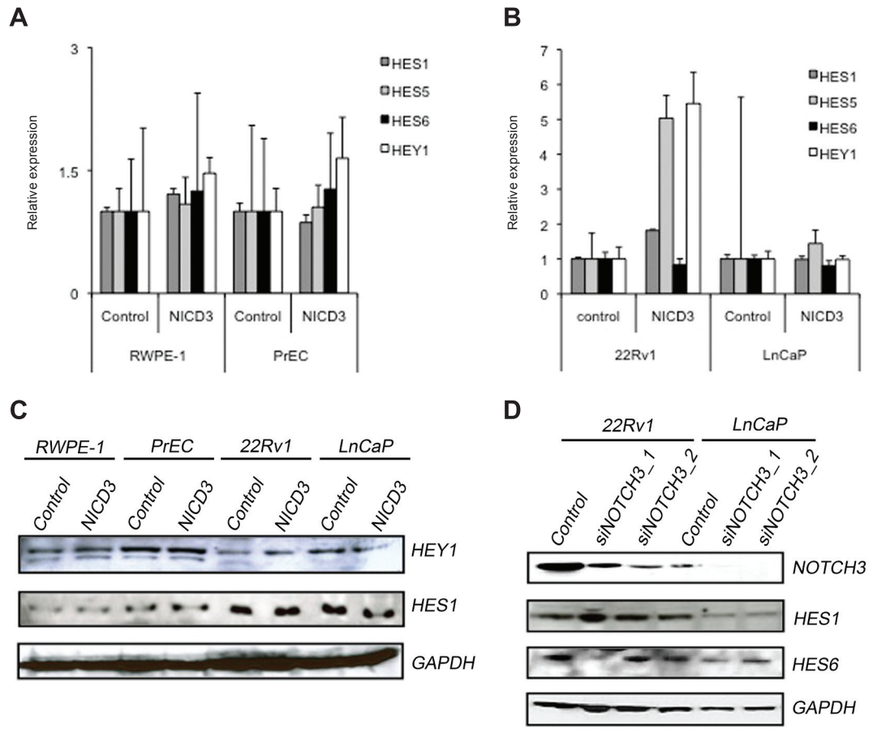

Figure 3 — HES6 stands apart from the canonical Notch signaling pathway

A and **B** qPCR analysis of HEY1, HES1, HES5, and HES6 levels after NICD3 expression in benign and androgen-responsive cancer cell lines. Notch signaling was responsive to NICD3 only in 22Rv1 cancer cells.

C Immunoblot for HEY1 and HES1 validate the qPCR findings that NICD3 expression in 22Rv1 increases HEY1 protein levels.

D Immunoblot shows that the levels of HES6 remain unchanged after NOTCH3 knockdown in cancer cell lines.

To confirm that HES6 is not under Notch3 control, we used siRNAs to knockdown Notch3 in the cancer cells with highest Notch3 and HES6 levels, 22Rv1 and LnCaP and determined the protein levels of HES6 and of HES1, a known Notch3 target (30). Upon effective Notch3 knockdown (Fig. 3D), HES1 levels correlated with levels of Notch1 protein (Fig. 2B): expression of this Notch target was maintained in 22RV1 cells, but not in LnCaP cells (Fig. 3D). These data indicate that HES1 is a Notch target in prostate cancer cells and suggest that its expression in 22RV1 is redundantly supported by Notch1 and Notch3 but only by Notch1 in LnCaP cells. HES6 expression, in contrast, was unaffected by Notch3 knockdown (Fig. 3D). Thus, HES6 expression appears to be independent of Notch signaling. Neither engineered expression of NICD3 (Fig. 3B and 3C) nor Notch3 knockdown by siRNA (Fig. 3D) affected

HES6 levels. Although HES6 may interact with Notch signaling components, these results suggest that HES6 stands apart from the canonical Notch signaling pathway.

Prostate cancer cells are resistant to γ-secretase inhibition

By pharmacologically inhibiting γ-secretase, and monitoring cleavage of Notch1 protein into its active moiety, NICD1, we tested the effects of Notch pathway inhibition on cell growth and viability. The two benign cell lines PrEC and RWPE–1 showed high levels of NICD1, but among 5 different cancer lines only one — 22Rv1 — had detectable NICD1 levels (Fig. 4A). Treatment of these cells with increasing concentrations of γ-secretase inhibitor DAPT showed that 1 to 3 μM of DAPT were sufficient to block γ-secretase activity and eliminate NICD1 protein levels (Fig. 4B and 4C). Nevertheless, cell viability responses both in benign and cancer cells to DAPT required drug concentrations that were 30 to 40 times higher, most likely corresponding to off-target effects (Fig. 4D and Table 1). These results cast further doubt on the notion that Notch signaling is required for prostate cancer cell survival or growth.

A

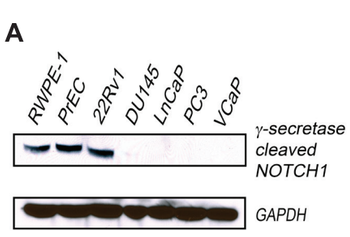

B

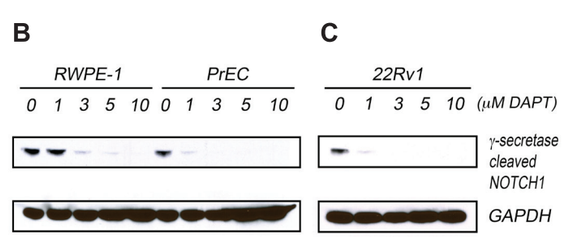

C

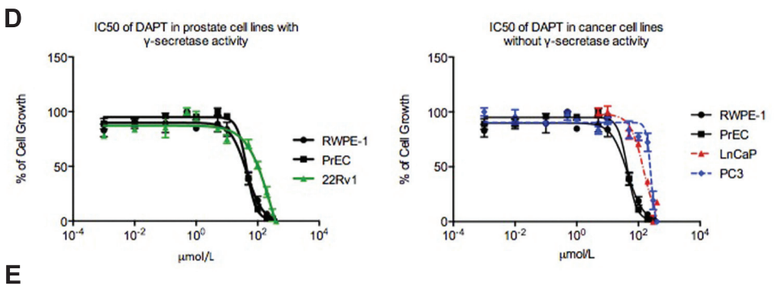

D

E

	RWPE-1	PrEC	22Rv1	LnCaP	PC3
IC50 (μM)	44.07	44.04	282.6	149.4	259.8
R^2	0.9592	0.9843	0.9322	0.9310	0.9295

Previous Page:

Figure 4 — Prostate cancer cells are resistant to γ-secretase inhibition

A Immunoblot shows γ-secretase cleaved NICD1 in the two benign cell lines PrEC and RWPE-1, and 22Rv1 cancer cell line.

B and **C** γ-secretase is inhibited in both benign and 22Rv1 cancer cells with 1 to 3 uM of DAPT. Immunoblot shows the levels of NICD1 protein after 48 hours treatment to the indicated concentrations of DAPT.

D and **E** Prostate cells are resistant to γ-secretase inhibitor DAPT. Effects of DAPT on benign and tumor cells proliferation following incubation with increasing concentrations of DAPT. Error bars, mean ± SEM of triplicates. The table shows all cell lines were insensitive to DAPT with IC50 above 40μM, much higher concentrations than the ones required to inhibit γ-secretase.

Androgens downregulate Notch receptors while upregulating HES/HEY family members

Since there was a clear difference between two out of three androgen-responsive cell lines (22Rv1 and LnCaP) and androgen insensitive cell lines in Notch component expression (Fig. 1A), we investigated how androgens affect the expression of different Notch pathway members in prostate cancer. For these studies, we utilized cell culture experiments and primary cancer tissue from human patients treated with androgen deprivation. We stimulated LnCaP with DHT and collected RNA for qPCR at time points up to 72 hours. Monitoring levels of transcripts encoding *PSA*, an androgen responsive gene (31), indicated effective androgen responses (Supplementary Fig. S4). Interestingly, we found that DHT modulated receptors and targets in opposite directions. *NOTCH4* was undetectably low, regardless of androgen treatment. The expression of Notch receptors *NOTCH1*, *NOTCH2*, and *NOTCH3* decreased over time with DHT administration whereas levels of *HES1*, *HES6* and *HEY1* increased (Fig. 5A and 5B). *HES1* and *HEY1* were particularly increased in the first 12 hours of DHT treatment. The effect diminished at later time points. *HES6* did not increase as quickly or dramatically as *HES1* and *HEY1*, but the response was more durable (Fig. 5B). These results indicate that HES/HEY family members respond to androgen stimulation independently of canonical Notch signaling. This response occurs in two phases — rapid and transient induction of Notch targets HEY1 and HES1, and slow, sustained induction of HES6.

To further investigate the long-term effects of androgen withdrawal, we assayed HES/HEY family member expression in LnCaP96, an LnCaP subline adapted to androgen independent growth (32). In LnCaP96, mRNA levels for the androgen-regulated gene, *PSA* were undetectable, whereas *PSA* was highly expressed in parental LnCaP cells (Fig. 5C). Compared to LnCaP levels, *NOTCH3* levels in LnCaP96 were unchanged, whereas *HES6* expression was significantly reduced (Fig. 5D). In agree-

ment with these in vitro results, we found a significant reduction in HES6 staining intensity in cancers from men who had undergone a long-term ADT, compared to androgen-naïve cancers (Fig. 5E and 5F). In light of the dependence of Notch receptor expression by androgen, these results raise the possibility that androgens induce HES/HEY family members in a Notch receptor-independent manner.

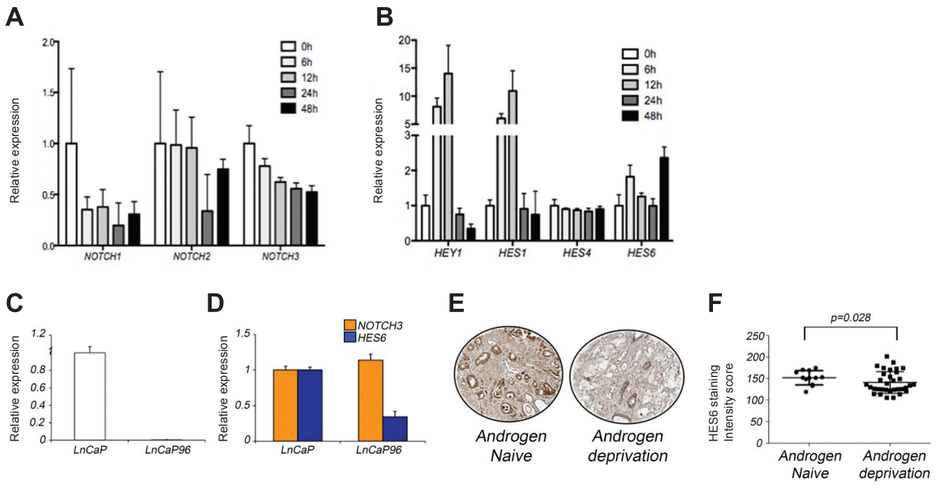

Figure 5 — Androgens downregulate Notch receptors and upregulate HES/HEY family members

A and **B** Effects on LnCaP Notch receptors and HES/HEY family members expression after incubation with 10 nM of DHT. Transcript levels of *NOTCH1*, *NOTCH2*, and *NOTCH3* decreased overtime and *HEY1*, *HES1* and *HES6* dramatically increased. Error bars, mean ± SEM of of three technical triplicates.

C and **D** In the long-term androgen deprived subline LnCaP96, *PSA* levels are undetectable, *NOTCH3* remains unchangeable and *HES6* expression is significantly reduced. Error bars, mean ± SEM of of three technical triplicates.

E and **F** Photomicrographs of HES6 immunohistochemistry in prostate cancer glands with and without previous androgen deprivation. There is a significant decrease in HES6 expression (F) after androgen deprivation (*p=0.028, Mann–Whitney test).

HES6 contributes to prostate cancer aggressiveness

As shown by qPCR array, *HES6* transcripts were approximately 4–fold enriched in cancer cells compared to benign. In previous work, immunohistochemical analysis of HES6 protein in human clinical samples (33) confirmed that the protein was upregulated in cancer and further demonstrated that strong nuclear HES6 protein expression increased as a function of Gleason grade, a potent indicator of metastatic potential in prostate cancer.

The ability to metastasize has been correlated with *in vitro* cell behaviors, including clonogenic growth and invasion through various matrices (34, 35). We up- and down-regulated HES6 expression and assayed the effects on standard growth in culture, clonogenic growth, cell migration and invasion.

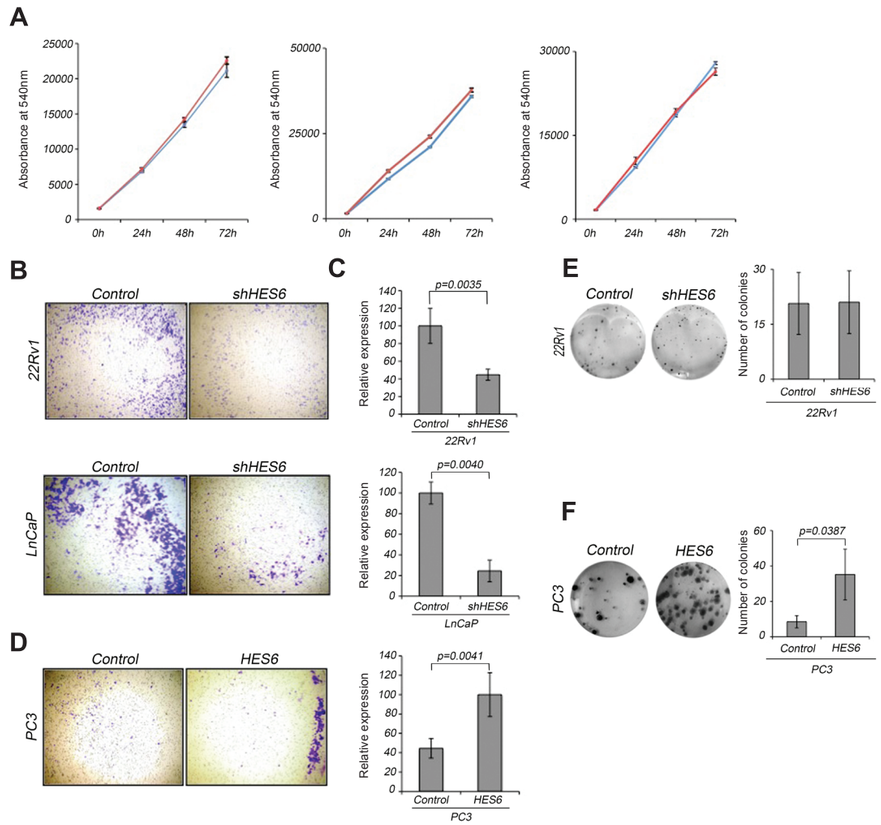

Figure 6 — HES6 promotes cancer cells invasion and colony formation

A Following HES6 shRNA knockdown in 22RV1 and LnCaP (left and middle) and HES6 overexpression in PC3 (right), cells were plated for alamarBlue proliferation assays. Growth curves show HES6 does not change proliferation in the three cell lines.

B Representative images of invasive 22Rv1 and LnCaP cells after HES6 shRNA knockdown.

C Quantification of 22Rv1 and LnCaP HES6 knockdown invaded cells. Error bars, mean ± SEM.

D Representative images of invasive PC3 cells overexpressing (left) and quantification of invaded cells (right). Error bars, mean ± SEM.

E Representative pictures (left) and quantification (right) of colony-forming efficiency of 22Rv1 cells with HES6 knockdown. Error bars, mean ± SEM.

F Representative pictures (left) and quantification (right) of colony-forming efficiency of PC3 cells overexpressing HES6. Error bars, mean ± SEM.

Using lentiviral plasmid transfer, we reversed baseline levels of HES6 (Fig. 2A) by stably engineered its expression into PC3 cells and knocked it down in 22Rv1 and LnCaP cells (Supplementary Fig. 5A and 5B). Whereas HES6 overexpression or knockdown did not have a noticeable effect on cell viability or growth rate (Fig. 5A), HES6 significantly affected cell invasion. HES6 knockdown in 22Rv1 and LnCaP significantly impaired cell invasion through a matrigel membrane and PC3 cells overexpressing HES6 showed a significant increase in their ability to invade compared to controls (Fig. 6B–D). In line with these observations, HES6 affects the clonogenic potential of cancer cells. HES6 knockdown in 22Rv1 and LnCaP cell did not significantly decrease the number of colonies, but HES6 overexpression in PC3 increased the capacity of the cells to form colonies 4 times (Fig. 6E and 6F). As previously suggested by studies that showed that HES6 distinguishes prostate cancers with and without the ability to metastasize (6), these results strongly suggest that HES6 confers biological properties to cancer cells that enable them to escape the prostate and generate metastatic clones.

HES6 controls a number of pathways that contribute to cancer progression

To determine the pathways activated by HES6 in benign cells and the mechanisms involved in the invasion and clonogenic advantage observed in cancer cells, we engineered HES6 overexpression and knockdown and comprehensively profiled changes in gene expression. Despite previous indicators that HES6 can downregulate Notch signaling, we saw no evidence that any Notch target was significantly modulated by HES6 (Fig. 7A). In contrast, HES6 modulated expression of a number of other pathways. The pathways activated by HES6 were different among benign and malignant cells (Fig. 7A). In benign cells, HES6 induced overexpression of genes, such as IRF4, LCK and BMX that are involved in immunosurveillance and kinases that increase cell survival (Fig 7B).

Next Page:

Figure 7 — HES6 controls different pathways in benign and cancer cell lines

A HES6 expression in RWPE–1 and PC3, and knockdown in 22Rv1 and LnCaP altered the expression of 63 genes that are members of different pathways.

B C D E qPCR analysis of differentially expressed transcripts after HES6 overexpression in RWPE–1 (B) and PC3 (C), or HES6 knockdown in 22Rv1 (D) and LnCaP (E). Error bars, mean ± SEM of three technical replicates.

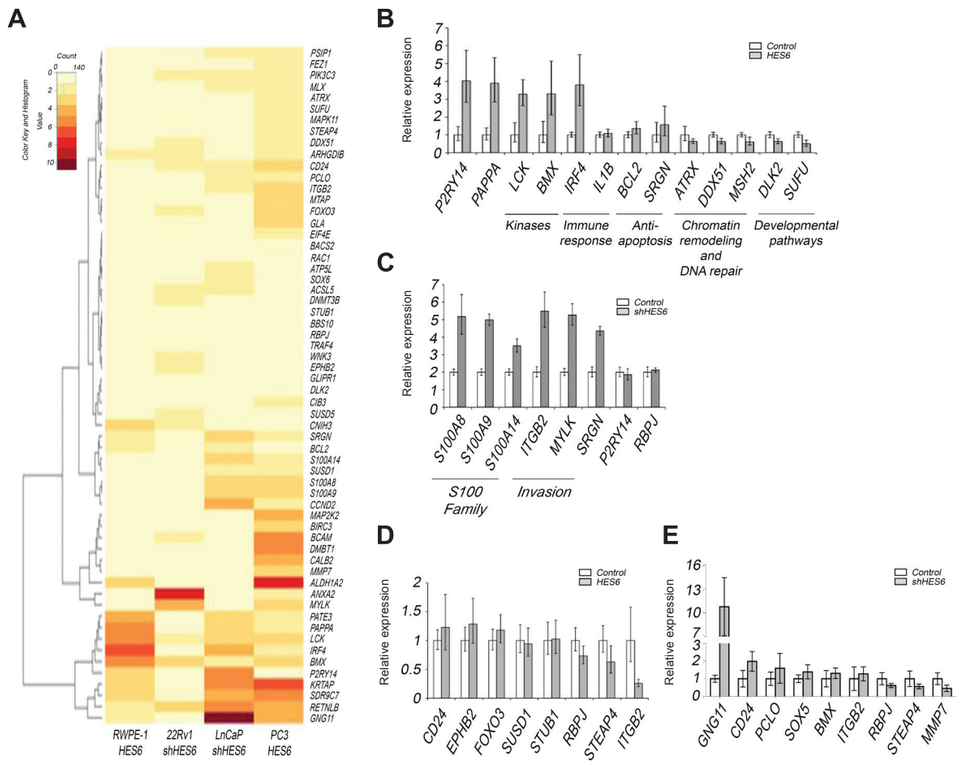

Two significantly highly expressed genes, P2RY14 and PAPPA, were implicated lung tumor growth (36, 37). HES6 overexpression in RWPE–1 significantly downregulated ATRX and DDX51 genes that encode proteins involved in chromatin remodeling and telomere lengthening. Interestingly, we found downregulation of DLK2, a gene encoding a protein that inhibits Notch signaling and one that was previously implicated in prostate tumorigenesis (38). Also downregulated was suppressor of fused (SUFU), considered a tumor suppressor gene through its inhibitory influence on the Hedgehog pathway (Fig. 7B). Repression of SUFU by HES6 could represent a new mechanism of inducing Hedgehog signaling in prostate cancer, which could participate in prostate cancer development, metastasis and androgen-independent growth (39, 40). In PC3 prostate cancer cells, HES6 increased most significantly genes involved in cell structure, motility, and tumor cells invasion and metastasis (Fig. 7C). Significantly overexpressed genes included three members of S100 family, S100A8, S100A9, and S100A14, serglycin (SRGN), myosin light chain kinase (MYLK), and the integrin beta 2 (ITGB2). These genes were previously implicated in cancer progression of several tumors, including the prostate: S100 proteins are overexpressed in prostate cancer and present in circulating tumor cells (41, 42); SRGN promoted metastasis in nasopharyngeal carcinoma (43); MYLK was identified in a microarray

study as one of the most discriminative genes between normal and prostate cancer (44); and integrin beta 2, as well as other integrins, are essential for different types of cancer cells to interact with the extracellular matrix and trigger intracellular signals to support survival and migration (45). In LnCaP and 22Rv1 cells, HES6 knockdown modulated a set of genes that only partially overlapped with those affected in PC3 cells, but the most highly affected pathways in all cancer cell lines were strikingly similar. HES6 knockdown in these 2 cell lines significantly diminished expression of genes involved in migration and invasion, including metalloproteinase 7 (MMP7) and ITGB2 (Fig. 7D and 7E). In LnCaP cells, HES6 knockdown significantly increase the expression of the G-protein GNG11, which beyond inducing cell senescence (46), is downregulated in splenic marginal zone lymphoma (47). HES6 downregulation in LnCaP significantly increased CD24 (Fig. 7E). This cell surface protein plays important roles in cell-cell and cell-extracellular matrix interactions and some studies showed that it is highly expressed high grade prostate cancers (48). However, progenitor cancer cells with the ability to initiate new tumors, compared with differentiated cells, possess lower CD24 expression (49). In this context, HES6 may provide tumor-initiation properties to prostate cancer cells and the knockdown of HES6 lead to an increase of CD24 contributing to a less aggressive phenotype of cancer cells.

Discussion

Our results confirm differential expression of Notch pathway members in aggressive prostate cancer and indicate a role for HES6 in tumor progression. These effects result from a direct action of HES6 or activation of other pathways. These data suggest that Notch signaling, and particularly HES6, may be useful in distinguishing indolent from lethal prostate cancers.

In our studies, Notch receptor expression and Notch signaling activation is inversely correlated with malignant phenotype of cancer cells. We found that prostate benign cells have higher Notch1 and Notch2 expression and more Notch pathway activation than cancer cells. Notch pathway blockade, a proposed therapeutic modality for breast cancer (50) had no effect on prostate cancer viability. To the extent that in vitro assays reflect cancer biology in vivo, these results suggest that Notch blockade may not be therapeutically helpful in prostate cancer patients.

In contrast, HES6, although homologous to Notch pathway targets, is regulated independently from Notch and may be helpful in prostate cancer diagnostic and prognostic settings. HES6 interacts with Notch signaling components (9), but is not regulated by Notch receptors. HES6 modulates pathways involved in cancer colony formation, invasion and migration such as integrins, and these pathways are potential targets for prostate cancer therapy. We found a significant decrease in HES6 expression in cell lines cultured in androgen-deprived media and in prostate cancer specimens from patients treated with ADT. However, in a variable time frame, prostate cancer becomes resistant to ADT and cancer cells are able to reactivate AR signaling. In this setting, it is possible that other genes possibly assume the role of HES6.

Our results show that HES6 reflects and mediates the aggressive phenotype in hormone-naïve prostate cancers. The identification of the invasion and clonogenic advantages conferred by HES6 to cancer cells, and other cellular pathways it activates may open new avenues to interfere with prostate cancer progression.

References

1 Catalona WJ, Smith DS, Ratliff TL, Dodds KM, Coplen DE, Yuan JJ, et al. Measurement of prostate-specific antigen in serum as a screening test for prostate cancer. N Engl J Med. 1991;324:1156–61.

2 Schroder FH, Hugosson J, Carlsson S, Tammela T, Maattanen L, Auvinen A, et al. Screening for prostate cancer decreases the risk of developing metastatic disease: findings from the European Randomized Study of Screening for Prostate Cancer (ERSPC). Eur Urol. 2012;62:745–52.

3 Schroder FH, Hugosson J, Roobol MJ, Tammela TL, Ciatto S, Nelen V, et al. Prostate-cancer mortality at 11 years of follow-up. N Engl J Med. 2012;366:981–90.

4 Wilt TJ, Brawer MK, Jones KM, Barry MJ, Aronson WJ, Fox S, et al. Radical prostatectomy versus observation for localized prostate cancer. N Engl J Med. 2012;367:203–13.

5 Penney KL, Sinnott JA, Fall K, Pawitan Y, Hoshida Y, Kraft P, et al. mRNA expression signature of Gleason grade predicts lethal prostate cancer. J Clin Oncol. 2011;29:2391–6.

6 Ross AE, Marchionni L, Vuica-Ross M, Cheadle C, Fan J, Berman DM, et al. Gene expression pathways of high grade localized prostate cancer. Prostate. 2011.

7 Bray SJ. Notch signalling: a simple pathway becomes complex. Nat Rev Mol Cell Biol. 2006;7:678–89.

8 Haapa-Paananen S, Kiviluoto S, Waltari M, Puputti M, Mpindi JP, Kohonen P, et al. HES6 gene is selectively overexpressed in glioma and represents an important transcriptional regulator of glioma proliferation. Oncogene. 2012;31:1299–310.

9 Gratton MO, Torban E, Jasmin SB, Theriault FM, German MS, Stifani S. Hes6 promotes cortical neurogenesis and inhibits Hes1 transcription repression activity by multiple mechanisms. Mol Cell Biol. 2003;23:6922–35.

10 Evans GS, Chandler JA. Cell proliferation studies in the rat prostate: II.The effects of castration and androgen-induced regeneration upon basal and secretory cell proliferation. Prostate. 1987;11:339–51.

11 English HF, Santen RJ, Isaacs JT. Response of glandular versus basal rat ventral prostatic epithelial cells to androgen withdrawal and replacement. Prostate. 1987;11:229–42.

12 Valdez JM, Zhang L, Su Q, Dakhova O, Zhang Y, Shahi P, et al. Notch and TGFbeta form a reciprocal positive regulatory loop that suppresses murine prostate basal stem/progenitor cell activity. Cell Stem Cell. 2012;11:676–88.

13 Wang XD, Shou J, Wong P, French DM, Gao WQ. Notch1 — expressing cells are indispensable for prostatic branching morphogenesis during development and re-growth following castration and androgen replacement. J Biol Chem. 2004;279:24733–44.

14 Kleeberger W, Bova GS, Nielsen ME, Herawi M, Chuang AY, Epstein JI, et al. Roles for the stem cell associated intermediate filament Nestin in prostate cancer migration and metastasis. Cancer Res. 2007;67:9199–206.

15 Carvalho FL, Simons BW, Antonarakis ES, Rasheed Z, Douglas N, Villegas D, et al. Tumorigenic potential of circulating prostate tumor cells. Oncotarget. 2013;4:413–21.

16 Barbieri CE, Baca SC, Lawrence MS, Demichelis F, Blattner M, Theurillat JP, et al. Exome sequencing identifies recurrent SPOP, FOXA1 and MED12 mutations in prostate cancer. Nat Genet. 2012;44:685–9.

17 Baia GS, Caballero OL, Orr BA, Lal A, Ho JS, Cowdrey C, et al. Yes-associated protein 1 is activated and functions as an oncogene in meningiomas. Mol Cancer Res. 2012;10:904–13.

18 Kortenhorst MS, Wissing MD, Rodriguez R, Kachhap SK, Jans JJ, Van der Groep P, et al. Analysis of the genomic response of human prostate cancer cells to histone deacetylase inhibitors. Epigenetics. 2013;8.

19 Ross AE, Marchionni L, Phillips TM, Miller RM, Hurley PJ, Simons BW, et al. Molecular effects of genistein on male urethral development. J Urol. 2011;185:1894–8.

20 Gentleman RC, Carey VJ, Bates DM, Bolstad B, Dettling M, Dudoit S, et al. Bioconductor: open software development for computational biology and bioinformatics. Genome Biol. 2004;5:R80.

21 Ihaka R, and Gentleman, R. R: A Language for Data Analysis and Graphics. Journal of Computational and Graphical Statistics. 1996.

22 Smyth GK. Linear models and empirical bayes methods for assessing differential expression in microarray experiments. Stat Appl Genet Mol Biol. 2004;3:Article3.

23 Benjamini YH, Y. Controlling the False Discovery Rate: A Practical and Powerful Approach to Multiple Testing. Journal of the Royal Statistical Society. 1995;57:289–300.

24 Bello D, Webber MM, Kleinman HK, Wartinger DD, Rhim JS. Androgen responsive adult human prostatic epithelial cell lines immortalized by human papillomavirus 18. Carcinogenesis. 1997;18:1215–23.

25 Garraway LA, Lin D, Signoretti S, Waltregny D, Dilks J, Bhattacharya N, et al. Intermediate basal cells of the prostate: in vitro and in vivo characterization. Prostate. 2003;55:206–18.

26 Webber MM, Bello D, Quader S. Immortalized and tumorigenic adult human prostatic epithelial cell lines: characteristics and applications Part 2. Tumorigenic cell lines. Prostate. 1997;30:58–64.

27 van Bokhoven A, Varella-Garcia M, Korch C, Johannes WU, Smith EE, Miller HL, et al. Molecular characterization of human prostate carcinoma cell lines. Prostate. 2003;57:205–25.

28 Yu X, Zou J, Ye Z, Hammond H, Chen G, Tokunaga A, et al. Notch signaling activation in human embryonic stem cells is required for embryonic, but not trophoblastic, lineage commitment. Cell Stem Cell. 2008;2:461–71.

29 Fan X, Mikolaenko I, Elhassan I, Ni X, Wang Y, Ball D, et al. Notch1 and notch2 have opposite effects on embryonal brain tumor growth. Cancer Res. 2004;64:7787–93.

30 Morimoto M, Nishinakamura R, Saga Y, Kopan R. Different assemblies of Notch receptors coordinate the distribution of the major bronchial Clara, ciliated and neuroendocrine cells. Development. 2012;139:4365–73.

31 Wang LG, Liu XM, Kreis W, Budman DR. Down-regulation of prostate-specific antigen expression by finasteride through inhibition of complex formation between androgen receptor and steroid receptor-binding consensus in the promoter of the PSA gene in LNCaP cells. Cancer Res. 1997;57:714–9.

32 Pflug BR, Reiter RE, Nelson JB. Caveolin expression is decreased following androgen deprivation in human prostate cancer cell lines. Prostate. 1999;40:269–73.

33 Qi J, Nakayama K, Cardiff RD, Borowsky AD, Kaul K, Williams R, et al. Siah2—dependent concerted activity of HIF and FoxA2 regulates formation of neuroendocrine phenotype and neuroendocrine prostate tumors. Cancer Cell. 2010;18:23–38.

34 Cifone MA, Fidler IJ. Correlation of patterns of anchorage-independent growth with in vivo behavior of cells from a murine fibrosarcoma. Proc Natl Acad Sci U S A. 1980;77:1039–43.

35 Pouliot N PH, Burrows A. Investigating Metastasis Using In Vitro Platforms. In: Jandial R, editor. Metastatic Cancer: Clinical and Biological Perspectives. Madame Curie Bioscience Database: Landes Bioscience; 2000.

36 Pan H, Hanada S, Zhao J, Mao L, Ma MZ. Protein secretion is required for pregnancy-associated plasma protein-A to promote lung cancer growth in vivo. PLoS One. 2012;7:e48799.

37 Wu X, Zang W, Cui S, Wang M. Bioinformatics analysis of two microarray gene-expression data sets to select lung adenocarcinoma marker genes. Eur Rev Med Pharmacol Sci. 2012;16:1582–7.

38 Kumar A, White TA, MacKenzie AP, Clegg N, Lee C, Dumpit RF, et al. Exome sequencing identifies a spectrum of mutation frequencies in advanced and lethal prostate cancers. Proc Natl Acad Sci U S A. 2011;108:17087–92.

39 Chen BY, Lin DP, Liu JY, Chang H, Huang PH, Chen YL, et al. A mouse prostate cancer model induced by Hedgehog overexpression. J Biomed Sci. 2006;13:373–84.

40 Karhadkar SS, Bova GS, Abdallah N, Dhara S, Gardner D, Maitra A, et al. Hedgehog signalling in prostate regeneration, neoplasia and metastasis. Nature. 2004;431:707–12.

41 Grebhardt S, Veltkamp C, Strobel P, Mayer D. Hypoxia and HIF–1 increase S100A8 and S100A9 expression in prostate cancer. Int J Cancer. 2012;131:2785–94.

42 Smirnov DA, Zweitzig DR, Foulk BW, Miller MC, Doyle GV, Pienta KJ, et al. Global gene expression profiling of circulating tumor cells. Cancer Res. 2005;65:4993–7.

43 Li XJ, Ong CK, Cao Y, Xiang YQ, Shao JY, Ooi A, et al. Serglycin is a theranostic target in nasopharyngeal carcinoma that promotes metastasis. Cancer Res. 2011;71:3162–72.

44 Fujita A, Gomes LR, Sato JR, Yamaguchi R, Thomaz CE, Sogayar MC, et al. Multivariate gene expression analysis reveals functional connectivity changes between normal/tumoral prostates. BMC Syst Biol. 2008;2:106.

45 Hood JD, Cheresh DA. Role of integrins in cell invasion and migration. Nat Rev Cancer. 2002;2:91–100.

46 Hossain MN, Sakemura R, Fujii M, Ayusawa D. G-protein gamma subunit GNG11 strongly regulates cellular senescence. Biochem Biophys Res Commun. 2006;351:645–50.

47 Ruiz-Ballesteros E, Mollejo M, Rodriguez A, Camacho FI, Algara P, Martinez N, et al. Splenic marginal zone lymphoma: proposal of new diagnostic and prognostic markers identified after tissue and cDNA microarray analysis. Blood. 2005;106:1831–8.

48 Quek SI, Ho ME, Loprieno MA, Ellis WJ, Elliott N, Liu AY. A multiplex assay to measure RNA transcripts of prostate cancer in urine. PLoS One. 2012;7:e45656.

49 Ponti D, Costa A, Zaffaroni N, Pratesi G, Petrangolini G, Coradini D, et al. Isolation and in vitro propagation of tumorigenic breast cancer cells with stem/progenitor cell properties. Cancer Res. 2005;65:5506–11.

50 Watters JW, Cheng C, Majumder PK, Wang R, Yalavarthi S, Meeske C, et al. De novo discovery of a gamma-secretase inhibitor response signature using a novel in vivo breast tumor model. Cancer Res. 2009;69:8949–57.

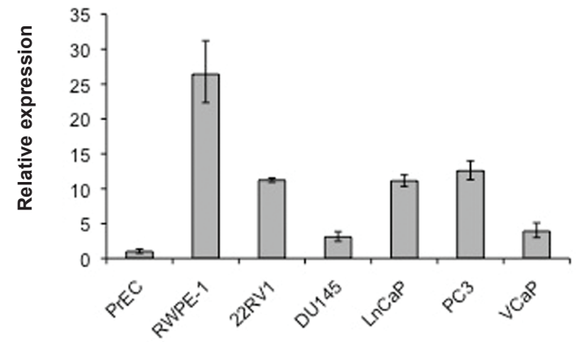

Supplementary Figure 1 — qRT-PCR analysis for *NOTCH3* expression in prostate cell lines. Error bars, mean ± SEM of three technical replicates.

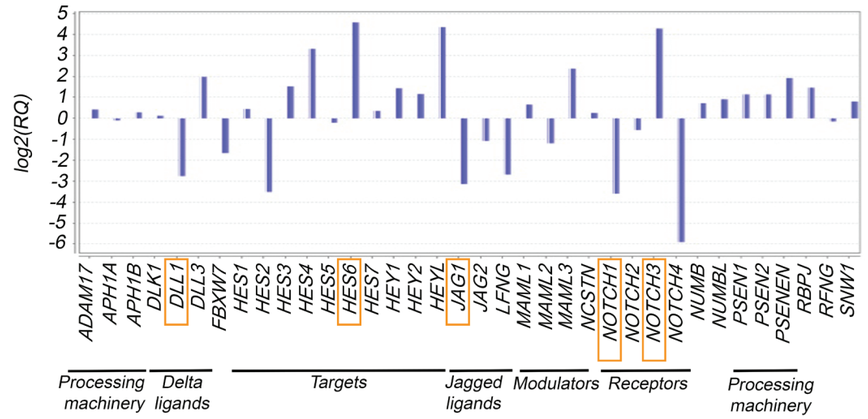

Supplementary Figure 2 — qPCR analysis of Notch pathway members expression in cancer cell lines relative to PrEC. The exclusion of RWPE–1 from the analysis causes a significant increase in *NOTCH3* in cancer cells.

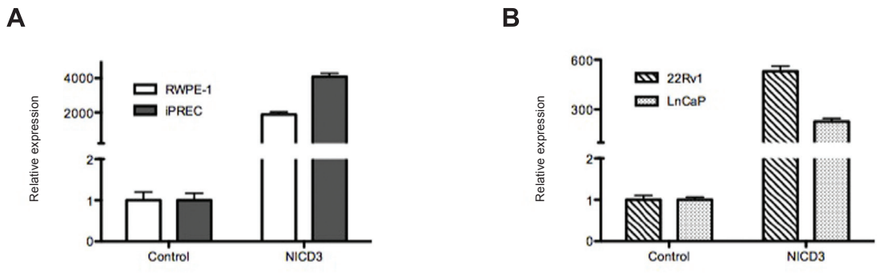

Supplementary Figure 3 — qPCR shows increase in *NOTCH3* transcripts after overexpression of NICD3. We used TaqMan primers to detect increase in NICD3 transcripts because the antibody used to detect NOTCH3 protein expression in western blots (Pro2311; Cell Signaling) recognizes the transmembrane domain and is unable to detect the intracellular portion of the receptor.

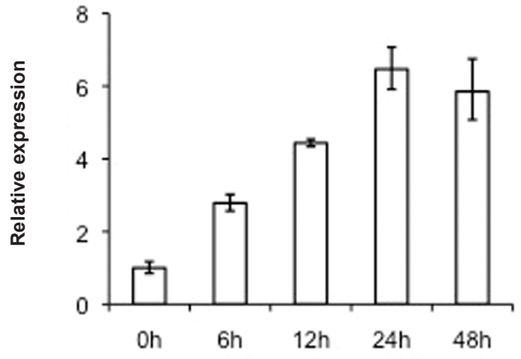

Supplementary Figure 4 — qPCR shows *PSA* transcript levels at several time points after DHT stimulation of LnCaP cells.

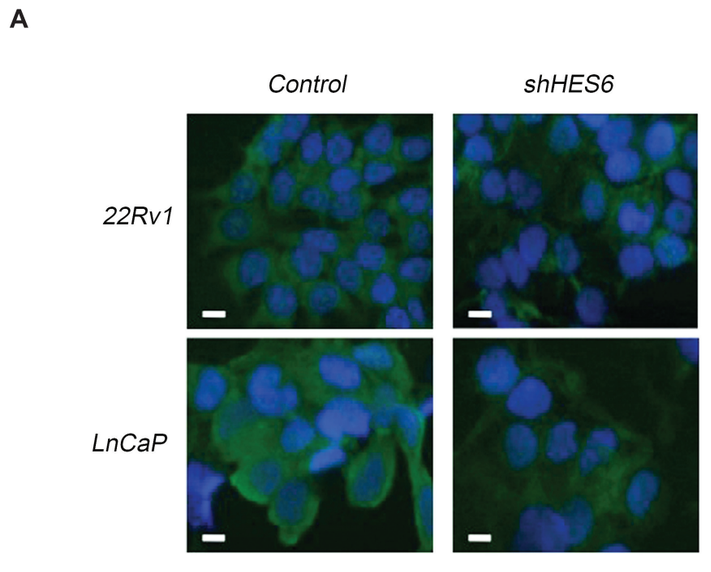

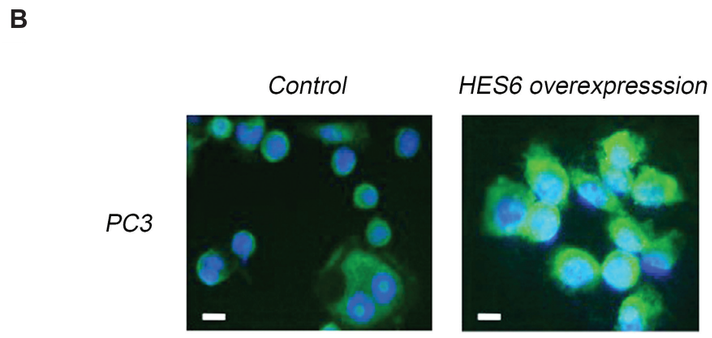

Supplementary Figure 5 — Manipulation of HES6 protein levels in cancer cell lines

A and **B** Photomicrographs of HES6 immunofluorescence in 22Rv1 (top panel) and LnCaP (lower panel) cells after HES6 knockdown, and PC3 (**B**) cells overexpressing HES6. Scale bar, 200μm.

Gene Name	Gene Symbol	Assay Id
Eukaryotic 18S rRNA	18S	Hs99999901_s1
Actin, beta	ACTB	Hs99999903_m1
Hypoxanthine phosphoribosyltransferase 1	HPRT 1	Hs99999909_m1
Glucuronidase, beta	GUSB	Hs99999908_m1
Jagged 1	JAG 1	Hs00164982_m1
Jagged 2	JAG 2	Hs00171432_m1
Numb homolog (Drosophila)-like	NUMBL	Hs00191080_m1
Delta-like 1 (Drosophila)	DLL 1	Hs00194509_m1
Mastermind-like 1 (Drosophila)	MAML 1	Hs00207373_m1
Anterior pharynx defective 1 homolog A (C. elegans)	APH1A	Hs00211268_m1
Delta-like 3 (Drosophila)	DLL 3	Hs00213561_m1
F-box and WD repeat domain containing 7	FBXW7	Hs00217794_m1
Anterior pharynx defective 1 homolog B (C. elegans)	APH1B	Hs00229911_m1
Presenilin 1	PSEN1	Hs00240518_m1
Presenilin 2 (Alzheimer disease 4)	PSEN2	Hs00240982_m1
SNW domain containing 1	SNW1	Hs00273351_m1
Mastermind-like 3 (Drosophila)	MAML3	Hs00298519_s1
Nicastrin	NCSTN	Hs00299716_m1
Notch 1	NOTCH 1	Hs01062011_m1
Notch 2	NOTCH 2	Hs01050719_m1
Notch 3	NOTCH 3	Hs01128541_m1
Notch 4	NOTCH 4	Hs00965889_m1
Mastermind-like 2 (Drosophila)	MAML 2	Hs00418423_m1
Presenilin enhacer 2 homolog (C. elegans)	PSENEN	Hs00708570_s1
Recombination signal binding protein for immunoglobulin kappa J region	RBPJ	Hs00794653_m1
ADAM metallopeptidase domain 17	ADAM 17	Hs01041915_m1
LFNG O-fucosylpeptide 3–beta-N-acetylglucosaminyltransferase	LFNG	Hs01046129_m1
RFNG O-fucosylpeptide 3–beta-N-acetylglucosaminyltransferase	RFNG	Hs01357010_g1
Delta-like 1 homolog (Drosophila)	DLK 1	Hs00171584_m1
Hairy and enhancer of slip 1 (Drosophila)	HES 1	Hs00172878_m1
Hairy and enhancer of slip 2 (Drosophila)	HES 2	Hs00219505_m1
Hairy and enhancer of slip 3 (Drosophila)	HES 3	Hs01367669_g1
Hairy and enhancer of slip 4 (Drosophila)	HES 4	Hs00368353_g1
Hairy and enhancer of slip 5 (Drosophila)	HES 5	Hs01387464_g1
Hairy and enhancer of slip 6 (Drosophila)	HES 6	Hs00936587_g1
Hairy and enhancer of slip 7 (Drosophila)	HES 7	Hs00261517_m1
Hairy/enhancer of slip related with YRPW motif 1	HEY 1	Hs00232618_m1
Hairy/enhancer of slip related with YRPW motif 2	HEY 2	Hs00232622_m1
Hairy/enhancer of slip related with YRPW motif-like	HEYL	Hs00232718_m1
Numb homolog (Drosophila)	NUMB	Hs00377772_m1
Ribosomal protein 18	RPL 18	Hs00965812_g1

Supplementary Table S1 —

Gene Name	Gene Symbol	Forward	Reverse
Prostate-spesific antigen	PSA	TGAACCAGAGGAGTTCTTGAC	TGACGTGATACCTTGAAGCA
Hypoxanthine phosphoribosyltransferase 1	HPRT	TGGGAGGCCATCACATTGTA	CCAGCAGGTCAGCAAAGAATT
DNA (cytosine–5)-methyltransferase 3 beta	DNMT3B	AGGGAAGACTCGATCCTCGTC	GTGTGTAGCTTAGCAGACTGG
Purinergic receptor P2Y G-protein coupled 14	P2RY14	TACGTGCCCAGCTCTAAGAGT	GTCACCAAGGATCTTGAAAGGAA
Pregnancy-associated plasma protein A, pappalysin 1	PAPPA	ACAAAGACCCACGCTACTTTTT	CATGAACTGCCCATCATAGGTG
Serglycin	SRGN	GGACTACTCTGGATCAGGOTT	CAAGAGACCTAAGGTTGTCATGG
Suppressor of fused homolog (Drosophila)	SUFU	GCCTGAGTGATCTCTATGGTGA	TCTCTCTTCAGACGAAAGGTCAA
Interleukin 1 beta	IL1B	ATGATGGCTTATTACAGTGGCAA	GTCGGAGATTCGTAGCTGGA
BMX non-receptor tyrosine kinase	BMX	GAGTGCTGAAGATACCTCGGG	CGTTGTCATATTGGGCTAGAGTG
Alpha thalassemia/mental retardation syndrome X-linked	ATRX	GCAACCTTGGTCGAAAGGAGT	GGCTCTGGGTGACAAATGTAG
B-cell CLL/lymphoma 2	BCL2	GGTGGGGTCATGTGTGTGG	CGGTTCAGGTACTCAGTCATCC
Baculoviral IAP repeat containing 3	BIRC3	TTTCCGTGGCTCTTATTCAAACT	GCACAGTGGTAGGAACTTCTCAT
DEAD (Asp-Glu-Ala-Asp) box polypeptide 51	DDX51	GGCTGGCTGAGCCTAACTG	GGACTGGAAAGTAGGACGAGAT
Delta-like 2 homolog (Drosophila)	DLK2	GTACCATTGTGTGTGCTTACCA	CAGGCAGTCATCCACATTTACC
Interferon regulatory factor 4	IRF4	GCTGATCGACCAGATCGACAG	CGGTTGTAGTCCTGCTTGC
Lymphocyte-specific protein tyrosine kinase	LCK	TGCCATTATCCCATAGTCCCA	GAGCCTTCGTAGGTAACCAGT
Myosin light chain kinase	MYLK	CCCGAGGTTGTCTGGTTCAAA	GCAGGTGTACTTGGCATCGT
Ras-related C3 botulinum toxin substrate 1 (rho family, small GTP binding protein Rac1)	RAC1	ATGTCCGTGCAAAGTGGTATC	CTCGGATCGCTTCGTCAAACA
Integrin, beta 2 (complement component 3 receptor 3 and 4 subunit)	ITGB2	AAGTGACGCTTTACCTGCGAC	AAGCATGGAGTAGGAGAGGTC
WNK lysine deficient protein kinase 3	WNK3	ACTTCTCCTAGTGGCAGATTCC	GCAGCTCACACCAAGCAAC
Aldehyde dehydrogenase 1 family, member A2	ALDH1A2	TTGCAGGGCGTCATCAAAAC	ACACTCCAATGGGTTCATGTC
Basal cell adhesion molecule (Lutheran blood group)	BCAM	CAGGTCACAATGCACGACAC	CACCACGCACACGTAGTCT
CD24 molecule	CD24	CTCCTACCCACGCAGATTTATTC	AGAGTGAGACCACGAAGAGAC
Forkhead box O3	FOXO3	ACGGCTGACTGATATGGCAG	CGTGATGTTATCCAGCAGGTC
Mitogen-activated protein kinase kinase 2	MAP2K2	AGGTCCTGCACGAATGCAA	CGTCCATGTGTTCCATGCAA
Matrix metallopeptidase 7 (matrilysin, uterine)	MMP7	GAGTGAGCTACAGTGGGAACA	CTATGACGCGGGAGTTTAACAT
Methylthioadenosine phosphorylase	MTAP	ACCACCGCCGTGAAGATTG	GCATCAGATGGCTTGCCAA
SRY (sex determining region Y)-box 6	SOX6	TACCTCTACCTCACCACATAAGC	ACATCGGCAAGACTCCCTTTG
STIP1 homology and U-box containing protein 1, E3 ubiquitin protein ligase	STUB1	AGCAGGGCAATCGTCTGTTC	CAAGGCCCGGTTGGTGTAATA
Sushi domain containing 1	SUSD1	GGGCAGCCAGGTTCGTTAT	TCTGGAGGGTTGCCACAGT
TNF receptor-associated factor 4	TRAF4	CAGGAGAGTGTCTACTGTGAGA	CCACACCACATTGGTTGGG
Recombination signal binding protein for immunoglobulin kappa J region	RBPJ	AACAAATGGAACGCGATGGTT	GGCTGTGCAATACTTCTTTCCTT

Supplementary Table S2 A —

Gene Name	Gene Symbol	Forward	Reverse
S100 calcium binding protein A14	S100A14	GAGACGCTGACCCCTTCTG	CTTGGCCGCTTCTCCAATCA
S100 calcium binding protein A8	S100A8	ATGCCGTCTACAGGGATGAC	ACTGAGGACACTCGGTCTCTA
S100 calcium binding protein A9	S100A9	GGTCATAGAACACATCATGGAGG	GGCCTGGCTTATGGTGGTG
STEAP family member 4	STEAP4	CCTCAGCCCTTCAAATCTCAG	ACATGGCATGATTAGGACAAACT
Acyl-CoA synthetase long-chain family member 5	ACSL5	CTCAACCCGTCTTACCTCTTCT	GCAGCAACTTGTTAGGTCATTG
Annexin A2	ANXA2	GAGCGGGATGCTTTGAACATT	TAGGCGAAGGCAATATCCTGT
Rho GDP dissociation inhibitor (GDI) beta	ARHGDIB	GACTGGGGTGAAAGTGGATAAAG	TCGTCGGTGAAGAAGGACTTG
ATP synthase H+ transporting mithochondrial Fo complex subunit G	ATP5L	ATGGCCCAATTTGTCCGTAAC	TGGCGTAGTACCAAAATGTGG
Bardet-Biedl syndrome 10	BBS10	CCGAGGGACGGCAAGTTTT	TGGGATGCTCTAAGTGTAGCG
Breast carcinoma amplified sequence 2	BCAS2	TGGATGCGCTGCCGTATTTT	GGTATCTGCGAGTTTCCTCCTC
Calbindin 2	CALB2	AGCGCCGAGTTTATGGAGG	TGGTTTGGGTGTATTCCTGGA
Cyclin D2	CCND2	TTTGCCATGTACCCACCGTC	AGGGCATCACAAGTGAGCG
Calcium and integrin binding family member 3	CIB3	GCGTATCAGGACTGCACATTT	GCAGGTGGTATAGTCGAGGG
Cornichon homolog 3 (Drosophila)	CNIH3	GAGCCCCATAGACCAGTGC	CACCAGCTTTCGCAGAAGGA
Deleted in malignant brain tumors 1	DMBT1	CAAGGACTACAGACTACGCTTCA	TCCGAGGGAAATGGAGAACCT
Eukaryotic translation initiation factor 4E	EIF4E	GAAACCACCCCTACTCCTAATCC	AGAGTGCCCATCTGTTCTGTA
EPH receptor B2	EPHB2	GTGTGCAACGTGTTTGAGTCA	ACGCACCGAAAACTTCATCTC
Fasciulation and elongation protein zeta 1 (zygin I)	FEZ1	CCACTGGTGAGTCTGGATGAA	CGGAAGAAAAATTCTCAAGCTCG
Galactosidase alpha	GLA	TTGGATACTACGACATTGATGCC	TTCTGCCAGTCCTATTCAGGG
GLI pathogenesis-related 1	GLIPR1	TCCGATCAGAGGTGAAACCAA	GGCTTCAGCCGTGTATTATGTG
Guanine nucleotide binding protein (G protein), gamma 11	GNG11	CCTGCCCTTCACATCGAAGAT	CTTCTTTGCGAAGCTGCTCAA
Interleukin 22	IL22	GCTTGACAAGTCCAACTTCCA	GCTGACTCATACTGACTCCGT
Keratin associated protein 3–1	KRTAP3–1	ACCTGCCCACATGAGATCAG	GGCACATAGGTATCAGGCTTG
Mitogen-activated protein kinase 11	MAPK11	AAGCACGAGAACGTCATCGG	TCACCAAGTACACTTCGCTGA
MAX-like protein X	MLX	TGTCCACGTTACGCAAGGATG	GGTGTGCCTTCACAATCTGCT
MutS homolog 2, colon cancer, nonpolyposis type 1 (E. coli)	MSH2	CACTGTCTGCGGTAATCAAGT	CTCTGACTGCTGCAATATCCAAT
Prostate and testis expressed 3	PATE3	ATCACTTCAGTGCATAACATGCC	CTCGCCCTTCTGAGCAGTA
Piccolo (presynaptic cytomatrix protein)	PCLO	TGTTACCACTACATCAGCACTGA	AGCCATGAAGGGTTGGTTGTT
Phosphoinositide–3–kinase, class 3	PIK3C3	GTCTGGCCTAATGTAGAAGCAG	GGCAAGACGGCTCATCTGAT
PC4 and SFRS 1 interacting protein 1	PSIP1	CAACAGGCAGCAACTAAACAATC	TCATGGTCGGTATCTTCCTTTGA
Resistin like beta	RETNLB	CCGTCCTCTTGCCTCCTTC	CTTTTGACACTAGCACACGAGA
Short chain dehydrogenase/reductase family 9C, member 7	SDR9C7	CAGCGGGATACCTCCTATCG	GCCTTGTTCGCCCACTTTG
Sushi domain containing 5	SUSD5	GTGGTACAGGATTGCTCCTTTG	CCACTTCCTTTGCTACACACAG

Supplementary Table S2 B —

CHAPTER 5 —
PTEN LOSS DISTINGUISHES PROSTATE CANCER PATIENTS' CANDIDATES FOR ACTIVE SURVEILLANCE

PTEN LOSS DISTINGUISHES PROSTATE CANCER PATIENTS' CANDIDATES FOR ACTIVE SURVEILLANCE

PTEN Loss is Associated with Upgrading of Prostate Cancer from Biopsy to Radical Prostatectomy

Tamara L. Lotan[1,2*], Filipe LF. Carvalho[1*], Sarah B. Peskoe[3], Jessica L. Hicks[1], Jennifer Good[4], Helen Fedor[1], Elizabeth Humphreys[5], Misop Han[5], Elizabeth A. Platz[3], Jeremy A. Squire[4,6], Angelo M. De Marzo[1,2,5], David M. Berman[1,4,5]
Departments of [1]Pathology, [2]Oncology, Johns Hopkins University School of Medicine; [3]Department of Epidemiology, Johns Hopkins Bloomberg School of Public Health; [4]Department of Pathology and Molecular Medicine, Queen's University, Kingston, ON, Canada; [5]Department of Urology and the James Buchanan Brady Urological Institute, Johns Hopkins University School of Medicine, [6]Department of Pathology, University of Sao Paulo, Ribeirão Preto, Brazil.

*These authors contributed equally to this work

Word count 2793

Running Title PTEN Loss at Biopsy is Associated with Prostate Cancer Upgrading at Radical Prostatectomy

Keywords: Prostatic adenocarcinoma; PTEN; upgrading; radical prostatectomy; biopsy.

Financial Support Funding for this research was provided in part by a Prostate Cancer Foundation Young Investigator Award (TLL) and a grant from David Koch administered by the Patrick C. Walsh Prostate Cancer Research Fund (TLL). PhD grant from Fundação para Ciência e Tecnologia (SFRH/ BD/ 69819/ 2010 to FLFC)

To whom correspondence should be addressed
Tamara Lotan, MD
855 N. Wolfe Street Baltimore, MD 21205
(410) 614–9196 (ph)
(410) 502–9911 (fax)
e-mail: tlotan1@jhmi.edu

David M. Berman, MD, PhD
18 Stuart St.
Kingston, ON K7L 2C4 Canada
613–533–6000 ext 75218
bermand@queensu.ca

Conflicts of Interest DMB has consulted and/or performed sponsored research for Myriad Genetics and Metamark Genetics; JAS has consulted for CymoGen Dx, LLC.

Abstract

Background Though active surveillance is increasingly recommended, approximately one third of patients with Gleason score 3+3=6 (GS6) cancer on biopsy are upgraded to higher GS at radical prostatectomy (RP). Clinical-pathologic parameters are only weak predictors of upgrading.

Objective To investigate whether PTEN loss in GS6 biopsies is associated with upgrading at RP.

Design, setting and participants 71 patients with GS6 tumors on needle biopsy upgraded to GS7 or higher cancer at RP (cases) were compared to 103 patients with GS6 on both biopsy and RP (controls). Patients were from tertiary care and community care settings.

Outcome Measurements and Statistical Analysis A previously validated immunohistochemical (IHC) assay for PTEN loss was performed on all biopsies, followed by fluorescence in situ hybridization (FISH) to detect PTEN gene deletion in biopsies with PTEN loss. The association of PTEN loss with upgrading and clinical-pathologic variables was assessed by logistic regression.

Results and limitations Upgraded patients were older than controls (61.8 vs. 59.3 years), had higher pre-operative PSA levels (6.53 vs. 5.26 ng/mL), and had a higher fraction of involved cores (0.42 vs. 0.36). PTEN loss by IHC was found in 18.3% (13/71) of upgraded cases compared to 6.8% (7/103) of controls (p=0.02). Of these biopsies with PTEN protein loss, FISH demonstrated homozygous PTEN deletion in 90% (9/10) of upgraded tumors compared to 67% (4/6) of controls. Tumors with PTEN loss were significantly more likely to be upgraded at RP than those without loss, even after adjusting for age, preoperative PSA, clinical stage and race (OR = 3.04 [1.08–8.55; p=0.035]).

Conclusions PTEN loss in GS6 biopsies is associated with upgrading at RP.

Patient summary A simple test can be conducted on low grade prostate cancer biopsies to help identify patients with potentially unsampled higher risk disease who may not be good candidates for active surveillance.

Introduction

Based on pathologic examination of the entire prostate, the Gleason grading system distinguishes between indolent Gleason score 3+3=6 (GS6) cancers and cancers with lethal potential, virtually all of which are Gleason score 3+4=7 (GS7) or higher [1–5]. If this information were available at the time of diagnosis, it would be relatively simple to identify appropriate candidates for deferred treatment or active surveillance (AS) in place of definitive therapy. However, a recent meta-analysis, including more than 14,000 cases, suggests that this is frequently not the case: a mean of 36% (range: 14–51%) of apparently indolent GS6 tumors on needle biopsy are "upgraded" to GS7 or higher at RP [6].

Currently, there are relatively few predictors of which patients with GS6 prostate tumors on needle biopsy are likely to harbor higher grade disease. Tumor upgrading from needle biopsy to RP can occur for multiple reasons, including tumor progression, pathology errors, and inter-observer variability in Gleason grading. However, a common cause is under-sampling of the highest Gleason score cancer [6]. Unfortunately, increasing the number of needle cores above the current standard of 12 does not substantially reduce the frequency of upgrading [7]. While MRI-based imaging is becoming more promising in this regard [8], imaging is expensive and not widely used. Further, prior studies have found that clinical-pathologic parameters such as higher preoperative PSA, lower prostate volume, and more extensive disease on biopsy are relatively weak predictors of upgrading [9–15]. To date, no molecular biomarkers have been validated for association with upgrading.

We and others have shown that PTEN, a tumor suppressor, is most commonly lost in prostate tumors with high Gleason grade and high stage [16–25]. Recently, we developed and validated a simple and inexpensive immunohistochemical (IHC) assay to assess PTEN status in prostate cancer [16]. Using this assay, we showed that PTEN protein loss, assessed by a simple dichotomous scoring system, is highly correlated with underlying genetic deletions of the PTEN gene and is associated with decreased time to biochemical recurrence, disease progression and metastasis in contemporary surgical cohorts [16–18]. Here, we demonstrate that PTEN loss in GS6 needle biopsy specimens is associated with GS upgrading in the final RP specimen.

Patients and Methods

Patients and tissue samples With institutional review board approval, the Johns Hopkins Hospital (JHH) Pathology database was queried for all needle biopsies performed at JHH (a tertiary care hospital) or Johns Hopkins Bayview Medical Center (BMC, a community care setting) that contained only GS6 tumor followed by a radical prostatectomy (RP) specimen that contained GS7 or higher tumor occurring between 2000–2011. Controls with GS6 tumor on biopsy followed by GS6 tumor on RP were selected from sequential biopsies occurring between 2000–2004 at JHH and 2000–2011 at BMC. As is routine at JHH and BMC, all RP specimens were entirely submitted and processed for histologic analysis. All biopsies and RP slides were re-reviewed and re-graded by trained uropathologists (DMB and TLL) using the 2005 modified International Society of Urologic Pathology (ISUP) grading system [26]. Each case was assigned a primary, secondary and tertiary (for RP specimens) Gleason pattern. Upgrading was defined by the Gleason score without reference to the tertiary component since studies from the era predating the use of tertiary grades support the negligible lethality associated with GS6 tumors [1]. A single block (generally consisting of two cores) containing the largest percentage involvement by tumor was selected for PTEN immunostaining described below.

PTEN Immunohistochemistry and interpretation PTEN IHC was performed as previously described and blindly scored by two uropathologists (TLL and DMB) using a previously validated dichotomous scoring system [16]. In cases where the two scoring uropathologists disagreed (17/174 or 10% of total), a third uropathologist (AMD) blindly scored the case to break the tie.

PTEN FISH Four-color FISH was performed and interpreted as described previously using the PTEN del-TECT probe (CymoGen Dx, LLC, New Windsor, NY) [23, www.ptendeletion.net]. A hematoxylin and eosin stained needle core section was available for comparison to confirm marked regions of interest.

Statistical analysis Means and proportions of pre-and post-operative characteristics of cases and controls were compared using the two-sample t-test and the chi-square test, respectively. Multivariable logistic regression was used to estimate the odds ratios (ORs) and 95% confidence intervals (CI) of a biopsy upgrade among men with PTEN loss. First, ORs were estimated adjusted for age at diagnosis. Next, results were adjusted for preoperative PSA (continuous, log-transformed) and clinical stage (binary, T2 or higher). Results were further adjusted for race (binary, nonwhite). Statistical analyses were performed using SAS 9.3 (Cary, NC).

Results

Pre-operative clinical-pathologic parameters The mean age of the 71 upgraded cases was slightly older than that of the 103 controls who were not upgraded (61.8 vs. 59.3 years; p=0.005) (Table 1). The racial makeup of the two cases and controls was not significantly different. The mean pre-operative serum PSA level was 23% higher in the upgraded cases (6.53 vs. 5.26 ng/mL; p= 0.009), but there was no difference in clinical stage distribution between the two groups. The majority of patients underwent RP within 3 months of biopsy diagnosis and there was no significant difference in the pre-operative interval between groups.

Variable	Controls	Cases	P
Age at diagnosis [mean (SD)]	59.3 (6.2)	61.8 (5.3)	0.005
Non-white (%)	21.4	29.6	0.22
Pre-operative PSA (ng/mL) [mean (SD)]	5.26 (2.95)	6.53 (3.40)	0.009
PSA density* [mean (SD)]	0.10 (0.07)	0.13 (0.08)	0.002
Clinical Stage (%)			
1 – T1c	83.7	89.4	0.57
2 – T2a	13.3	9.1	
3 – T2b	3.0	1.5	
% missing	4.9	7.0	
Days between biopsy and RP [mean (SD)]	90.6 (53)	103.7 (54)	0.12
Number of cores sampled [mean (SD)]	12.2 (1.1)	11.9 (1.1)	0.06
Less than 12 cores sampled (%)	3.9	8.5	0.20
Number involved cores [mean (SD)]	3.6 (2.2)	4.2 (2.3)	0.08
Fraction involved cores [mean (SD)]	0.3 (0.18)	0.36 (0.21)	0.04
Maximum percent tumor per core [mean (SD)]	48 (25)	51 (27)	0.40
Bilateral involved cores (%)	41.2	54.9	0.07
Perineural invasion (%)	22.3	25.4	0.64
PTEN loss by IHC (%)	6.8	18.3	0.02

*PSA density was calculated using the prostate weight at radical prostatectomy.

Table 1 — Pre-Operative Characteristics of Cases and Controls (103 Controls, 71 Cases)

Greater than 90% of both cases and controls had a 12–core biopsy performed, with a comparable number of cores examined in the cases compared to the controls (12.2 vs.11.9; p=0.06). The fraction of cores involved by tumor was slightly higher in the cases (0.36 vs. 0.30; p=0.04), however the maximum percent tumor per core was not significantly different between groups. Tumor was present on bilateral cores (from the left and right prostate) in a higher percentage of the upgraded cases compared to controls (54.9% vs. 41.2%, p=0.07). Finally, the fraction of cases with perineural invasion was not significantly different between groups.

Post-operative clinical-pathologic parameters: To validate the clinical significance of tumor upgrading, post-operative clinical-pathologic parameters for the two groups of patients were assessed (Table 2). Upgraded cases had smaller mean prostate weights at RP (54.4 vs. 59.8 grams) although this did not reach statistical significance (p=0.17). As expected, upgraded cases were significantly more likely to have had extraprostatic extension or seminal vesicle involvement at RP than controls (34.8% vs. 17.6%; p = 0.01). Accordingly, upgraded cases were more likely to have positive margins at RP (23.9% vs. 7.8%; p=0.003) as well as PSA recurrence (8.8% vs. 1.2%; p=0.03), with a mean follow-up period of 3.6 and 4.5 years respectively for the roughly 80% of patients with available information in each group.

Variable	Controls	Cases	P
Gland weight [mean (SD)]	59.8 (28.9)	54.4 (23.0)	0.17
Pathologic stage (%)			
T2	82.3	65.2	0.03
T3a	15.7	27.5	
T3b	2.0	7.3	
Node positive	0.0	1.5	0.23
% missing	1.0	2.8	
Path stage > T2 (%)	17.6	34.8	0.0107
% missing	1.0	2.8	
Positive margins	7.8	23.9	0.003
PSA recurrence (%)	1.2	8.8	
% missing	19.4	19.7	
Years of followup [mean (SD)]	4.5 (3.4)	3.6 (3.2)	0.10

Table 2 — Post-operative Characteristics of Cases and Controls (103 Controls, 71 Cases)

PTEN protein loss and PTEN gene status PTEN protein loss was present in 18.3% (13/71) of the upgraded tumors compared to only 6.8% (7/103) of the controls (p=0.02). A subgroup analysis of the two hospital populations included in the study showed nearly identical results in both patient populations (17.9% and 20% for cases in JHH and BMC respectively; and 6.9% and 6.4% for controls, respectively). PTEN protein loss was frequently focal within a given tumor sample (Figures 1 and 2) with heterogeneous PTEN staining in 85% (11/13) of the upgraded cases with PTEN loss and 100% (7/7) of the controls.

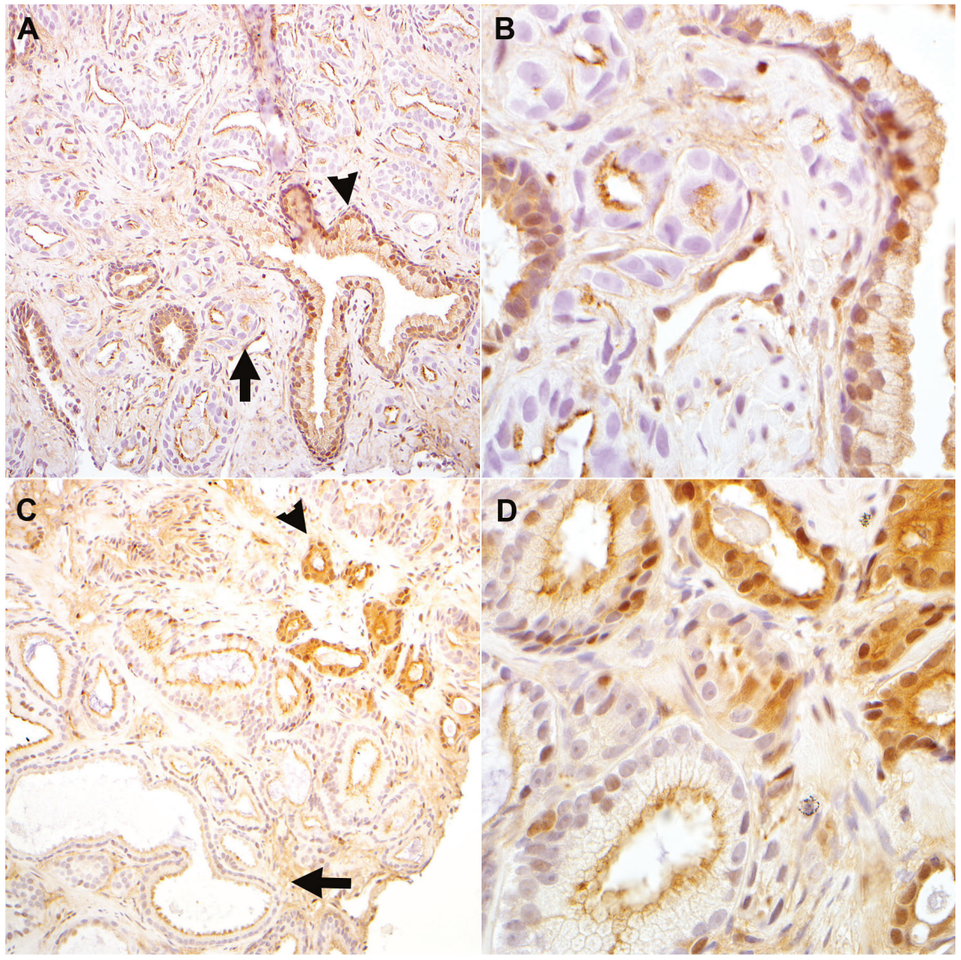

Figure 1 — Gleason Score 6 prostate biopsies that are upgraded to Gleason Score 7 at radical prostatectomy show PTEN protein loss by immunohistochemistry (IHC)

A Low power (200x magnification) photomicrograph of PTEN IHC in a GS6 needle biopsy specimen demonstrates PTEN protein loss in tumor glands (arrow) with preservation of PTEN staining in intermingled benign glands (arrowheads)

B High power (630x) image highlights infiltrating tumor glands with PTEN loss and surrounding benign glands with intact staining

C Low power (200x magnification) photomicrograph of tumor with heterogeneous PTEN loss, demonstrating PTEN loss in some tumor glands (arrow) and intact PTEN protein in adjacent tumor (arrowhead)

D High power (630x) image showing tumor glands with and without PTEN protein loss. Note the presence of apical membrane staining and rare nuclear PTEN in glands with cytoplasmic PTEN loss, though the significance of these findings is unclear.

A recently developed 4–color FISH assay [23] was used to assess for PTEN gene deletions in the 20 biopsies with decreased PTEN protein by IHC. PTEN FISH was evaluable in 86% of the non-upgraded controls (6/7) and 77% (10/13) of the upgraded cases. Biopsies that could not be evaluated included those where the FISH hybridization failed (n=2) or where the tumor area with decreased PTEN protein could not be aligned on the adjacent histologic section on which the FISH was performed (n=2). Among the evaluable upgraded cases, 90% (9/10) of the biopsies with decreased PTEN protein showed homozygous PTEN deletions by FISH, variably involving the adjacent gene probes for FAS and WAPAL (Figure 2).

Only one upgraded case (10%) with PTEN protein loss lacked PTEN gene deletion as assessed by FISH. Among the evaluable non-upgraded controls that showed unambiguous loss of PTEN protein by IHC, 67% had homozygous PTEN gene deletions (4/6), while 17% (1/6) had a hemizygous deletion and 17% (1/6) had no apparent PTEN deletion. In cases where PTEN protein loss was focal by IHC, PTEN FISH was evaluated in both the tumor areas with and without PTEN protein immunostaining. In these heterogeneous cases, the FISH for PTEN gene deletions was generally concordant with the IHC (Figure 2). Thus, FISH analysis confirmed the results of IHC analysis in 87% of evaluable cases.

Association of PTEN protein loss and upgrading: Logistic regression was performed to assess whether PTEN loss was independently associated with GS upgrading (Table 3).

The variables adjusted in the multivariable analysis were those that have been found to be associated with upgrading in the current and multiple prior studies, including patient age and race, pre-operative PSA level and clinical stage. Even after adjusting for all of these variables (Model B), the odds ratio of GS upgrading was 3.04 (95% confidence interval: 1.08-8.55; p= 0.035) for PTEN protein loss.

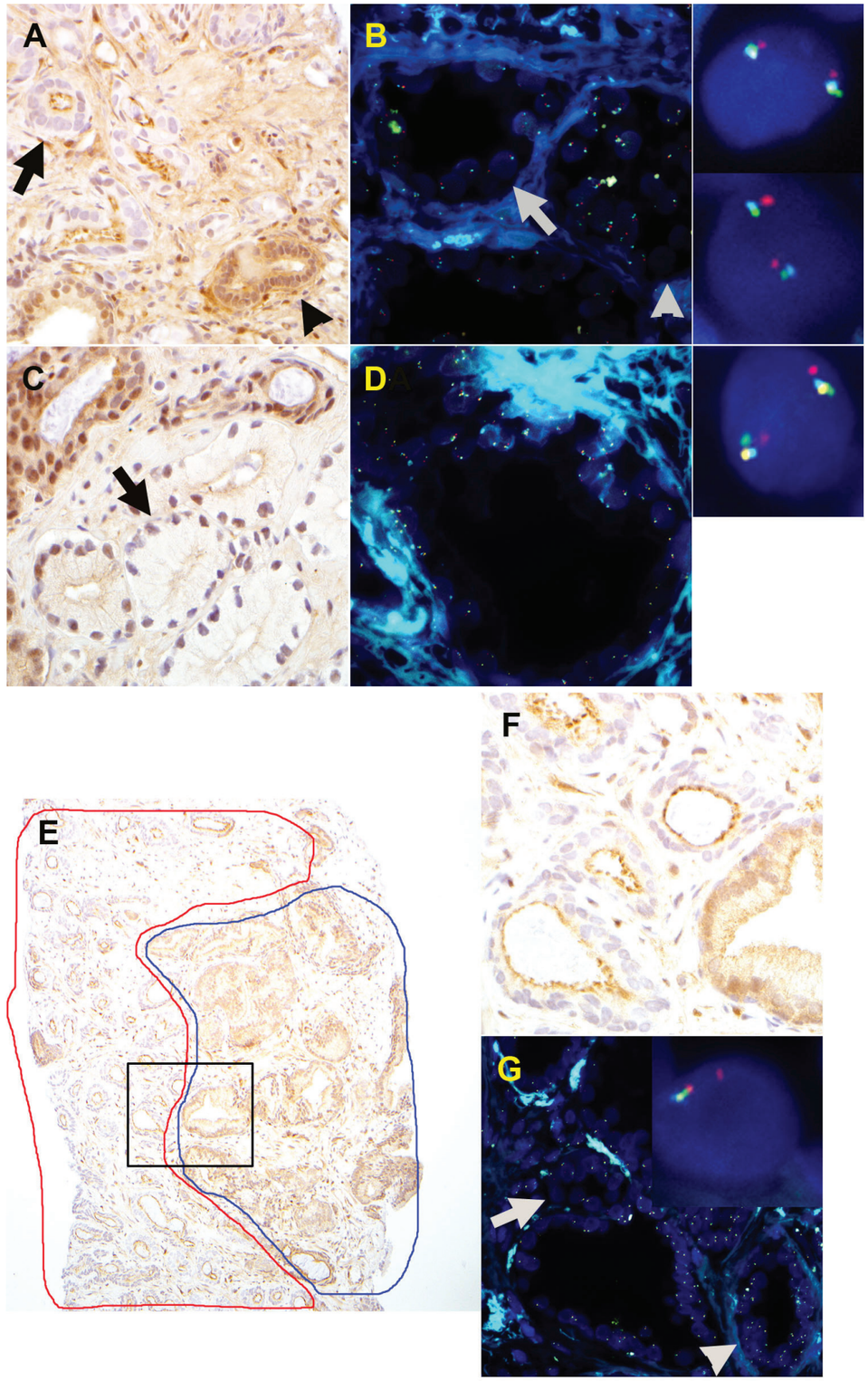

Previous Page:

Figure 2 — PTEN FISH results are highly concordant with PTEN immunohistochemistry (IHC)

A PTEN IHC image (200x magnification) demonstrating PTEN protein loss in tumor glands (arrow) and PTEN protein retention in nearby benign glands (arrowhead)

B PTEN FISH image captured from the tumor in (**A**) demonstrates glands with homozygous PTEN loss (orange signal; arrow and upper right panel) intermixed with glands with PTEN intact (orange signal; arrowhead, lower right panel). Peri-centromeric control probes (red) as well as flanking gene probes WAPAL (green) and FAS (aqua) are intact in all cells

C PTEN IHC image (200x magnification) from a separate Gleason score 6 biopsy that was not upgraded at radical prostatectomy demonstrating focal loss of cytoplasmic PTEN protein in tumor glands (arrow). Adjacent tumor glands stain positively

D PTEN FISH image captured from tumor in (**C**) demonstrates diploid tumor cells throughout (inset)

E PTEN IHC image (100x) demonstrates PTEN protein loss in tumor glands (red outline) with PTEN protein retention in adjacent benign glands (blue outline)

F Higher power (630x) image of boxed area from (**E**)

G PTEN FISH image captured from region delineated in (**E**) demonstrates intermixed glands with hemizygous PTEN, WAPAL and FAS deletion (arrow, inset) and diploid glands (arrowhead)

Model	OR (95% CI)	P
Age-adjusted	2.93 (1.08-7.95)	0.034
Multivariable-adjusted A*	2.81 (1.01-7.82)	0.047
Multivariable-adjusted B†	3.04 (1.08-8.55)	0.035

* Additionally adjusted for preoperative PSA (continuous, log-transformed), and clinical stage (binary, T2 or higher)

† Additionally adjusted for preoperative PSA (continuous, log-transformed), clinical stage (binary, T2 or higher), and race (binary, nonwhite)

Table 3 — Odds ratio for upgrading from GS 6 tumor with PTEN protein loss

Discussion

Biopsy GS underestimates the true GS in up to one third of cases, hindering the urologist's ability to select optimal candidates for active surveillance. Here, we have shown that PTEN protein loss, assessed by a simple immunohistochemical (IHC) assay, is associated with tumor upgrading in GS6 biopsies. To our knowledge, this study is the first to support the utility of a single molecular marker in this setting. Compared to other types of biomarker assays, such as gene expression profiling arrays, one important advantage of PTEN IHC is that it is an inexpensive test that can easily be introduced into the workflow of any accredited pathology laboratory. Scored by a simple binary system, we have demonstrated low inter-observer variability for PTEN IHC by trained pathologist reviewers [16]. However, in cases with

indeterminate results, PTEN FISH will likely play a key role in resolving ambiguities, analogous to its use in the setting of Her2 assessment in breast cancer. Additionally, in our cohort of GS6 biopsies, PTEN gene deletions were frequently quite focal, thus PTEN IHC had the important advantage of focusing FISH scoring on the appropriate area of the tumor, improving the speed and likely also the accuracy of FISH analysis.

The association of PTEN loss with tumor upgrading in GS6 needle biopsies suggests that Gleason pattern 3 tumor associated with adjacent pattern 4 differs at the genomic level from pattern 3 derived from a purely GS6 tumor [24,27]. Indeed, using radical prostatectomy (RP) specimens, we have found that PTEN protein loss in pattern 3 carcinoma from a GS7 cancer is significantly more common than that of pattern 3 carcinoma from a purely GS6 tumor (AMD and Bruce Trock, in preparation). These studies suggest that an integrated approach exploiting genomic markers in limited tumor biopsy specimens will very likely improve on the prognostic accuracy of our current pathologic grading system. Such improvements are sorely needed to avoid overtreatment of indolent prostate cancers.

In the current study, we report a very high correlation between PTEN IHC and FISH results. It is notable that such a large majority (87%) of cases with PTEN protein loss had underlying PTEN deletions in the current study. Given the general prevalence of hemizygous over homozygous deletions in previous PTEN FISH studies in localized prostate cancer [21,24], a surprising finding in the current study was that the majority of GS6 cases with PTEN protein loss showed homozygous PTEN gene deletion. This result may be attributable to the fact that we only performed PTEN FISH on cases showing PTEN protein loss by IHC. It is possible that the PTEN IHC assay may be relatively insensitive for detecting cases with hemizygous PTEN gene loss where protein levels may be somewhat lower compared to normal cases, but not markedly decreased due to the presence of one allele of the gene. It is also possible that focal/subclonal homozygous deletions in primary prostate cancer are more common than previously thought [28]. Future studies will examine whether hemizygous deletions may predict upgrading. If so, performance of IHC with FISH may represent the optimal strategy for risk assessment.

Our study has a number of important strengths for routine clinical practice. Although our patients were not enrolled in active surveillance protocols, 85% of them would have met the extended criteria for active surveillance recently evaluated at our institution [29], strongly suggesting that the results of the current study are relevant to this clinical setting. The vast majority of patients (>90%) in our study underwent an extended 12 core biopsy. Previous studies have demonstrated that biopsies consisting of fewer than 12 cores are associated with significantly higher upgrading rates than extended biopsies, which are currently the standard of care in the United States [12, 30]. Additionally, in our study, all RPs were entirely submitted for histologic examination, ensuring accurate Gleason score assignment. Finally, all biopsies and RPs were re-graded by urologic pathologists using the most updated (2005) Gleason scoring system [26]. Our findings are further validated by the clinical-pathologic variables we found associated with upgrading, which are highly consistent with contemporary studies in much larger cohorts, including patient age, pre-operative PSA, clinical stage and extent of tumor involvement on biopsy [9–15]. As expected, upgraded patients in the current study also fared significantly worse after surgery, with substantially higher rates of extraprostatic extension, surgical margin positivity and biochemical recurrence compared to controls who were not upgraded at RP.

There are a few potential weaknesses of the current study, perhaps the most important of which is the relatively small sample size. Because of this, it is essential that our results be validated in future studies with larger, prospective cohorts. Partly mitigating this weakness, our study did include patients from two clinical settings (tertiary vs. community care) yet each showed nearly identical rates of PTEN protein loss in upgraded cases and controls, suggesting that our findings will likely be reproducible in independent cohort analyses. An additional potential weakness is that we evaluated only one to two needle biopsy cores for most patients. Because we and others have showed that PTEN protein loss and underlying gene deletion is most commonly focal [24, 28], it is likely that we missed a number of cases with focal PTEN loss by evaluating PTEN status in only one core. Future studies and clinical implementation of our PTEN assay may require that all cancer-containing needle cores are evaluated for PTEN loss and this may substantially increase the sensitivity of our assay for predicting tumor upgrading in GS6 needle biopsies.

In sum, with additional validation in larger cohorts, the PTEN IHC assay described herein may become an important part of the evaluation of prostate cancer patients being considered for active surveillance. It may be used alone on multiple involved needle cores from a single patient, or perhaps optimally in concert with FISH. In combination with MRI or other imaging tests to ensure the absence of unsampled anterior tumors, PTEN IHC is an inexpensive and simple test to assess for the presence of potentially unsampled higher grade disease in otherwise low risk patients.

References

1 Pound CR, Partin AW, Eisenberger MA, Chan DW, Pearson JD, Walsh PC. Natural history of progression after PSA elevation following radical prostatectomy. JAMA 1999;281 1591–7.

2 Ross HM, Kryvenko ON, Cowan JE, Simko JP, Wheeler TM, Epstein JI. Do adenocarcinomas of the prostate with Gleason score (GS) </=6 have the potential to metastasize to lymph nodes?. Am.J.Surg.Pathol. 2012;36 1346–52.

3 Pierorazio PM, Walsh PC, Partin AW, Epstein JI. Prognostic Gleason grade grouping: data based on the modified Gleason scoring system. BJU Int. 2013;111 753–60.

4 Ellis CL, Walsh PC, Partin AW, Epstein JI. Multiple cores of Gleason score 6 correlate with favourable findings at radical prostatectomy. BJU Int. 2013;111 E306– 9.

5 Berman DM, Epstein JI. When is prostate cancer really cancer? Urologic Clinics of North America 2013;In press.

6 Epstein JI, Feng Z, Trock BJ, Pierorazio PM. Upgrading and downgrading of prostate cancer from biopsy to radical prostatectomy: incidence and predictive factors using the modified Gleason grading system and factoring in tertiary grades. Eur. Urol. 2012;61 1019–24.

7 Irani J, Blanchet P, Salomon L, Coloby P, Hubert J, Malavaud B, et al. Is an extended 20–core prostate biopsy protocol more efficient than the standard 12– core? A randomized multicenter trial. J.Urol. 2013;190 77–83.

8 Siddiqui MM, Rais-Bahrami S, Truong H, Stamatakis L, Vourganti S, Nix J, et al. Magnetic Resonance Imaging/Ultrasound-Fusion Biopsy Significantly Upgrades Prostate Cancer Versus Systematic 12–core Transrectal Ultrasound Biopsy. Eur. Urol. 2013.

9 Magheli A, Hinz S, Hege C, Stephan C, Jung K, Miller K, et al. Prostate specific antigen density to predict prostate cancer upgrading in a contemporary radical prostatectomy series: a single center experience. J.Urol. 2010;183 126–31.

10 Oh JJ, Hong SK, Lee JK, Lee BK, Lee S, Kwon OS, et al. Prostate-specific antigen vs prostate-specific antigen density as a predictor of upgrading in men diagnosed with Gleason 6 prostate cancer by contemporary multicore prostate biopsy. BJU Int. 2012;110 E494–9.

11 Truong M, Slezak JA, Lin CP, Iremashvili V, Sado M, Razmaria AA, et al. Development and multi-institutional validation of an upgrading risk tool for Gleason 6 prostate cancer. Cancer 2013.

12 Capitanio U, Karakiewicz PI, Valiquette L, Perrotte P, Jeldres C, Briganti A, et al. Biopsy core number represents one of foremost predictors of clinically significant gleason sum upgrading in patients with low-risk prostate cancer. Urology 2009;73 1087–91.

13 Gershman B, Dahl DM, Olumi AF, Young RH, McDougal WS, Wu CL. Smaller prostate gland size and older age predict Gleason score upgrading. Urol.Oncol. 2013;31 1033–7.

14 Freedland SJ, Kane CJ, Amling CL, Aronson WJ, Terris MK, Presti JC,Jr, et al. Upgrading and downgrading of prostate needle biopsy specimens: risk factors and clinical implications. Urology 2007;69 495–9.

15 Moussa AS, Kattan MW, Berglund R, Yu C, Fareed K, Jones JS. A nomogram for predicting upgrading in patients with low- and intermediate-grade prostate cancer in the era of extended prostate sampling. BJU Int. 2010;105 352–8.

16 Lotan TL, Gurel B, Sutcliffe S, Esopi D, Liu W, Xu J, et al. PTEN protein loss by immunostaining: analytic validation and prognostic indicator for a high risk surgical cohort of prostate cancer patients. Clin.Cancer Res. 2011;17 6563–73.

17 Chaux A, Peskoe SB, Gonzalez-Roibon N, Schultz L, Albadine R, Hicks J, et al. Loss of PTEN expression is associated with increased risk of recurrence after prostatectomy for clinically localized prostate cancer. Mod.Pathol. 2012;25 1543–9.

18 Antonarakis ES, Keizman D, Zhang Z, Gurel B, Lotan TL, Hicks JL, et al. An immunohistochemical signature comprising PTEN, MYC, and Ki67 predicts progression in prostate cancer patients receiving adjuvant docetaxel after prostatectomy. Cancer 2012;118 6063–71.

19 McMenamin ME, Soung P, Perera S, Kaplan I, Loda M, Sellers WR. Loss of PTEN expression in paraffin-embedded primary prostate cancer correlates with high Gleason score and advanced stage. Cancer Res. 1999;59 4291–6.

20 Sircar K, Yoshimoto M, Monzon FA, Koumakpayi IH, Katz RL, Khanna A, et al. PTEN genomic deletion is associated with p-Akt and AR signalling in poorer outcome, hormone refractory prostate cancer. J.Pathol. 2009;218 505–13.

21 Yoshimoto M, Cunha IW, Coudry RA, Fonseca FP, Torres CH, Soares FA, et al. FISH analysis of 107 prostate cancers shows that PTEN genomic deletion is associated with poor clinical outcome. Br.J.Cancer 2007;97 678–85.

22 Krohn A, Diedler T, Burkhardt L, Mayer PS, De Silva C, Meyer-Kornblum M, et al. Genomic deletion of PTEN is associated with tumor progression and early PSA recurrence in ERG fusion-positive and fusion-negative prostate cancer. Am.J.Pathol. 2012;181 401–12.

23 Yoshimoto M, Ludkovski O, DeGrace D, Williams JL, Evans A, Sircar K, et al. PTEN genomic deletions that characterize aggressive prostate cancer originate close to segmental duplications. Genes Chromosomes Cancer 2012;51 149–60.

24 Yoshimoto M, Ding K, Sweet JM, Ludkovski O, Trottier G, Song KS, et al. PTEN losses exhibit heterogeneity in multifocal prostatic adenocarcinoma and are associated with higher Gleason grade. Mod.Pathol. 2013;26 435–47.

25 Cuzick J, Yang ZH, Fisher G, Tikishvili E, Stone S, Lanchbury JS, et al. Prognostic value of PTEN loss in men with conservatively managed localised prostate cancer. Br J Cancer. 2013;108 2582–9.
26 Epstein JI, Allsbrook WC,Jr, Amin MB, Egevad LL. Update on the Gleason grading system for prostate cancer: results of an international consensus conference of urologic pathologists. Adv.Anat.Pathol. 2006;13 57–9.
27 Sowalsky AG, Ye H, Bubley GJ, Balk SP. Clonal progression of prostate cancers from Gleason grade 3 to grade 4. Cancer Res. 2013;73 1050–5.
28 Gumuskaya B, Gurel B, Fedor H, Tan HL, Weier CA, Hicks JL et al. Assessing the order of critical alterations in prostate cancer development and progression by IHC:
further evidence that PTEN loss occurs subsequent to ERG gene fusion. Prostate Cancer Prostatic Dis. 2013;16 209–15.
29 Reese AC, Landis P, Han M, Epstein JI, Carter HB. Expanded criteria to identify men eligible for active surveillance of low risk prostate cancer at Johns Hopkins: a preliminary analysis. J.Urol. 2013;May 13; Epub ahead of print.
30 Capitanio U, Karakiewicz PI, Valiquette L, Perrotte P, Jeldres C, Briganti A, et al. Biopsy core number represents one of foremost predictors of clinically significant gleason sum upgrading in patients with low-risk prostate cancer. Urology 2009;73 1087–91.

CHAPTER 6 —
BIOLOGICAL ACTIVITY OF PROSTATE CIRCULATING TUMOR CELLS

www.impactjournals.com/oncotarget/ Oncotarget, March, Vol.4, No 3

Tumorigenic potential of circulating prostate tumor cells

Filipe LF. Carvalho[1,3], Brian W. Simons[1,2], Emmanuel S. Antonarakis[3], Zeshaan Rasheed[3], Nora Douglas[1], Daniela Villegas[1], William Matsui[3], David M. Berman[1,3,4]

[1] Department of Pathology, Johns Hopkins University School of Medicine, Baltimore, MD, USA

[2] Department of Molecular and Comparative Pathobiology, Johns Hopkins University School of Medicine, Baltimore, MD, USA

[3] Department of Oncology, Johns Hopkins University School of Medicine, Baltimore, MD, USA.

[4] Departments of Pathology and Molecular Medicine and Cancer Biology and Genetics, Cancer Research Institute, Queen's University, Kingston, Ontario, Canada

***Correspondence to**: David M. Berman, **email**: filipelafuente@gmail.com*

Keywords: Circulating tumor cells; EpCAM; prostate cancer; prostate-specific antigen; TRAMP mouse

***Received**: February 21, 2013* ***Accepted**: March 04, 2013* ***Published**: March 05, 2013*

ABSTRACT:

Circulating tumor cells (CTCs) have received intense scientific scrutiny because they travel in the bloodstream and are therefore well situated to mediate hematogenous metastasis. However, the potential of CTCs to actually form new tumors has not been tested. Popular methods of isolating CTCs are biased towards larger, more differentiated, non-viable cells, creating a barrier to testing their tumor forming potential. Without relying on cell size or the expression of differentiation markers, our objective was to isolate viable prostate CTCs from mice and humans and assay their ability to initiate new tumors. Therefore, blood was collected from transgenic adenocarcinoma of the mouse prostate (TRAMP) mice and from human patients with metastatic castration-resistant prostate cancer (PCa). Gradient density centrifugation or red cell lysis was used to remove erythrocytes, and then leukocytes were depleted by magnetic separation using CD45 immunoaffinity beads. CTCs fractions from TRAMP mice and PCa patients were verified by immunocytochemical staining for cytokeratin 8 and EpCAM, and inoculated into immunodeficient mice. TRAMP tumor growth was monitored by palpation. Human tumor growth formation was monitored up to 8 months by ultrasensitive PSA assays performed on mouse serum. We found viable tumor cells present in the bloodstream that were successfully isolated from mice without relying on cell surface markers. Two out of nine immunodeficient mice inoculated with TRAMP CTCs developed massive liver metastases. CTCs were identified in blood from PCa patients but did not form tumors. In conclusion, viable CTCs can be isolated without relying on epithelial surface markers or size fractionation. TRAMP CTCs were tumorigenic, so CTCs isolated in this way contain viable tumor-initiating cells. Only two of nine hosts grew TRAMP tumors and none of the human CTCs formed tumors, which suggests that most CTCs have relatively low tumor-forming potential. Future studies should identify and target the highly tumorigenic cells.

INTRODUCTION

Elevated numbers of circulating tumor cells (CTCs) in several cancers, including prostate cancer (PCa) have been correlated with decrease patient survival [1-4]. Thus, CTCs may be potent mediators of prostate cancer metastasis. However, the biological properties of these cells have not been explored. Current methods to isolate these cells rely on physical properties (large size, density, electric charges, and deformability) and expression of the epithelial markers, mainly the epithelial cell adhesion molecule (EpCAM) [5]. Although these methods enable a molecular profiling of CTCs [6], they have important limitations regarding the selected cells. Cancer cells are variable in size, and larger cancer cells are more differentiated and less adept at forming new tumors [7-

9]. Therefore, CTCs isolated on the basis of large size may under-represent the underlying CTC population and bias them towards a less tumorigenic phenotype. Likewise, EpCAM expression is absent in subpopulations of CTCs that may be decisive for metastasis [10]. Gene expression profile of prostate cells varies during disease progression [11, 12]. Indeed, cancer cells that lose epithelial differentiation in favor of more mesenchymal character may contribute to carcinogenesis and be more potent initiators of metastasis [13-15]. Furthermore, upon isolation by current methods, CTCs are dead and therefore not usable in functional experiments. Indeed, at the time this publication was submitted, we could find no other published studies characterizing growth, differentiation potential, clonogenicity, or metastatic capacity of circulating tumor cells from any solid tumor.

An efficient xenografting method can be very useful in characterizing the molecular changes of individual tumors during disease progression and response to therapy [16]. Primary human prostate cancers are notoriously difficult to grow in the laboratory setting. Using optimized methods enhanced by co-engraftment with fetal urogenital mesenchyme, 100,000 or more primary human cancer cells are required to establish a tumor [17], suggesting that most primary human PCa cells lack tumorigenic potential. Some investigators have worked to enhance PCa grafting efficiency by growing primary prostate tumors under the kidney capsule of immunodeficient mice [17-19].

In contrast to primary cancers, advanced metastatic cancers may contain a higher fraction of highly tumorigenic cells. In this study, we utilized blood from men with metastatic castration-resistant PCa and from the transgenic adenocarcinoma of the mouse prostate (TRAMP) mice with metastatic disease. TRAMP is the most widely studied mouse model of prostate cancer, and in contrast to human-derived models, it metastasizes widely. In this model, a prostate-specific probasin promoter drives the expression of simian virus 40 (SV40) T antigen in the prostate. This viral oncogene induces malignant transformation of prostate cells at 12 weeks of age, and by 30 weeks, tumors progress to lung and lymph node metastases [20-22].

Our main goal was to isolate a viable unbiased population of CTCs and generate new tumors to test whether these circulating cancer cells have tumorigenic potential.

RESULTS

CTCs from TRAMP mouse produce metastases in immunodeficient host

We injected nucleated cell preparations from 700 mL blood (which is approximately 50% of the total blood volume) of TRAMP mice intravenously into nine highly immunodeficient NOD.Cg-*Prkdc*^{scid} *Il2rg*^{tm1Wjl}/SzJ (NSG) mouse recipients (Fig. 1). Three months after injection, seven of the mice showed no evidence of metastasis. The remaining two recipients developed massive tumor deposits in the liver (Fig. 2 E-H). In each mouse, gross inspection of the liver revealed more than 15 liver lesions larger than 1 mm (largest lesion 2cmx1.2cmx1.5cm) and 10 lesions smaller than 1 mm. The lungs, spleen and kidneys did not show evidence of metastatic lesions. Histologic examination of the liver lesions showed tumor cells with neuroendocrine carcinoma morphology typical of TRAMP tumors (Fig. 2 A-D). TRAMP cancers invaded diffusely through the liver parenchyma (Fig. 2 E-H). As seen in previous studies of TRAMP tumors, blood-derived TRAMP tumor cells in the liver lacked immunoreactivity for androgen receptor (AR) but stained strongly for SV40 T-Ag [23], consistent with primary TRAMP prostate tumors (Fig 2B and 2C). PCR analysis of DNA isolated from liver tumors confirmed that the tumors carried the TRAMP transgene. Since the NSG recipients lacked the transgene, these results confirmed that the tumors originated from TRAMP donor CTCs (Supplementary Fig. S1). In summary, tumor cells were readily identified in blood from all TRAMP animals, but injection of TRAMP blood cells yielded tumors in only 22% of recipients. When tumors did form, they recapitulated the highly

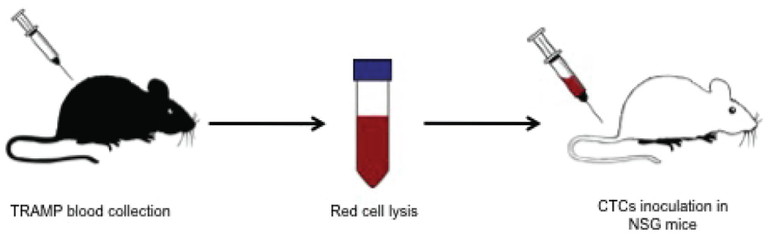

Figure 1: Schematic view of TRAMP CTCs isolation and xenograft. TRAMP mice were terminally bleed and the whole blood mixed with red cell lysis buffer. After red cell lysis, the remaining cells were injected in the tail vein of NSG mice.

invasive and aggressive features of the parental TRAMP tumors. These results indicate that in TRAMP mice, a small minority of CTCs have tumorigenic potential.

Isolation of viable human prostate cells from human blood

As a prerequisite to testing the tumor forming potential of human CTCs, we confirmed that we could isolate viable and growth-competent human prostate cancer cells from human blood. Human DU145 prostate cancer cells were spiked into blood of healthy individuals and recovered using density gradient centrifugation. Upon subsequent culture, these cells expanded at a rate similar to the parental cell line (Fig. 3A). These preliminary findings encouraged us to characterize CTCs present in patients with prostate cancer. Using the same approach, we identified cells expressing the epithelial marker cytokeratin 8 and EpCAM in blood from castration-resistant PCa patients, but not from healthy controls (Fig. 3B and data not shown). These results show that this method recovered viable PCa cells present in human blood.

Xenografts of human CTCs

After finding metastatic potential of TRAMP CTCs, we decided to inject human CTCs in immunodeficient mice (Fig. 4). Initially, we injected CTCs from PCa patients thought the tail vein of NSG mice (n=4) and measured the PSA in mice serum for 8 months. We observed transient spikes in PSA values, but not sustained elevation that would reflect tumor growth. We euthanized these four mice, performed gross and histologic examination of the viscera, and did not find evidence of engraftment. We then adapted a xenografting method optimized for primary human prostate cancers [17] to combine human CTCs with mouse fetal urogenital mesenchyme and engraft under the kidney capsule. Confirming that the fetal mesenchyme was active and competent to induce prostate growth, murine prostate epithelial cells grew as renal grafts only when recombined with fetal urogenital mesenchyme (Fig. 5A). This grafting method was also highly effective for human prostate cancer cell lines, as shown by grafts combining human LnCaP prostate cancer cells with fetal urogenital mesenchyme. LnCaP grafts engulfed and invaded the kidney (Fig. 5B), resulting in rapidly rising serum PSA in the mouse recipients (Fig. 5D). The seven human CTC grafts introduced under the kidney capsule showed either no rise in PSA or a transient rise followed by return to baseline. Macroscopic and microscopic evaluation of these grafts revealed multiple capillary vessels and scattered cells inside the matrigel matrix without tumor growth (Fig. 5C).

DISCUSSION

Our results indicate that viable prostate CTCs can be isolated using "negative selection" methods that avoid assumptions regarding size and surface marker expression.

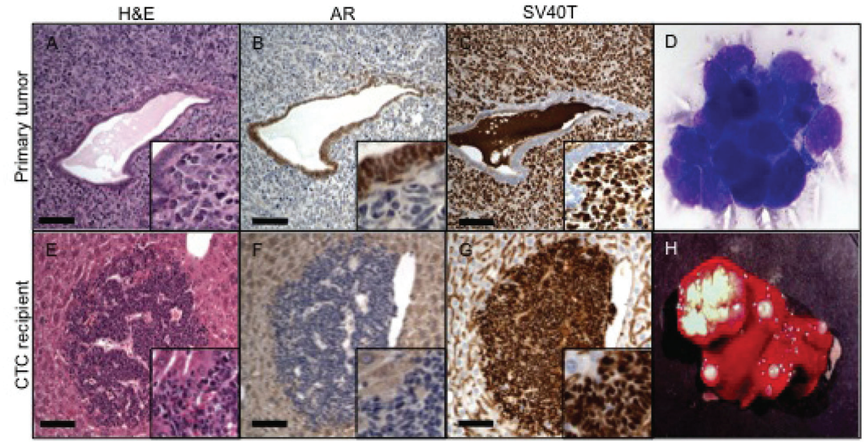

Figure 2: CTCs in the TRAMP mouse. *Top row.* H&E stain (A) of primary tumor cells surrounding a benign gland; AR (B) and SV 40 (C) exclusively stain two distinct cell populations: AR the benign cells and SV40 the tumor cells. (D) Large atypical cells found in the bloodstream of TRAMP showing adherent clumps. *Lower row.* Multiple metastasis in the liver of NSG mice. H&E stain of a metastatic lesion near a liver vessel (E). Tumor cells do not express AR (F) and are strongly positive for SV 40 (G). Gross appearance of the liver with massive metastasis (H). Scale bars, 100 μm.

When isolated in this way, CTCs can form new tumors. TRAMP CTCs successfully engrafted in 22% of cases and NSG recipients developed in a short period of time small-cell SV40-T Ag positive diffuse liver metastasis.

Using the same methodology on human PCa patients' blood samples, we identified circulating cells expressing EpCAM and cytokeratin 8, the same markers used by Food and Drug Administration (FDA)-cleared automated systems to identify CTCs (CellSearch, Veridex LLC, Raritan, NJ). The identification of these cells confirmed that we were grafting the same cells currently used as biomarkers to predict PCa patients' prognosis [1, 24]. These cells can be introduced into highly immunodeficient mice without adverse events, namely graft-versus-host disease. However, even using highly efficient xenografting techniques [17, 25], human CTCs did not form new tumors. The superior performance of TRAMP CTCs in xenografting assays may have methodological and biological explanations. In the TRAMP experiments, we collected 50% of the blood volume of each mouse, whereas the human sample represented less than 0.5% of blood volume. Therefore, sampling issues should affect human samples more. It is also possible that CTCs have growth requirements that differ from those of primary human prostate cancers. It would thus be possible that the renal capsule/SVM environment is not optimized for CTC growth. For example, the preferential metastatic niche for human prostate cancer is the bone. Bone-based environments might therefore provide better growth support for metastatic PCa, but bone metastasis models have yet to be successfully developed for prostate cancer [26]. Humanized mice represent another option for enhanced xenografting, as they have been shown to increase the take rate of human primary ovarian and lung cancer cells [27-29]. In addition to potential issues with the host

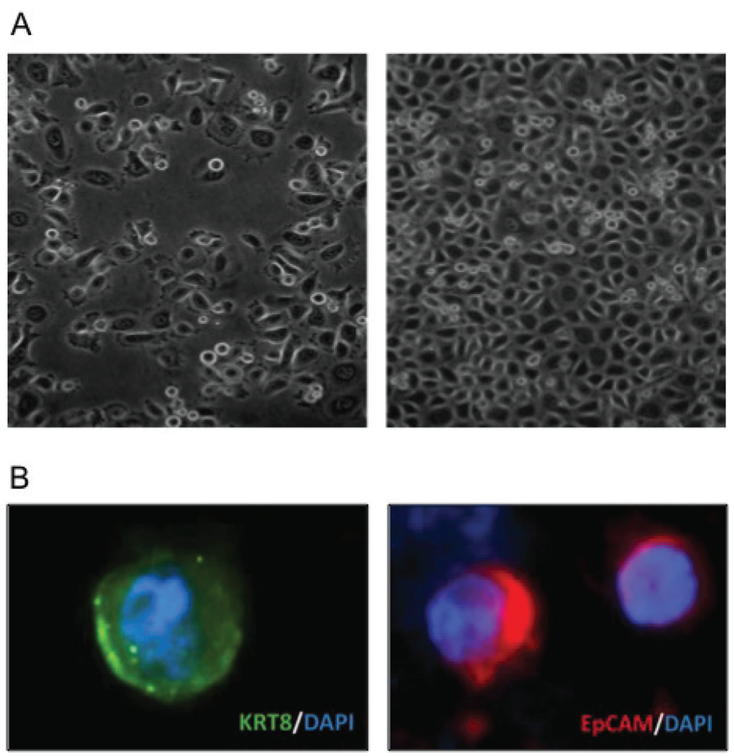

Figure 3: Isolation of tumor cells. (A) DU145 spiked in blood recovered using gradient centrifugation were viable 24 hours later (left) and had doubled by 48 hours (right). (B) CTCs isolated from patients' blood express the epithelial markers keratin 8 (left) and EpCAM (right).

environment, we posit that CTCs are not particularly potent at initiating new sites of tumor growth. Previous studies showed that 70% of men with clinically localized PCa undergoing radical prostatectomy have tumor cells in the bone marrow prior to surgery [30]. In the same study, almost 60% of these patients with tumor cells in bone marrow did not have biochemical recurrence after surgery, meaning the majority of the CTCs do not have the capacity to generate metastasis. These results are consistent with our findings that even CTCs isolated from patients with advanced metastatic castration-resistant PCa, did not show the ability to initiate new tumors. If it is true that most prostate CTCs are innocuous, future studies should focus on isolating the few CTCs that can actually promote cancer progression. Isolating CTCs without restrictions regarding size and epithelial differentiation should facilitate such studies.

MATERIALS AND METHODS

Patient selection

Patients treated at the Johns Hopkins Sidney Kimmel Comprehensive Cancer Center (Baltimore, MD) with castration-resistant PCa and radiologic evidence of distant osseous or soft tissue metastatic disease were recruited according to an institutional review board (IRB)-approved protocol. All patients signed a written informed consent. A total of 14 patients (Table 1) donated 7 mL of blood on one or more occasions for CTCs immunocytochemistry or xenograft. Blood from healthy individuals without evidence of PCa was spiked with DU145 cells.

Cell Culture

Human DU145 and LnCaP prostate cancer cells were obtained from the American Type Culture Collection, maintained in RPMI 1640 media (Gibco) supplemented with 10% fetal bovine serum (Gibco) and Penicillin-Streptomycin (Invitrogen).

Cell isolation

Blood drawn into a heparinized tube followed two different approaches (Fig. 1 and 4) to remove red blood cells and collect nucleated cells: red cell lysis or density gradient centrifugation. After red cell removal, nucleated cells present in blood were collected, incubated with anti-leukocyte antibody CD45 magnetic microbeads (Miltenyi Biotec), placed into magnetic depletion columns (Miltenyi Biotec) to deplete white blood cells and all tumor cells that flow through the columns were collected for further studies. As a "proof-of-principle" for isolation of viable circulating cells, human DU145 prostate cancer (1 x 10^6) cells were spiked in blood from healthy individuals and placed back in culture for 48 hours to monitor if the cells were viable and able to expand in culture. CTCs from PCa patients were either spread across microscopic slides for immunofluorescent analysis or xenografted in mice.

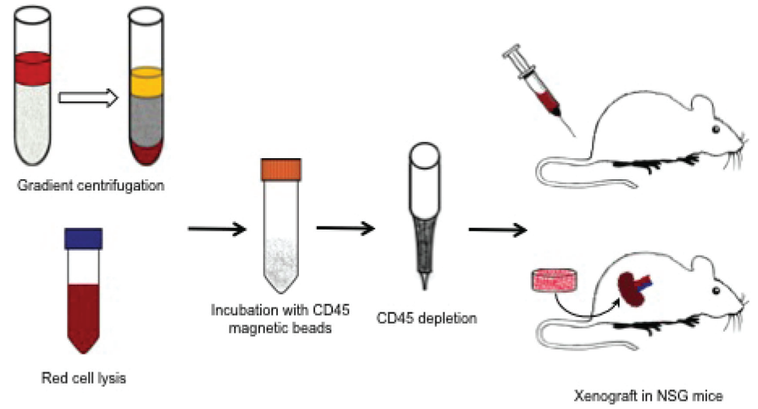

Figure 4: Blood from prostate cancer patients was either placed atop of a Ficoll-Paque PLUS gradient column or subject to red cell lysis; then the nucleated cells were incubated with CD45 magnetic beads and hematopoietic CD45-expressing cells removed from the mixture. The remaining cells were either injected into the tail vein of NSG mice or wrapped with mouse neonatal mesenchymal cells and grafted under the kidney capsule.

Generation of CTC xenografts and determination of engraftment with PSA

CTCs from both TRAMP mice and human prostate cancer patients were inserted into anesthetized male highly immunodeficient NOD.Cg-*Prkdc*^{scid} *Il2rg*^{tm1Wjl}/SzJ mice (Figure 1 and 4), also known as NOD SCID gamma (NSG) mice [31]. NSG mice lack functional T cells, B cells, and NK cells and have markedly reduced dendritic cell and macrophage activity. This high degree of immunodeficiency results in superior engraftment of human cells [32].

Approximately 700 mL of blood from TRAMP mice (n=9) went through the red cell lysis step and nucleated cells were afterwards injected into the tail vein of NSG mice. To confirm the existence of CTCs in TRAMPs blood, we spread TRAMP nucleated cells in a microscope slide and performed Wright's stain.

CTCs isolated from PCa patient blood were injected into the tail vein of NSG mice (n=4) or wrapped in mouse newborn seminal vesicle mesenchyme (SVM) and inserted under the renal capsule (n=7) as described previously [17]. Briefly, this technique consists in the isolation of SVM from newborn (day 0) C57BL/6 mice [17], 1 x 10^5 SVM cells were combined with CTCs isolated from patients in a matrigel (BD Biosciences) disk. The disk, containing

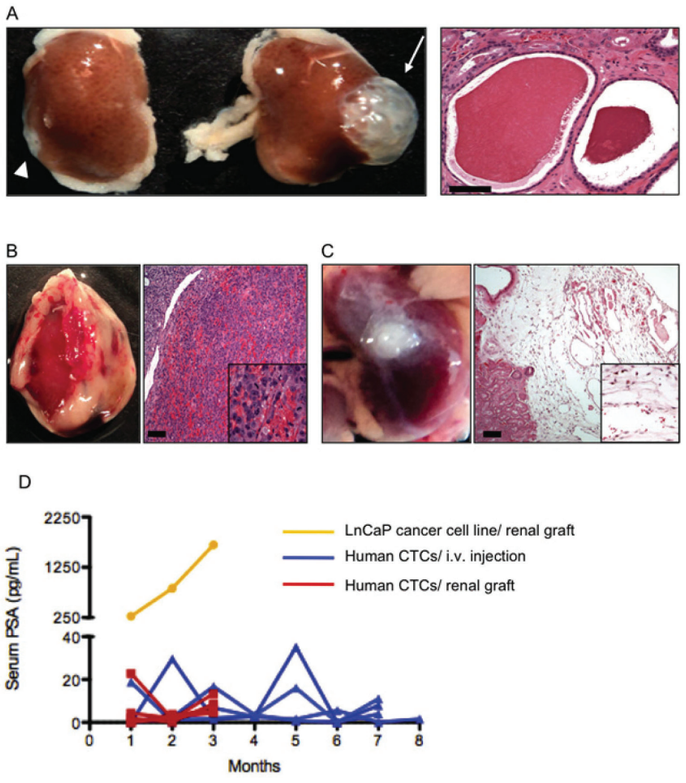

Figure 5: Renal grafts. (A) When combined with neonatal murine SVM and grafted in the kidney, benign murine prostate epithelium formed a prostate (arrow and right panel). Scale bar, 100 nm. Neither SVM (not shown) nor prostate epithelial cells alone (arrowhead) did so. (B) Human LnCaP prostate cancer cells engulfed and invaded the kidney. Scale bar, 100 µm. (C) Human CTCs failed to grow and form tumors when grafted under the kidney capsule (left panel). Microscopic analysis of the graft (right panel) revealed many capillary vessels and scattered cells. Scale bar, 100 µm. (D) PSA kinetics in mouse serum reflected these findings: mouse grafted with LnCaP had a rapidly rise in PSA and the hosts of human CTCs showed transient spikes in PSA but not sustained elevation that reflected tumor growth.

Table 1: Patients baseline demographics and clinical characteristics.

	Overall n=14
Age, yr, median (IQR)	69.5 (60 - 81)
Gleason Score, no. (%)	
Gleason 6	2 (14.3)
Gleason 7	2 (14.3)
Gleason 8	2 (14.3)
Gleason 9	7 (50.0)
Gleason 10	1 (7.1)
Primary Therapy	
Radical prostatectomy, no. (%)	3 (21.4)
Radiation therapy, no. (%)	3 (21.4)
Combination of prostatectomy and radiation, no. (%)	2 (14.3)
No primary treatment, no. (%)	6 (42.9)
Prior androgen deprivation therapy, no. (%)	14 (100)
Number of secondary hormonal therapies, median (IQR)	2 (1 - 5)
Three or more hormonal therapies, no. (%)	8 (57.1)
Prior Chemotherapy, no.	
One prior regimen, no. (%)	9 (64.3)
Two (or more) prior regimens, no. (%)	2 (14.3)
PSA when CTCs when were collected, median (IQR)	92.9 (3.1 - 4760.2)
Sites of metastases	
Bone only, no. (%)	5 (35.7%)
Soft tissue only (nodes, liver, lung)	1 (7.1%)
Soft tissue and bone	8 (57.1%)

CTCs and the SVM were combined and cultured 12 hours in RPMI supplemented with 1 mM of dihydrotestosterone, and then introduced under the renal capsule. To confirm the capacity of SVM to support prostate epithelial growth, benign primary mouse prostate epithelial cells (1 x 10^6) were combined with SVM and also grafted under the kidney capsule. PSA-producing cancer cells LnCaP (1 x 10^6) cells were also used as controls, to confirm that the grafting conditions supported human prostate cancer growth and to confirm the performance of ultrasensitive PSA tests (see below) on mouse serum. Since mice do not make PSA, human CTC engraftment was monitored monthly by ultrasensitive nano-PSA assays (Nanosphere Inc, Chicago, IL) performed on serum prepared from 50 mL of mouse blood [33]. NSG mice injected with TRAMP CTCs were euthanized 3 months after grafting, and the NSGs grafted with human circulating cells were euthanized 8 months after grafting. An expert veterinary pathologist performed comprehensive necropsies as well as histologic examination of the liver, lungs, spleen and the grafts from all animals.

Immunohistochemistry and immunofluorescence

Formalin-fixed, paraffin-embedded tissue samples from the liver, lungs, spleen and CTC xenografts were sectioned (4 mm) and immunohistochemistry was performed as described [34] using anti-SV40 T-Ag (clone Pab101 Santa Cruz, 1:1000) or anti-androgen receptor (clone N-20 Santa Cruz, 1:500) antibodies for immunodetection.

Immunofluorescent staining for cytokeratin 8 (1:500; clone M20 Abcam) and EpCAM (1:500; clone VU-1D9 Abcam) was performed to confirm the collection of CTCs from castration-resistant PCa patients. Cells obtained after CD45 depletion were spread onto a microscope slide, stained as previously described [35] and

analyzed under a 100x oil immersion objective using a Nikon E400 fluorescence microscope (Nikon).

CONCLUSIONS

These results demonstrate that viable CTCs can be isolated without *a priori* assumptions about surface markers and, using transgenic mouse models of PCa cancer, CTCs were able to form metastasis in new hosts. Nevertheless, CTCs were surprising inefficient at initiating new sites of tumor growth. Our work highlights the need to better define subpopulations of CTCs that have the ability to produce metastasis. Future studies should identify and target the highly tumorigenic cells.

ACKNOWLEDGEMENTS

The design and conduct of this research was funded by a PhD grant from Fundação para Ciência e Tecnologia (SFRH/ BD/ 69819/ 2010) to F. LF. Carvalho.

REFERENCE

1. Scher HI, Jia X, de Bono JS, Fleisher M, Pienta KJ, Raghavan D and Heller G. Circulating tumour cells as prognostic markers in progressive, castration-resistant prostate cancer: a reanalysis of IMMC38 trial data. Lancet Oncol. 2009; 10(3):233-239.
2. Strijbos MH, Gratama JW, Schmitz PI, Rao C, Onstenk W, Doyle GV, Miller MC, de Wit R, Terstappen LW and Sleijfer S. Circulating endothelial cells, circulating tumour cells, tissue factor, endothelin-1 and overall survival in prostate cancer patients treated with docetaxel. Eur J Cancer. 46(11):2027-2035.
3. Patel AS, Allen JE, Dicker DT, Peters KL, Sheehan JM, Glantz MJ and El-Deiry WS. Identification and enumeration of circulating tumor cells in the cerebrospinal fluid of breast cancer patients with central nervous system metastases. Oncotarget. 2011; 2(10):752-760.
4. Faltas B. Circulating tumor cells in the cerebrospinal fluid: "tapping" into diagnostic and predictive potential. Oncotarget. 2011; 2(11):822.
5. Danila DC, Fleisher M and Scher HI. Circulating tumor cells as biomarkers in prostate cancer. Clin Cancer Res. 17(12):3903-3912.
6. Danila DC, Anand A, Sung CC, Heller G, Leversha MA, Cao L, Lilja H, Molina A, Sawyers CL, Fleisher M and Scher HI. TMPRSS2-ERG status in circulating tumor cells as a predictive biomarker of sensitivity in castration-resistant prostate cancer patients treated with abiraterone acetate. Eur Urol. 60(5):897-904.
7. Wang ZP, Eisenberger MA, Carducci MA, Partin AW, Scher HI and Ts'o PO. Identification and characterization of circulating prostate carcinoma cells. Cancer. 2000; 88(12):2787-2795.
8. Al-Hajj M, Wicha MS, Benito-Hernandez A, Morrison SJ and Clarke MF. Prospective identification of tumorigenic breast cancer cells. Proc Natl Acad Sci U S A. 2003; 100(7):3983-3988.
9. He X, Marchionni L, Hansel DE, Yu W, Sood A, Yang J, Parmigiani G, Matsui W and Berman DM. Differentiation of a highly tumorigenic basal cell compartment in urothelial carcinoma. Stem Cells. 2009; 27(7):1487-1495.
10. Kirby BJ, Jodari M, Loftus MS, Gakhar G, Pratt ED, Chanel-Vos C, Gleghorn JP, Santana SM, Liu H, Smith JP, Navarro VN, Tagawa ST, Bander NH, Nanus DM and Giannakakou P. Functional characterization of circulating tumor cells with a prostate-cancer-specific microfluidic device. PLoS One. 7(4):e35976.
11. Huang Z, Hurley PJ, Simons BW, Marchionni L, Berman DM, Ross AE and Schaeffer EM. Sox9 is required for prostate development and prostate cancer initiation. Oncotarget. 2012; 3(6):651-663.
12. Vainio P, Lehtinen L, Mirtti T, Hilvo M, Seppanen-Laakso T, Virtanen J, Sankila A, Nordling S, Lundin J, Rannikko A, Oresic M, Kallioniemi O and Iljin K. Phospholipase PLA2G7, associated with aggressive prostate cancer, promotes prostate cancer cell migration and invasion and is inhibited by statins. Oncotarget. 2011; 2(12):1176-1190.
13. Poczatek RB, Myers RB, Manne U, Oelschlager DK, Weiss HL, Bostwick DG and Grizzle WE. Ep-Cam levels in prostatic adenocarcinoma and prostatic intraepithelial neoplasia. J Urol. 1999; 162(4):1462-1466.
14. Mani SA, Guo W, Liao MJ, Eaton EN, Ayyanan A, Zhou AY, Brooks M, Reinhard F, Zhang CC, Shipitsin M, Campbell LL, Polyak K, Brisken C, Yang J and Weinberg RA. The epithelial-mesenchymal transition generates cells with properties of stem cells. Cell. 2008; 133(4):704-715.
15. Brennen WN, Chen S, Denmeade SR and Isaacs JT. Quantification of Mesenchymal Stem Cells (MSCs) at Sites of Human Prostate Cancer. Oncotarget. 2013.
16. Jimeno A, Feldmann G, Suarez-Gauthier A, Rasheed Z, Solomon A, Zou GM, Rubio-Viqueira B, Garcia-Garcia E, Lopez-Rios F, Matsui W, Maitra A and Hidalgo M. A direct pancreatic cancer xenograft model as a platform for cancer stem cell therapeutic development. Mol Cancer Ther. 2009; 8(2):310-314.
17. Toivanen R, Berman DM, Wang H, Pedersen J, Frydenberg M, Meeker AK, Ellem SJ, Risbridger GP and Taylor RA. Brief report: a bioassay to identify primary human prostate cancer repopulating cells. Stem Cells. 29(8):1310-1314.
18. Zhao H, Nolley R, Chen Z and Peehl DM. Tissue slice grafts: an in vivo model of human prostate androgen signaling. Am J Pathol. 177(1):229-239.
19. Priolo C, Agostini M, Vena N, Ligon AH, Fiorentino M, Shin E, Farsetti A, Pontecorvi A, Sicinska E and Loda M. Establishment and genomic characterization of mouse xenografts of human primary prostate tumors. Am J Pathol. 176(4):1901-1913.
20. Greenberg NM, DeMayo F, Finegold MJ, Medina D, Tilley WD, Aspinall JO, Cunha GR, Donjacour AA, Matusik RJ and Rosen JM. Prostate cancer in a transgenic mouse. Proc Natl Acad Sci U S A. 1995; 92(8):3439-3443.
21. Gingrich JR, Barrios RJ, Morton RA, Boyce BF, DeMayo FJ, Finegold MJ, Angelopoulou R, Rosen JM and Greenberg NM. Metastatic prostate cancer in a transgenic mouse. Cancer Res. 1996; 56(18):4096-4102.
22. Gingrich JR, Barrios RJ, Kattan MW, Nahm HS, Finegold MJ and Greenberg NM. Androgen-independent prostate cancer progression in the TRAMP model. Cancer Res. 1997; 57(21):4687-4691.
23. Chiaverotti T, Couto SS, Donjacour A, Mao JH, Nagase H, Cardiff RD, Cunha GR and Balmain A. Dissociation of epithelial and neuroendocrine carcinoma lineages in the transgenic adenocarcinoma of mouse prostate model of prostate cancer. Am J Pathol. 2008; 172(1):236-246.
24. Danila DC, Heller G, Gignac GA, Gonzalez-Espinoza R, Anand A, Tanaka E, Lilja H, Schwartz L, Larson S, Fleisher M and Scher HI. Circulating tumor cell number and prognosis in progressive castration-resistant prostate cancer. Clin Cancer Res. 2007; 13(23):7053-7058.
25. Taylor RA, Toivanen R, Frydenberg M, Pedersen J, Harewood L, Australian Prostate Cancer B, Collins AT, Maitland NJ and Risbridger GP. Human epithelial basal cells are cells of origin of prostate cancer, independent of CD133 status. Stem Cells. 30(6):1087-1096.
26. Singh AS, Macpherson GR, Price DK, Schimel D and Figg WD. Evaluation of human fetal bone implants in SCID mice as a model of prostate cancer bone metastasis. Oncol Rep. 2006; 15(3):519-524.
27. Bankert RB, Balu-Iyer SV, Odunsi K, Shultz LD, Kelleher RJ, Jr., Barnas JL, Simpson-Abelson M, Parsons R and Yokota SJ. Humanized mouse model of ovarian cancer recapitulates patient solid tumor progression, ascites formation, and metastasis. PLoS One. 6(9):e24420.
28. Simpson-Abelson MR, Sonnenberg GF, Takita H, Yokota SJ, Conway TF, Jr., Kelleher RJ, Jr., Shultz LD, Barcos M and Bankert RB. Long-term engraftment and expansion of tumor-derived memory T cells following the implantation of non-disrupted pieces of human lung tumor into NOD-scid IL2Rgamma(null) mice. J Immunol. 2008; 180(10):7009-7018.
29. Richmond A and Su Y. Mouse xenograft models vs GEM models for human cancer therapeutics. Dis Model Mech. 2008; 1(2-3):78-82.
30. Ellis WJ, Pfitzenmaier J, Colli J, Arfman E, Lange PH and Vessella RL. Detection and isolation of prostate cancer cells from peripheral blood and bone marrow. Urology. 2003; 61(2):277-281.
31. Shultz LD, Lyons BL, Burzenski LM, Gott B, Chen X, Chaleff S, Kotb M, Gillies SD, King M, Mangada J, Greiner DL and Handgretinger R. Human lymphoid and myeloid cell development in NOD/LtSz-scid IL2R gamma null mice engrafted with mobilized human hemopoietic stem cells. J Immunol. 2005; 174(10):6477-6489.
32. Carreno BM, Garbow JR, Kolar GR, Jackson EN, Engelbach JA, Becker-Hapak M, Carayannopoulos LN, Piwnica-Worms D and Linette GP. Immunodeficient mouse strains display marked variability in growth of human melanoma lung metastases. Clin Cancer Res. 2009; 15(10):3277-3286.
33. Thaxton CS, Elghanian R, Thomas AD, Stoeva SI, Lee JS, Smith ND, Schaeffer AJ, Klocker H, Horninger W, Bartsch G and Mirkin CA. Nanoparticle-based bio-barcode assay redefines "undetectable" PSA and biochemical recurrence after radical prostatectomy. Proc Natl Acad Sci U S A. 2009; 106(44):18437-18442.
34. Kleeberger W, Bova GS, Nielsen ME, Herawi M, Chuang AY, Epstein JI and Berman DM. Roles for the stem cell associated intermediate filament Nestin in prostate cancer migration and metastasis. Cancer Res. 2007; 67(19):9199-9206.
35. Outeiro TF, Putcha P, Tetzlaff JE, Spoelgen R, Koker M, Carvalho F, Hyman BT and McLean PJ. Formation of toxic oligomeric alpha-synuclein species in living cells. PLoS One. 2008; 3(4):e1867.

Tumorigenic potential of circulating prostate tumor cells - Carvalho et al

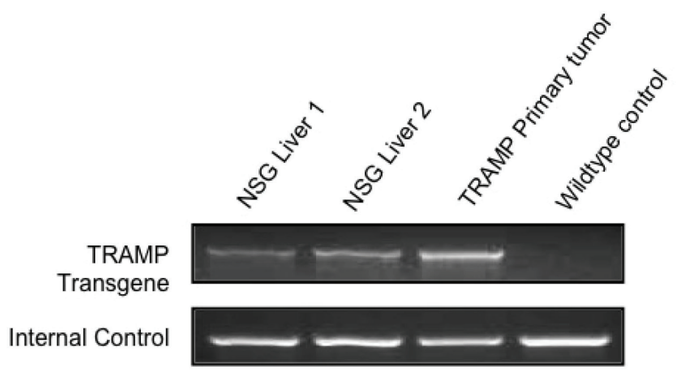

Supplementary figure S1: PCR analysis of genomic DNA isolated from liver tumors. PCR product of TRAMP transgene was detected in the liver of NSG mice with metastasis, confirming the tumors originated from TRAMP tumor.

PART III — DISCUSSION AND CONCLUSIONS

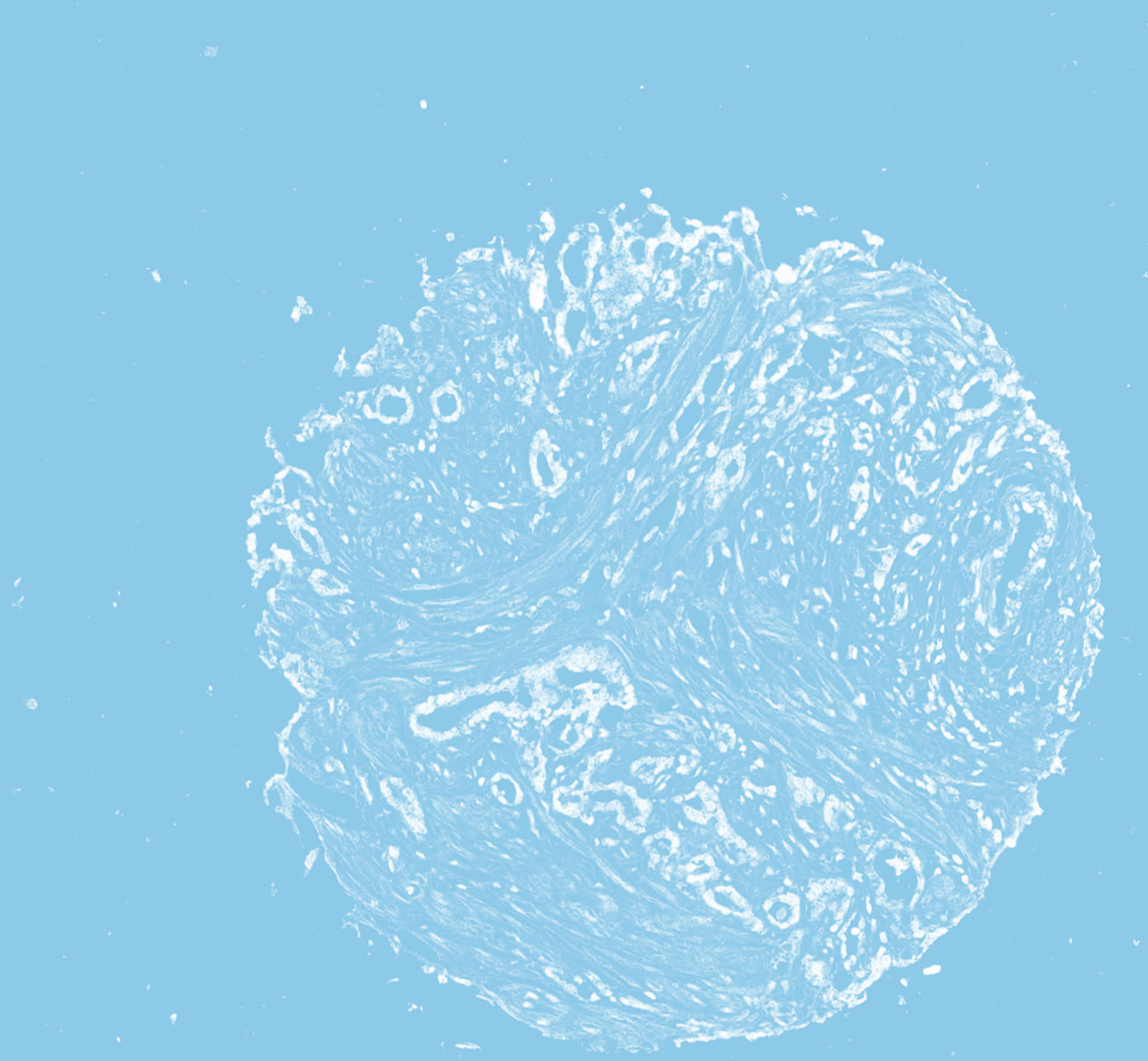

CHAPTER 7 —
GENERAL DISCUSSION

GENERAL DISCUSSION

Prostate cancer is the most common visceral cancer diagnosed in men and, respectively, the second and third most frequently cause of cancer deaths in the United States and Europe (17, 18). Widespread PSA screening and aggressive treatment substantially reduced mortality rates of prostate cancer (19, 20). However, the progresses in prostate cancer early detection lead to an overdiagnosis and overtreatment of indolent low grade cancers that would not be diagnosed clinically during life (20, 21). This fueled the debate about PSA screening because all treatments for prostate cancer have potential long-term consequences for urinary and sexual function (22). Thus, it is mandatory to implement treatment strategies only in men who are likely to benefit from them and do not harm those patients with indolent tumors. A growing consensus in urological community supports an initial defer of treatment of indolent tumors using a strategy called active surveillance (23, 24). Men managed through active surveillance are monitored periodically to evaluate tumor progression so the patients can be treated within the window of opportunity to cure the cancer. In addition, the outcome of patients managed through active surveillance and subsequently required therapeutic intervention is identical with patients that initially received treatment (25, 26). Therefore, active surveillance is an important alternative to avoid or delay morbidity of prostate cancer treatment in a large subset of patients (27, 28).

Prominent academic institutions established active surveillance programs, but the correct selection of candidates for these protocols and prediction of tumor progression are major challenges. A significant part of this quandary is due to the fact that prostate biopsies often fail to distinguish low-grade from high-grade tumors either due to sampling errors and imperfection of Gleason grading (29–31). Several studies estimate that between 20% and 30% of tumors are incorrectly classified as low-grade and in reality contain high-grade features (28, 31, 32). In addition, Gleason score is still the strongest predictor of prognosis and there is a lack of precise molecular correlates of tumor progression. For this reason my work focused on three different stages of prostate cancer evolution and cutoff of therapeutic intervention: cellular pathways involved in tumorigenesis and aggressiveness, Gleason score upgrading, and tumor-initiation capacity of cells that escape from the prostate to generate metastasis.

Several new concepts emerged from this work describing the dynamics of Notch signaling prostate cancer progression, the pivotal role of HES6 in tumor aggressiveness, the value of PTEN protein loss predicting Gleason score upgrade, and the isolation of viable CTCs to determine their biological activity. I will discuss in detail the most relevant results of the manuscripts presented in the previous chapters, because these findings may open new avenues for diagnostic and therapeutic targets in prostate cancer.

Notch signaling in prostate: double-edge sword

Recent genome-wide expression profiles comparing low grade (Gleason ≤ 6) with high-grade (Gleason ≥ 8) tumors revealed enrichment for Notch pathway in aggressive cancers. In these studies, cancer cells with metastatic and lethal potential (Gleason ≥ 8) upregulated the Notch ligand JAGGED2, the NOTCH3 receptor, and a potential Notch target gene HES6. Although Notch signaling was recognized as an important pathway in several tumors (34), the contribution of these pathway members to prostate tumorigenesis was largely unkown. Moreover, in prostate cancer there were contradictory results about the oncogenic or tumor suppressive role of Nocth1 receptor in mouse and human models (35–37) contributing to a cloudy understanding of the role of Notch in prostate carcinogenesis.

In line with the gene expression studies performed in human tissue samples, our study confirmed that among all the members of Notch pathway the most highly express gene in cancer cell lines compared to benign was HES6. In these studies along with HES6, Notch3 was the other member of the pathway overexpressed in high grade cancer. However, in our global gene expression comparison between benign and cancer cell lines, we did not find a significant change for Notch3. After performing a subanalysis to find out the individual pattern of Notch pathway members expression in each cell line, we realized that one of the benign cell lines — RWPE1 — was the cell line with highest levels of Notch3, wiping out a higher expression in global analysis. When the subanalysis was performed without this cell line, HES6 and Notch3 were the most highly expressed genes in cancer cell lines. Another interesting finding was the fact that both Notch3 and HES6 were increased in two out of three androgen-responsive cancer cell lines (22Rv1 and LnCaP). So, we wondered if HES6 was a downstream target of Notch3 and they were regulated by androgens. Although HES6 is structurally homologous to known Notch3 targets, such as HES1 and HEY1, it was unknown whether Notch signaling regulates HES6. Our studies showed that HES6 acts independently of Notch3 and androgen stimulation increases HES6 transcript levels.

Another important aspect is the dynamics of Notch signaling in prostate cells. Notch signaling largely emerged as having oncogenic effects in several tumor types and tumor suppressive functions were restricted to cutaneous squamous cell carcinomas (38). However, recent studies revealed tumor suppressive roles for Notch pathway in a wide variety of tumors (39–43). Yet none of these studies address potential tumor suppressive function in the prostate. We found that benign prostate cells expressed higher levels of Notch1 and Notch2 receptors and more Notch pathway activation than cancer cells. Additional experiments demonstrated that prostate cancer cells do not respond to gamma secretase inhibition.

The last section of our Notch signaling studies focused on the independent roles of HES6 in tumor progression. By manipulating HES6 protein levels in benign and cancer cell lines, we discovered that HES6 controls the expression of genes involved in cell invasion, apoptosis, chromatin remodeling, DNA repair, and modulators of Hedgehog and Notch pathways.

Notch signaling dynamics and HES6 roles in prostate cancer bring up many interesting questions for future research projects. Previous studies showed that although HES6 is structurally related with HES family members, it plays a feedback negative regulation of Notch signaling during neural stem cell differentiation by inhibiting Notch-responsive HES proteins (44, 45). So, besides HES6 independent functions controlling important pathways for tumor progression, future studies should explore potential inhibitory effects of HES and HEY targets levels in the context of cancer.

Another angle of this Notch story that is worth pursuing in the future relates with the ligands and receptors differentially expressed in benign compared to cancer cells. In line with previous studies (46, 47), we also found an upregulation of Notch3 receptor in cancer cells. It was out of the scope of our study, but functional roles for Notch3 are being progressively implicated in the progression of different cancer types (48–53), including the prostate (54). For that reason, an interesting future line of research could be the comprehensive characterization of Notch3 functions' in prostate tumors. Although, in our studies there was not a significant increase in Notch ligands expression, Gleason score 8 prostate cancers are enriched for Jagged2 (6). Because Jagged2 ligand and Notch3 receptor are overexpressed in high grade tumors, it is legitimate to speculate if there is an increased binding affinity between Jagged2 and Notch3 in cancer. Binding affinities of Notch receptors and ligands remain largely unknown, but there are descriptions for specific ligand-receptor preferences. Delta4 and Notch1 actively interact to promote blood vessel formation (55–58) and recent work implicated Jagged2-Notch3 interaction in the context of T cell maturation (59). Because selective inhibitory antibodies against individual receptors are available (60), a better understanding of preferential ligand-receptor binding pairs is extremely relevant. By identifying which ligand-receptor interactions determine cancer phenotypes enable the specific Notch signaling blockade without the side effects of pan-notch inhibition (61). In conclusion, further studies characterizing Notch pathway modulation are likely to translate into powerful diagnostic and therapeutic tools for prostate cancer.

Loose PTEN to gain prognosis

In addition to understanding the biology of prostate tumorigenesis, I was also interested in studying molecular biomarkers to improve patient selection for active surveillance. As mentioned above, depending on the studies, 25% to 30% of supposedly indolent Gleason score 6 on needle biopsy are “upgraded” to Gleason score 7 or higher in the radical prostatectomy specimen. Several factors contribute to tumor upgrading, such as sampling error, tumor progression, and inter-observer variability in Gleason grading. Unfortunately other clinical-pathological parameters such as PSA kinetics, prostate volume, more extensive disease on biopsy cores, or increasing number of sampled needle cores, are modest predictors of Gleason grade upgrade. Thus, no molecular biomarkers were previously evaluated with the purpose of predicting tumor upgrading from needle biopsy to radical prostatectomy.

The loss of the tumor suppressor PTEN is one of the most common somatic aberrations in prostate cancer (62–69). Previous studies using applied IHC in high-risk cancers found that loss of PTEN protein staining is associated with poor clinical outcome (70, 71). Hence, we hypothesize whether PTEN IHC assay applied in a cohort of Gleason score 6 biopsies can predict Gleason upgrading in the radical prostatectomy specimen.

Our study showed a significant difference between PTEN protein loss in upgraded tumors compared to the controls ($p=0.02$). To confirm the IHC results, we performed FISH to determine PTEN gene deletions and found that 90% of the biopsies with decreased PTEN protein showed homozygous PTEN deletions. We then applied logistic regression models to determine the association of PTEN loss with tumor upgrade and found that, even adjusting for all predictors of upgrading described in multiple studies, tumors with PTEN loss were still significantly more likely upgraded at radical prostatectomy.

This is one of the first studies supporting the effectiveness of a single molecular marker in predicting Gleason score upgrading from needle biopsy to radical prostatectomy. This finding opens several new lines of research and further validation of our results. Even though PTEN IHC is a quick and cheap assay, the logistic of collecting needle biopsies and radical prostatectomies takes a significant amount of time. Thus, to complete the study within the period of my Ph.D. research work, our cohort included patients whose biopsies and radical prostatectomies were performed at Johns Hopkins Hospital and Johns Hopkins Bayview Medical Center. This contributes for the relatively small retrospective cohort enriched for white ethnical background. In addition, although all our needle biopsies had Gleason score 6 tumors, our selection criteria did not meet the active surveillance used at Johns Hopkins Hospital (72). Therefore, our PTEN assay needs further validation in a larger prospective active surveillance cohort and include ethnical origins other than whites, such as african-american, which have adverse outcomes even with low-grade disease (73).

In summary, PTEN IHC is a useful assay to predict Gleason score 6 upgrade, enabling better patient selection for active surveillance.

Beyond detection of prostate circulating tumor cells

Finally, the last stage of prostate cancer progression that I addressed was the biological activity of prostate circulating tumor cells (CTCs). The majority of prostate-related deaths are consequence of hematogenously metastatic spread of tumor cells to the bone (74). In general, there is a temporal gap between the time cancer cells infiltrate distant organs and the development of metastatic lesions. Also, increasing evidence supports the notion that tumor cells can disseminate from the earliest pre-neoplastic lesions, sometimes even before the formation of primary tumors (75–77). In prostate cancer, tumor recurrence is associated with pathological stage and Gleason score, but a provocative study demonstrated the presence of prostate cells in the bone marrow of 70% of patients with prostate cancer before radical prostatectomy (78). However, 15% of the patients with prostate cells in the bone marrow did not recur after 5 years of follow up. Several factors, such as short follow up time or tumor dormancy, can explain the absence of clinical recurrence, but it is reasonable to wonder if these cells cause or are simply a byproduct of metastasis.

Less than 0.1% of the circulating cancer cells are estimated to survive the journey of infiltrating and colonizing distant organs (79, 80). So, a panoply of techniques and cell surface markers are currently used to isolate CTCs (81). Most of these methods rely on cell size or expression of the epithelial differentiation marker EpCAM that isolate only a fraction of CTCs. In addition, cells are unviable at the end of the protocols currently used to identify CTCs, precluding functional experiments. Although in patients with prostate cancer, high CTCs counts predict early death (82) and recurrence after radical prostatectomy (78), several lines of evidence showed that tumor cells downregulate EpCAM during epithelial-to-mesenchymal transition (EMT) to invade surrounding tissues (83) and metastasis-initiating cells need plasticity to switch between epithelial and mesenchymal states to entry in the bloodstream and for extravasate into distant organs. Therefore, I developed an unbiased method to isolate viable CTCs and generated mouse xenografts to determine their tumor-initiating capacity.

I used blood from men with castration-resistant prostate cancer and from TRAMP mice with metastatic disease. To preserve CTCs viability, I used gradient density centrifugation or red cell lysis followed by magnetic depletion of leucocytes with CD45 immunoaffinity beads. CTCs isolation from TRAMP mice and prostate cancer patients was confirmed by immunocytochemical staining, and inoculated into immunodeficient mice. Three months after injection, CTCs from TRAMP mice yielded invasive and highly aggressive tumors in 22% of recipients. Human CTCs did not successfully form tumors either when injected directly in the bloodstream or grafted under the kidney capsule to enhance grafting efficiency. Our results confirm that our CTCs isolation approach isolates viable CTCs with tumor-forming capacity without relying on cell surface markers. The success of TRAMP CTCs xenografts may have methodological and biological explanations: the amount of blood used in mouse experiments represented half of blood volume of each mouse whereas the human samples represented less than 0.5% of blood volume. It is also possible that the xenograft techniques developed so far for primary prostate tumors do not meet the growth requirements of CTCs or these cells need more than 8 months to establish a tumor. As mentioned above, prostate cancer cells have a latency period of in the bone longer than our follow up, which may have not allowed us to observe tumors. Most importantly, to our knowledge, this was the first study proposing an unbiased method to isolate viable CTCs and demonstrating in vivo their tumorigenic capacity.

During the last decade, techniques to isolate circulating-free DNA present in the blood and identify genomic mutations present exclusively in tumors emerged as promising tools for cancer screening and monitoring therapeutic response (84). The sensitivity improvement of these assays and the rapid widespread of these technologies in several academic institutions will most likely relegate CTCs to a secondary plane as a diagnostic and therapy-response biomarkers, due to the lack of reliable cell surface markers and isolation techniques that identify the cells with true metastatic properties. Therefore, I believe that the study of CTCs should focus more on functional studies to identify lethal cell clones, their genetic and epigenetic alterations, rather than using several cell surface markers to enumerate different cell populations. Once the metastatic cell clones are identified, a plethora of assays to generate tumor-tissue in vitro, single-cell genomic analysis, and high-throughput drug screens can be performed to gain insights in individual tumors during disease progression and response to therapy.

To conclude this general discussion, I would like to quote Susan Lindquist, a biologist whose pioneering works in yeast contributed for the understanding of protein folding in disease. Asked about her feelings about the current times in scientific research, Susan Lindquist answered: “This is the greatest intellectual revolution, and it is happening right now, and I’m lucky enough to be in the middle of it.” I feel the same! We have amazing tools to sequence whole-genomes in a few days or using overnight assays to determine the expression of thousands of genes. Throughout my PhD research work, I took advantage of these high-end techniques to indentify target genes and explore the biology of prostate cancer progression and, at the same, contribute to biomarker discovery for active surveillance.

CHAPTER 8 —
MAIN CONCLUSIONS

MAIN CONCLUSIONS

1 Expression analysis of Notch pathway components in prostate cells revealed HES6 as the most differentially expressed gene between benign and cancer cells. HES6 transcritps are 4–fold higher in cancer.

2 Other targets of the Notch pathway such as HEY1, HEY2, and HES4 are also overexpressed in cancer cells. In contrast, many central Notch signaling components, as DLL1, JAG1, NOTCH1, NOTCH2, and NOTCH4 receptors, are downregulated in cancer.

3 Most of prostate androgen-responsive cell lines have a high expression of both NOTCH3 and HES6. However, NOTCH3 and HES6 act independently in prostate cancer progression.

4 Benign prostate cells have significantly higher expression of Notch1 and Notch2 receptors and preserved canonical Notch signaling. Consequently, Notch receptors are cleaved by g-secretase and strongly activate RBPJ. On the contrary, the majority of prostate cancer cells have lower expression of Notch1 and Notch2 receptors, which are not cleaved by g-secretase. For this reason, pharmacological inhibition of the Notch pathway does not affect prostate cancer cells viability and growth. Therefore, targeting Notch is unlikely to be a successful strategy for treating prostate cancer.

5 Androgens affect the expression of Notch receptors and targets in opposite directions. Androgen stimulation decreases NOTCH1, NOTCH2, and NOTCH3 expression over time whereas HES1, HES6, and HEY1 increase. Thus, androgens may induce HES/HEY family members in a Notch receptor-independent manner.

6 HES6 is a key player of Notch prostate cancer progression and metastatic potential. HES8 significantly affected the clonogenic potential and invasion capacity of cancer cells.

7 HES6 controls members of several pathways, such as kinases, apoptosis, hedgehog, and integrins, that are implicated in the invasion and clonogenic advantage observed in cancer cells.

8 PTEN IHC is an useful assay to predict upgrading of Gleason score 6 cancers from biopsies to radical prostatectomy.

9 PTEN protein loss in both nuclear and cytoplasmic compartments is present in 18.3% of upgraded cases comparing to only 6.8% of not upgraded tumors (p=0.02)

10 FISH confirmed that 90% of the biopsies with decreased PTEN protein expression have homozygous deletion of PTEN gene.

11 Logistic regression determined PTEN loss as an independent predictor of tumor upgrading. Even after adjusting for age, preoperative PSA, clinical stage and race, Gleason score 6 tumors with PTEN protein loss on biopsy are significantly more likely to be upgraded at radical prostatectomy [OR=3.04 (1.08–8.55; p=0.035)].

12 A novel unbiased approach can isolate viable CTCs present in the bloodstream of TRAMP mice and prostate cancer patients with castration-resistant disease.

13 CTCs isolated using gradient density centrifugation or red cell lysis followed by magnetic separation of CD45 cells express cytokeratin 8 and EpCAM.

14 CTCs from TRAMP mice isolated using our method, are able to form new tumors in immunodeficient hosts.

15 None of human CTCs formed tumors, suggesting a relatively low tumor-forming potential.

16 Rather than quantifying heterogeneous cell populations present in the blood, future studies should identify and target the highly tumorigenic fraction of CTCs.

PART IV — BIBLIOGRAPHY

References

1 Hurley PJ, Marchionni L, Simons BW, Ross AE, Peskoe SB, Miller RM, et al. Secreted protein, acidic and rich in cysteine-like 1 (SPARCL1) is down regulated in aggressive prostate cancers and is prognostic for poor clinical outcome. Proc Natl Acad Sci U S A. 2012;109:14977–82.

2 Carvalho FL, Simons BW, Antonarakis ES, Rasheed Z, Douglas N, Villegas D, et al. Tumorigenic potential of circulating prostate tumor cells. Oncotarget. 2013;4:413–21.

3 Kleeberger W, Bova GS, Nielsen ME, Herawi M, Chuang AY, Epstein JI, et al. Roles for the stem cell associated intermediate filament Nestin in prostate cancer migration and metastasis. Cancer Res. 2007;67:9199–206.

4 Barbieri CE, Baca SC, Lawrence MS, Demichelis F, Blattner M, Theurillat JP, et al. Exome sequencing identifies recurrent SPOP, FOXA1 and MED12 mutations in prostate cancer. Nat Genet. 2012;44:685–9.

5 Baia GS, Caballero OL, Orr BA, Lal A, Ho JS, Cowdrey C, et al. Yes-associated protein 1 is activated and functions as an oncogene in meningiomas. Mol Cancer Res. 2012;10:904–13.

6 Ross AE, Marchionni L, Vuica-Ross M, Cheadle C, Fan J, Berman DM, et al. Gene expression pathways of high grade localized prostate cancer. Prostate. 2011.

7 Ankerst DP, Boeck A, Freedland SJ, Thompson IM, Cronin AM, Roobol MJ, et al. Evaluating the PCPT risk calculator in ten international biopsy cohorts: results from the Prostate Biopsy Collaborative Group. World J Urol. 2012;30:181–7.

8 Kortenhorst MS, Wissing MD, Rodriguez R, Kachhap SK, Jans JJ, Van der Groep P, et al. Analysis of the genomic response of human prostate cancer cells to histone deacetylase inhibitors. Epigenetics. 2013;8.

9 Gentleman RC, Carey VJ, Bates DM, Bolstad B, Dettling M, Dudoit S, et al. Bioconductor: open software development for computational biology and bioinformatics. Genome Biol. 2004;5:R80.

10 Ihaka R, and Gentleman, R. R: A Language for Data Analysis and Graphics. Journal of Computational and Graphical Statistics. 1996.

11 Smyth GK. Linear models and empirical bayes methods for assessing differential expression in microarray experiments. Stat Appl Genet Mol Biol. 2004;3:Article3.

12 Benjamini Y, and Hochberg, Y. Controlling the false discovery rate: a practical and powerful approach to multiple testing. Royal Statistical Society. 1995;Series B.

13 Shultz LD, Lyons BL, Burzenski LM, Gott B, Chen X, Chaleff S, et al. Human lymphoid and myeloid cell development in NOD/LtSz-scid IL2R gamma null mice engrafted with mobilized human hemopoietic stem cells. J Immunol. 2005;174:6477–89.

14 Carreno BM, Garbow JR, Kolar GR, Jackson EN, Engelbach JA, Becker-Hapak M, et al. Immunodeficient mouse strains display marked variability in growth of human melanoma lung metastases. Clin Cancer Res. 2009;15:3277–86.
15 Toivanen R, Berman DM, Wang H, Pedersen J, Frydenberg M, Meeker AK, et al. Brief report: a bioassay to identify primary human prostate cancer repopulating cells. Stem Cells.29:1310–4.
16 Thaxton CS, Elghanian R, Thomas AD, Stoeva SI, Lee JS, Smith ND, et al. Nanoparticle-based bio-barcode assay redefines "undetectable" PSA and biochemical recurrence after radical prostatectomy. Proc Natl Acad Sci U S A. 2009;106:18437–42.
17 Siegel R, Naishadham D, Jemal A. Cancer statistics, 2013. CA Cancer J Clin. 2013;63:11–30.
18 Ferlay J, Steliarova-Foucher E, Lortet-Tieulent J, Rosso S, Coebergh JW, Comber H, et al. Cancer incidence and mortality patterns in Europe: estimates for 40 countries in 2012. Eur J Cancer. 2013;49:1374–403.
19 Catalona WJ, Smith DS, Ratliff TL, Dodds KM, Coplen DE, Yuan JJ, et al. Measurement of prostate-specific antigen in serum as a screening test for prostate cancer. N Engl J Med. 1991;324:1156–61.
20 Schroder FH, Hugosson J, Roobol MJ, Tammela TL, Ciatto S, Nelen V, et al. Prostate-cancer mortality at 11 years of follow-up. N Engl J Med. 2012;366:981–90.
21 Schroder FH, Hugosson J, Roobol MJ, Tammela TL, Ciatto S, Nelen V, et al. Screening and prostate-cancer mortality in a randomized European study. N Engl J Med. 2009;360:1320–8.
22 Huang GJ, Sadetsky N, Penson DF. Health related quality of life for men treated for localized prostate cancer with long-term followup. J Urol. 2010;183:2206–12.
23 Cooperberg MR, Carroll PR, Klotz L. Active surveillance for prostate cancer: progress and promise. J Clin Oncol. 2011;29:3669–76.
24 Heidenreich A, Abrahamsson PA, Artibani W, Catto J, Montorsi F, Van Poppel H, et al. Early detection of prostate cancer: European association of urology recommendation. Eur Urol. 2013;64:347–54.
25 Klotz L, Zhang L, Lam A, Nam R, Mamedov A, Loblaw A. Clinical results of long-term follow-up of a large, active surveillance cohort with localized prostate cancer. J Clin Oncol. 2010;28:126–31.
26 van den Bergh RC, Roemeling S, Roobol MJ, Aus G, Hugosson J, Rannikko AS, et al. Outcomes of men with screen-detected prostate cancer eligible for active surveillance who were managed expectantly. Eur Urol. 2009;55:1–8.
27 Iremashvili V, Pelaez L, Manoharan M, Jorda M, Rosenberg DL, Soloway MS. Pathologic prostate cancer characteristics in patients eligible for active surveillance: a head-to-head comparison of contemporary protocols. Eur Urol. 2012;62:462–8.
28 Suardi N, Briganti A, Gallina A, Salonia A, Karakiewicz PI, Capitanio U, et al. Testing the most stringent criteria for selection of candidates for active surveillance in patients with low-risk prostate cancer. BJU Int. 2010;105:1548–52.
29 Davies JD, Aghazadeh MA, Phillips S, Salem S, Chang SS, Clark PE, et al. Prostate size as a predictor of Gleason score upgrading in patients with low risk prostate cancer. J Urol. 2011;186:2221–7.
30 Kvale R, Moller B, Wahlqvist R, Fossa SD, Berner A, Busch C, et al. Concordance between Gleason scores of needle biopsies and radical prostatectomy specimens: a population-based study. BJU Int. 2009;103:1647–54.
31 Conti SL, Dall'era M, Fradet V, Cowan JE, Simko J, Carroll PR. Pathological outcomes of candidates for active surveillance of prostate cancer. J Urol. 2009;181:1628–33; discussion 33–4.
32 Smaldone MC, Cowan JE, Carroll PR, Davies BJ. Eligibility for active surveillance and pathological outcomes for men undergoing radical prostatectomy in a large, community based cohort. J Urol. 2010;183:138–43.
33 Penney KL, Sinnott JA, Fall K, Pawitan Y, Hoshida Y, Kraft P, et al. mRNA expression signature of Gleason grade predicts lethal prostate cancer. J Clin Oncol. 2011;29:2391–6.
34 Sethi N, Kang Y. Notch signalling in cancer progression and bone metastasis. Br J Cancer. 2011;105:1805–10.
35 Shou J, Ross S, Koeppen H, de Sauvage FJ, Gao WQ. Dynamics of notch expression during murine prostate development and tumorigenesis. Cancer Res. 2001;61:7291–7.
36 Wang XD, Leow CC, Zha J, Tang Z, Modrusan Z, Radtke F, et al. Notch signaling is required for normal prostatic epithelial cell proliferation and differentiation. Dev Biol. 2006;290:66–80.
37 Bin Hafeez B, Adhami VM, Asim M, Siddiqui IA, Bhat KM, Zhong W, et al. Targeted knockdown of Notch1 inhibits invasion of human prostate cancer cells concomitant with inhibition of matrix metalloproteinase–9 and urokinase plasminogen activator. Clin Cancer Res. 2009;15:452–9.
38 Dotto GP. Notch tumor suppressor function. Oncogene. 2008;27:5115–23.
39 Kuang SQ, Fang Z, Zweidler-McKay PA, Yang H, Wei Y, Gonzalez-Cervantes EA, et al. Epigenetic inactivation of Notch-Hes pathway in human B-cell acute lymphoblastic leukemia. PLoS One. 2013;8:e61807.
40 Avila JL, Kissil JL. Notch signaling in pancreatic cancer: oncogene or tumor suppressor? Trends Mol Med. 2013;19:320–7.

41 Lobry C, Ntziachristos P, Ndiaye-Lobry D, Oh P, Cimmino L, Zhu N, et al. Notch pathway activation targets AML-initiating cell homeostasis and differentiation. J Exp Med. 2013;210:301–19.
42 Kim HA, Koo BK, Cho JH, Kim YY, Seong J, Chang HJ, et al. Notch1 counteracts WNT/beta-catenin signaling through chromatin modification in colorectal cancer. J Clin Invest. 2012;122:3248–59.
43 Cui H, Kong Y, Xu M, Zhang H. Notch3 functions as a tumor suppressor by controlling cellular senescence. Cancer Res. 2013;73:3451–9.
44 Gratton MO, Torban E, Jasmin SB, Theriault FM, German MS, Stifani S. Hes6 promotes cortical neurogenesis and inhibits Hes1 transcription repression activity by multiple mechanisms. Mol Cell Biol. 2003;23:6922–35.
45 Fior R, Henrique D. A novel hes5/hes6 circuitry of negative regulation controls Notch activity during neurogenesis. Dev Biol. 2005;281:318–33.
46 Serafin V, Persano L, Moserle L, Esposito G, Ghisi M, Curtarello M, et al. Notch3 signalling promotes tumour growth in colorectal cancer. J Pathol. 2011;224:448–60.
47 Park JT, Chen X, Trope CG, Davidson B, Shih Ie M, Wang TL. Notch3 overexpression is related to the recurrence of ovarian cancer and confers resistance to carboplatin. Am J Pathol. 2010;177:1087–94.
48 Hassan KA, Wang L, Korkaya H, Chen G, Maillard I, Beer DG, et al. Notch pathway activity identifies cells with cancer stem cell-like properties and correlates with worse survival in lung adenocarcinoma. Clin Cancer Res. 2013;19:1972–80.
49 Ye YZ, Zhang ZH, Fan XY, Xu XL, Chen ML, Chang BW, et al. Notch3 overexpression associates with poor prognosis in human non-small-cell lung cancer. Med Oncol. 2013;30:595.
50 Park JT, Li M, Nakayama K, Mao TL, Davidson B, Zhang Z, et al. Notch3 gene amplification in ovarian cancer. Cancer Res. 2006;66:6312–8.
51 van Nes J, Chan A, van Groningen T, van Sluis P, Koster J, Versteeg R. A NOTCH3 transcriptional module induces cell motility in neuroblastoma. Clin Cancer Res. 2013;19:3485–94.
52 Eto K, Kawakami H, Kuwatani M, Kudo T, Abe Y, Kawahata S, et al. Human equilibrative nucleoside transporter 1 and Notch3 can predict gemcitabine effects in patients with unresectable pancreatic cancer. Br J Cancer. 2013;108:1488–94.
53 Ling H, Sylvestre JR, Jolicoeur P. Cyclin D1-Dependent Induction of Luminal Inflammatory Breast Tumors by Activated Notch3. Cancer Res. 2013;73:5963–73.
54 Danza G, Di Serio C, Ambrosio MR, Sturli N, Lonetto G, Rosati F, et al. Notch3 is activated by chronic hypoxia and contributes to the progression of human prostate cancer. Int J Cancer. 2013;133:2577–86.
55 Andrawes MB, Xu X, Liu H, Ficarro SB, Marto JA, Aster JC, et al. Intrinsic Selectivity of Notch 1 for Delta-like 4 Over Delta-like 1. J Biol Chem. 2013;288:25477–89.
56 Ridgway J, Zhang G, Wu Y, Stawicki S, Liang WC, Chanthery Y, et al. Inhibition of Dll4 signalling inhibits tumour growth by deregulating angiogenesis. Nature. 2006;444:1083–7.
57 Noguera-Troise I, Daly C, Papadopoulos NJ, Coetzee S, Boland P, Gale NW, et al. Blockade of Dll4 inhibits tumour growth by promoting non-productive angiogenesis. Nature. 2006;444:1032–7.
58 Hellstrom M, Phng LK, Hofmann JJ, Wallgard E, Coultas L, Lindblom P, et al. Dll4 signalling through Notch1 regulates formation of tip cells during angiogenesis. Nature. 2007;445:776–80.
59 Van de Walle I, Waegemans E, De Medts J, De Smet G, De Smedt M, Snauwaert S, et al. Specific Notch receptor-ligand interactions control human TCR-alpha-beta/gammadelta development by inducing differential Notch signal strength. J Exp Med. 2013;210:683–97.
60 Wu Y, Cain-Hom C, Choy L, Hagenbeek TJ, de Leon GP, Chen Y, et al. Therapeutic antibody targeting of individual Notch receptors. Nature. 2010;464:1052–7.
61 Capaccione KM, Pine SR. The Notch signaling pathway as a mediator of tumor survival. Carcinogenesis. 2013;34:1420–30.
62 Cairns P, Okami K, Halachmi S, Halachmi N, Esteller M, Herman JG, et al. Frequent inactivation of PTEN/MMAC1 in primary prostate cancer. Cancer Res. 1997;57:4997–5000.
63 Feilotter HE, Nagai MA, Boag AH, Eng C, Mulligan LM. Analysis of PTEN and the 10q23 region in primary prostate carcinomas. Oncogene. 1998;16:1743–8.
64 Pesche S, Latil A, Muzeau F, Cussenot O, Fournier G, Longy M, et al. PTEN/MMAC1/TEP1 involvement in primary prostate cancers. Oncogene. 1998;16:2879–83.
65 Suzuki H, Freije D, Nusskern DR, Okami K, Cairns P, Sidransky D, et al. Interfocal heterogeneity of PTEN/MMAC1 gene alterations in multiple metastatic prostate cancer tissues. Cancer Res. 1998;58:204–9.
66 Vlietstra RJ, van Alewijk DC, Hermans KG, van Steenbrugge GJ, Trapman J. Frequent inactivation of PTEN in prostate cancer cell lines and xenografts. Cancer Res. 1998;58:2720–3.
67 Wang SI, Parsons R, Ittmann M. Homozygous deletion of the PTEN tumor suppressor gene in a subset of prostate adenocarcinomas. Clin Cancer Res. 1998;4:811–5.
68 Whang YE, Wu X, Suzuki H, Reiter RE, Tran C, Vessella RL, et al. Inactivation of the tumor suppressor PTEN/MMAC1 in advanced human prostate cancer through loss of expression. Proc Natl Acad Sci U S A. 1998;95:5246–50.

69 Verhagen PC, van Duijn PW, Hermans KG, Looijenga LH, van Gurp RJ, Stoop H, et al. The PTEN gene in locally progressive prostate cancer is preferentially inactivated by bi-allelic gene deletion. J Pathol. 2006;208:699–707.
70 McMenamin ME, Soung P, Perera S, Kaplan I, Loda M, Sellers WR. Loss of PTEN expression in paraffin-embedded primary prostate cancer correlates with high Gleason score and advanced stage. Cancer Res. 1999;59:4291–6.
71 Lotan TL, Gurel B, Sutcliffe S, Esopi D, Liu W, Xu J, et al. PTEN protein loss by immunostaining: analytic validation and prognostic indicator for a high risk surgical cohort of prostate cancer patients. Clin Cancer Res. 2011;17:6563–73.
72 Tosoian JJ, Trock BJ, Landis P, Feng Z, Epstein JI, Partin AW, et al. Active surveillance program for prostate cancer: an update of the Johns Hopkins experience. J Clin Oncol. 2011;29:2185–90.
73 Sundi D, Ross AE, Humphreys EB, Han M, Partin AW, Carter HB, et al. African american men with very low-risk prostate cancer exhibit adverse oncologic outcomes after radical prostatectomy: should active surveillance still be an option for them? J Clin Oncol. 2013;31:2991–7.
74 Alva A, Hussain M. The changing natural history of metastatic prostate cancer. Cancer J. 2013;19:19–24.
75 Rhim AD, Mirek ET, Aiello NM, Maitra A, Bailey JM, McAllister F, et al. EMT and dissemination precede pancreatic tumor formation. Cell. 2012;148:349–61.
76 Podsypanina K, Du YC, Jechlinger M, Beverly LJ, Hambardzumyan D, Varmus H. Seeding and propagation of untransformed mouse mammary cells in the lung. Science. 2008;321:1841–4.
77 Husemann Y, Geigl JB, Schubert F, Musiani P, Meyer M, Burghart E, et al. Systemic spread is an early step in breast cancer. Cancer Cell. 2008;13:58–68.
78 Morgan TM, Lange PH, Porter MP, Lin DW, Ellis WJ, Gallaher IS, et al. Disseminated tumor cells in prostate cancer patients after radical prostatectomy and without evidence of disease predicts biochemical recurrence. Clin Cancer Res. 2009;15:677–83.
79 Acharyya S, Oskarsson T, Vanharanta S, Malladi S, Kim J, Morris PG, et al. A CXCL1 paracrine network links cancer chemoresistance and metastasis. Cell. 2012;150:165–78.
80 Weiss L. Metastasis of cancer: a conceptual history from antiquity to the 1990s. Cancer Metastasis Rev. 2000;19:I–XI, 193–383.
81 Danila DC, Fleisher M, Scher HI. Circulating tumor cells as biomarkers in prostate cancer. Clin Cancer Res. 2011;17:3903–12.
82 Scher HI, Jia X, de Bono JS, Fleisher M, Pienta KJ, Raghavan D, et al. Circulating tumour cells as prognostic markers in progressive, castration-resistant prostate cancer: a reanalysis of IMMC38 trial data. Lancet Oncol. 2009;10:233–9.
83 Mani SA, Guo W, Liao MJ, Eaton EN, Ayyanan A, Zhou AY, et al. The epithelial-mesenchymal transition generates cells with properties of stem cells. Cell. 2008;133:704–15.
84 Schwarzenbach H, Hoon DS, Pantel K. Cell-free nucleic acids as biomarkers in cancer patients. Nat Rev Cancer. 2011;11:426–37.

PART V — ABSTRACT / RESUMO

Abstract

This thesis covers molecular mechanisms involved in major steps of prostate cancer progression such as the roles of Notch pathway and HES6 in tumor aggressiveness, identification of PTEN loss as a predictor of Gleason score upgrading, and the isolation of cells with tumor-initiation capacity that escape from the prostate to generate metastasis.

PSA screening contributes to the early detection of prostate cancer. However, the results of randomized PSA screening studies raised issues of overdiagnosis and overtretament of indolent prostate cancers. One way to decrease prostate cancer overtreatment is through “Active surveillance”. Some of the most widely and accepted criteria to enroll patients in active surveillance protocols are early stage tumors with low grade Gleason score. Although the Gleason grading system is the strongest prognostic predictor after radical prostatectomy, due to sampling errors it is less powerful when analyzed in biopsies. So, one of the major questions that remain to be addressed is how to find biomarkers or pathways that can distinguish indolent from lethal tumors.

Recent work supports the notion that expression levels of Notch pathway members can serve this purpose. Gene expression profiling analysis on cancer cells from localized prostate cancers that were purely high-grade (Gleason 4+4=8) or purely low grade (Gleason 3+3=6) revealed that Notch signaling was the theme most associated with genes that distinguish between indolent and aggressive cancer cells. Our studies showed significantly higher expression of NOTCH3 and HES6 transcripts in cancer cells compared with benign cells. The expression of these Notch pathway receptor and target was particularly high in androgen-responsive lines 22Rv1 and LnCaP. Prostate cancer cells responded to Notch stimulation by induction of Notch canonical targets, HES1 and HEY1, but not HES6. We found that androgen stimulation also induced HES1 and HEY1, while downregulating Notch receptors, suggesting that androgens can activate Notch target genes in a receptor-independent manner. To study the dynamics of Notch signaling in prostate cells, we used a Notch-sensitive RBPJ reporter assay and realized that prostate cancer cells downregulated Notch signaling. Consequently Notch pathway blockade with γ-secretase inhibitor was unable to restrain cancer cell growth or viability. In contrast, HES6 expression was independent of Notch signaling, but as mentioned above, relied on androgen levels in culture. We confirmed androgen-dependent HES6 expression in human prostate cancer tissues from patients treated with androgen deprivation. We complemented HES6 expression studies with functional assays using shRNA downregulation of HES6 in cancer cells. We revealed functions for this gene product in prostate cancer cells to form colonies from single cells and cell invasion. By molecular profiling of

pathways controlled by HES6 we identified potential roles for this transcription factor in regulating hedgehog signaling, apoptosis, and cell migration. Thus, our work contraindicate an oncogenic role for Notch signaling in the prostate, but implicates HES6 as a protagonist in prostate cancer progression.

Having mind the clinical challenge that tumor progression represents for men with low grade cancer on active surveillance programs, we took advantage of PTEN loss, a characteristic genomic alteration of high Gleason score and metastatic tumors, and explore its potential to identify high risk cancers. We design a retrospective case-control study with 71 patients with GS 6 tumors on needle biopsy that were upgraded to GS 7 or higher cancer at RP (cases) and compared them to 103 patients whose GS 6 tumors on needle biopsy were not upgraded at RP (controls). Then, we performed IHC and scored for PTEN protein loss on prostate needle core biopsies with Gleason score 6. Biopsies with PTEN protein loss by IHC were further analysed using FISH to detect PTEN gene deletion. Our IHC results showed PTEN protein loss in 18.3% (13/71) of upgraded cases compared to 6.8% (7/103) of controls (p=0.02). In the cases where IHC did not detect PTEN expression, FISH confirmed homozygous PTEN deletion in 90% (9/10) of upgraded tumors compared to 67% (4/6) of interpretable controls who were not upgraded. Multivariate analyses adjusted for age, preoperative PSA, clinical stage and race, established that Gleason score 6 tumors with PTEN protein loss on biopsy were significantly more likely to be upgraded at radical prostatectomy [odds ratio = 3.04 (1.08–8.55; p=0.035)] compared to those without PTEN loss. Overall, PTEN IHC is a simple and cheap assay that effectively distinguishes men candidates for active surveillance with low risk cancers from men with intermediate or higher risk cancers.

Finally, cancer cells from high Gleason grade (Gleason score ≥ 7) tumors have the potential to escape from the prostate and generate metastasis in distant organs. The promise that detection of CTCs might change cancer prognosis and therapeutic response monitoring, lead to the development of several detection methods. However, most of these methods are biased towards isolation of subpopulations of CTCs that might not represent cells with true metastatic-initiation capacity. Thus, we developed an unbiased approach to isolate viable CTCs from a transgenic mouse model of prostate cancer (TRAMP) and men with castration-resistant disease. After identifying the presence of CTCs, we inoculated into immunodeficient mice to determine the tumorigenic potential of these cells. Three months after injecting CTCs from TRAMP into immunodeficient hosts, these developed metastasis with highly aggressive features, similar to the primary tumors. Although CTCs from prostate cancer patients did not formed tumors, our isolation method showed to be effective in isolating viable CTCs without relying on cell surface markers or size fractionation. Future studies should focus on identifying and target the highly tumorigenic cells to have significant impact in prostate cancer prognosis.

Resumo

Esta tese abrange os mecanismos moleculares envolvidos em algumas das principais etapas de progressão do cancro da próstata como o papel da via do Notch e do HES6 na agressividade tumoral, a identificação da perda de PTEN como preditor do aumento do score de Gleason e o isolamento de células neoplásicas prostáticas na circulação sanguínea e com capacidade de gerar metástases.

O rastreio baseado no PSA contribui para a detecção precoce do cancro da próstata. Contudo, resultados recentes de ensaios clínicos randomizados indicam que o screening com PSA leva a um sobrediagnóstico e sobretratamento de cancros da próstata indolentes. Uma forma de diminuir este sobretratamento consiste na “vigilância ativa”. A maioria dos doentes que integram programas de vigilância ativa têm tumores em estadio inicial e de baixo score de Gleason. No entanto, apesar do sistema de classificação de Gleason ser o principal preditor de prognóstico após prostatectomia radical, os erros de amostragem na biopsia fazem com que este parâmetro seja muito menos poderoso quando avaliado em biópsias. Por esse motivo, torna-se fundamental encontrar biomarcadores ou vias moleculares que distingam tumores indolentes dos letais.

Trabalhos recentes mostraram que os níveis de expressão de membros da via de sinalização Notch podem responder a esta problemática. A analise da expressão génica de células cancerígenas presentes em tumores localizados que eram puramente de alto grau (Gleason 4+4=8) ou puramente baixo grau (Gleason 3+3=6) revelou que o Notch era a via mais associada a genes que distinguem entre tumores indolentes e agressivos. Os nossos estudos mostraram um aumento significativo do nível de transcritos NOTCH3 e HES6 nas células cancerígenas comparando com células benignas. A expressão deste receptor e alvo da via foi particularmente elevada nas linhas celulares que respondem a androgénios, 22Rv1 e LnCaP. De forma a verficar se HES6 seria controlado pela sinalização Notch, estimulamos linhas celulares de cancro da próstata que responderam, com a indução de alvos canónicos, como HES1 e HEY1, mas não HES6. Adicionalmente, a estimulação das células com androgénios induziu a expressão dos alvos HES1 e HEY1, mas diminuiu a expressão dos receptores respectivos. Estes resultados sugerem que os androgénios activam alvos da via Notch de uma forma independente dos receptores. Para estudar a dinâmica desta via de sinalização em células prostáticas, usamos um vector com o gene RBPJ associado a um sinalizador de luciferase. Os resultados deste ensaio mostraram que as células de cancro da próstata diminuem a intensidade da sinalização Notch. Em consequência, o bloqueio farmacológico da via com um inibidor da γ-secretase foi incapaz de suprimir a multiplicação das células tumorais. Por outro lado, a expressão de HES6 mostrou-se independente da via de sinalização de Notch, mas como atrás mencionado, dependerá dos níveis

de androgénios no meio de cultura. Confirmamos a dependência da expressão de HES6 dos androgénios através da análise imunohistoquímica de tumores do cancro da próstata provenientes de doentes submetidos a terapêutica hormonal. Estes estudos da expressão de HES6 foram complementados com estudos funcionais utilizando o silenciamento deste gene nas células cancerígenas por RNA de interferência. Os nossos estudos mostraram que este gene está envolvido na formação de colónias de células malignas e na invasão da membrana basal. Depois de realizar o perfil molecular das vias controladas por HES6, identificamos potencias funções deste gene na regulação da via do hedgehog, apoptose e migração celular. Assim, o nosso trabalho sugere que a via de sinalização de Notch possivelmente não tem um papel oncogénico no cancro da próstata, mas implicam HES6 como um protagonista na progressão desta neoplasia.

Tendo em conta o desafio que representa para o urologista saber se os tumores dos doentes em vigilância ativa vão progredir para estádios mais avançados, decidimos explorar o potencial do gene PTEN como biomarcador. Estudos prévios mostraram que a perda do gene PTEN é frequente em tumores de elevado grau de Gleason e em metástases. Por isso a nossa hipótese consistiu em verificar se a perda da expressão da proteína PTEN em biópsias de tumores Gleason 6 predizia o aumento do score de Gleason na prostatectomia radical. Realizamos, então, um estudo retrospectivo caso-controlo, com 71 doentes portadores de carcinomas Gleason 6 na biopsia, mas cuja peça operatória de prostatectomia radical mostrou tumores com score de Gleason mais elevados (Casos); os quais foram comparados com 103 doentes cujo score de Gleason na biopsia e na peca operatória se manteve como 6 (Controlos). Avaliamos por imunohistoquímica a perda de expressão da proteína PTEN em todas as biópsias Gleason 6. As biópsias que apresentavam perda de proteína por imunohisotquimica foram analisadas com FISH para detectar deleções do gene PTEN. Os resultados de imunohistoquímica mostraram perda de expressão de PTEN em 18,3% (13/71) dos casos comparando com 6,8% (7/103) dos controlos (p=0,02). Em casos onde não se detectou expressão de PTEN, a técnica de FISH confirmou deleção homozigotica de PTEN em 90% (9/10) comparando com 67% (4/6) dos controlos. A analise multivariada ajustada para a idade, PSA pré-operatório, estadio clínico e raça, estabeleceu que nos tumores com um score de Gleason 6 com perda de expressão proteica de PTEN na biopsia existia uma probabilidade significativamente maior de ser atribuído um score de Gleason mais elevado na prostatectomia radical [odds ratio = 3.04 (1.08–8.55; p=0.035)]. Concluímos que a imunohistoquímica para PTEN, um teste simples e barato, distingue de forma eficaz pacientes com tumores de baixo grau candidatos a vigilância ativa dos portadores de tumores de risco intermédio ou alto.

Finalmente, tumores com elevado score de Gleason (superior ou igual a 7) têm o potencial para invadir e gerar metástases em órgãos distantes. A expectativa de que a detecção de células tumorais circulantes (CTCs) poderá melhorar o prognóstico ou a monitorização da resposta terapêutica, levou ao desenvolvimento de vários métodos para detectar estas células. Contudo, a maioria dos métodos de detecção de CTCs têm o viés de isolarem subpopulações de células que podem não representar aquelas com verdadeira capacidade de iniciar metástases. Por isso, desenvolvemos uma abordagem independente de isolamento de CTCs viáveis, utilizando um modelo de ratinho trangénico de cancro da próstata (TRAMP) e o sangue de pacientes com tumores hormono-resistentes. Depois de identificarmos a presença de CTCs isoladas por este método, inoculamos essas células em ratinhos imunodeficientes para determinar o potencial tumorigenico das CTCs. Três meses após inocularmos CTCs provenientes dos ratinhos TRAMP nos hospedeiros imunodeficientes, estes desenvolveram metástases com características muito agressivas, semelhantes aos dos tumores primários. Apesar das CTCs provenientes de doentes com cancro da próstata não terem formado tumores, o nosso método provou isolar eficazmente e de forma independente CTCs viáveis. Para que ocorra um impacto significativo destes achados no prognóstico dos pacientes com cancro da próstata, estudos futuros devem centrar-se na identificação das CTCs altamente tumorigénicas, as quais poderão constituir um alvo terapêutico preferencial.

CURRICULUM VITAE

Filipe Crista La Fuente Isaac de Carvalho

Home
1401 Blair Mill Rd, Apt 924
Silver Spring, 20910
USA

Contacts:
fcarval1@jhmi.edu
(202) 664-9226

Positions and Employment

2001-2007	M.D., Faculty of Medicine, University of Porto, Portugal
2008	Intern, Curry Cabral Hospital, Lisbon, Portugal
2009-2010	Urology Resident, Centro Hospitalar do Porto, Porto, Portugal
2010-Present	PhD dissertation work, Johns Hopkins University, Baltimore, USA

Honors and Awards:

2004 Award Maximiliano Lemos, Faculty of Medicine, University of Porto, Portugal
2004 Award Vicente Jose de Carvalho, Faculty of Medicine, University of Porto, Portugal
2005 Award Professor Aureliano Pessegueiro, Faculty of Medicine, University of Porto, Portugal
2010 PhD Scholarship from the Foundation for Science and Technology, Portugal
2012 Best Poster "Prostate cancer: Basic research", 27th Annual European Association Urology Congress
2012 Young promising speaker, 27th Annual European Association Urology Congress

Credentials:

2008 United States Medical Licensing Examination, Step 1 – Score 234/98
2009 United States Medical Licensing Examination, Step 2 CK – Score 230/95
2009 United States Medical Licensing Examination, Step 2 CS – Pass

Educational Activities:

2006 President of Organizing Committee of YES – Young European Scientist Meeting
2011 Poster presentation on circulating tumor cells at 4th Multi-institutional Prostate Cancer Retreat
2011 Poster presentation on circulating tumor cells at 6th Johns Hopkins Prostate cancer research day

Publications

Research papers:

Peer-reviewed publications:

1. Henriques-Coelho T, Oliveira SM, Moura RS, Roncon-Albuquerque R Jr, Neves AL, Santos M, Nogueira-Silva C, **La Fuente Carvalho F**, Brandão-Nogueira A,

Correia-Pinto J, Leite-Moreira AF. Thymulin inhibits monocrotaline-induced pulmonary hypertension modulating IL-6 expression and suppressing p38 pathway. Endocrinology, 2008, 149(9): 4367-73. PMID: 18511508

2. Outeiro TF, Putcha P, Tetzlaff JE, Spoelgen R, Koker M, **Carvalho F**, Hyman BT, McLean PJ. Formation of toxic oligomeric alpha-synuclein species in living cells. PLoS One. 2008 Apr 2;3(4):e1867. PMCID: PMC2270899

3. Cavadas V, Branco F, **Carvalho FL**, Osório L, Gomes MJ, Silva-Ramos M. The quality of reporting of randomized controlled trials in pelvic organ prolapse. Int Urogynecol J. 2011 Sep;22(9):1117-25. PMID: 21484364

4. Branco F, Cavadas V, Osório L, **Carvalho F**, Martins L, Dias L, Castro-Henriques A, Lima E. The incidence of cancer and potential role of sirolimus immunosuppression conversion on mortality among a single-center renal transplantation cohort of 1,816 patients. Transplant Proc. 2011 Jan-Feb;43(1):137-41. PMID: 21335171

5. de Oliveira RM, Marijanovic Z, **Carvalho F**, Miltényi GM, Matos JE, Tenreiro S, Oliveira S, Enguita FJ, Stone R, Outeiro TF. Impaired proteostasis contributes to renal tubular dysgenesis. PLoS One. 2011;6(6):e20854. Epub 2011 Jun 9. PMCID: PMC3111453

6. Osório L, **Carvalho FL**, Branco F, Cavadas V, Autorino R, Soares J. Endoscopic Removal of an Intravesical Calcified Sling Using Pneumatic Lithotripsy and Cystoscopic Resection. Urol Int. 2011 Aug 18. PMID: 21849767

7. **Carvalho F LF**, Simons B W, Antonarakis ES, Rasheed Z, Douglas N, Villegas D, Matsui W, Berman DM. Tumorigenic potential of circulating prostate tumor cells. Oncotarget, 2013;4(3):413-21. PMCID: PMC3717304

Submitted:

Carvalho F LF, Marchionni L, Ross AE, Schaeffer EM, Berman DM. HES6 promotes prostate cancer aggressiveness and independently of Notch signaling

Lotan TL*, **Carvalho FL***, Peskoe SB, Hicks JL, Good J, Fedor H, Humphreys E, Han M, Platz EA, Squire JA, De Marzo AM, Berman DM. PTEN Loss Predicts Upgrading of Prostate Cancer from Biopsy to Radical Prostatectomy

*co-first authors

In preparation:

Carvalho F LF, Simons B W, Eberhart, Eberhart CG, Berman DM. Notch signaling in prostate cancer: A moving target.

Abstracts:

1. Oliveira SM, Henriques-Coelho T, **La Fuente-Carvalho F**, Brandao-Nogueira A, Santos M, Correia Pinto J, Leite-Moreira AF. Immunomodulatory effects of thymulin in monocrotalin-induced pulmonary hypertension. Eur J Heart Fail 2006;5 (Abstr. Suppl.):168.

2. Henriques-Coelho T, **Carvalho FLF**, Oliveira SM, Brandao-Nogueira A, Santos M, Roncon-Albuquerque Jr R, Correia-Pinto J, Leite-Moreira AF. Beneficial effects of thymulin in MCT-induced pulmonary hypertension and its modulation of IL-6 gene expression**.** Eur Heart J 2006;27 (Abstr. Supp.): 901-902.

3. Henriques-Coelho T, **Carvalho FLF**, Oliveira SM, Brandao-Nogueira A, Santos M, Roncon-Albuquerque Jr R, Correia-Pinto J, Leite-Moreira AF. Beneficial effects of thymulin in MCT-induced pulmonary hypertension and its modulation of IL-6 gene expression. Circulation 2006;114 (Abstr. Suppl.):130.

4. **Carvalho F.L.**, Rasheed Z., Antonarakis E., Simons B., Matsui W., Berman D.M. Harnessing the biological activity of circulating prostate cancer cells. Eur Urol (Abstr. Suppl.):e652

5. **Carvalho F.L.**, Berman D.M. HES6 interacts with Notch signaling in prostate cancer progression. Eur Urol (Abstr. Suppl.):e656

Research Support

SFRH / BD / 69819 / 2010 09/01/2010-09/01/2014
Foundation for Science and Technology – Portuguese Ministry of Education and Science
Notch signaling pathway as a mediator for early detection and modulation of aggressiveness of prostate cancer
This project provided mentored training with Drs Stephen Baylin and David Berman with the goal of achieving a PhD degree.

1 F32 CA186460-01 (in revision) Expected 04/2014-04/2017
National Cancer Institute – National Institutes of Health
Epigenetic Alterations Induced by SWI/SNF Complex and KRAS in Lung Oncogenesis
This fellowship will be supervised by Dr. Stephen Baylin with the main goal of improving my scientific and management skills to establish as an independent investigator.

U.PORTO